CENTRO DE INVESTIGACIÓN Y DE ESTUDIOS

AVANZADOS DEL INSTITUTO POLITÉCNICO NACIONAL

UNIDAD ZACATENCO

DEPARTAMENTO DE FARMACOLOGÍA

“Modulación de sustancias liberadas por la microbiota intestinal mediante la ingestión de alimentos bioactivos en un modelo de ratón transgénico para la enfermedad de Alzheimer, y sus implicaciones en el metabolismo de los astrocitos”

TESIS

Que presenta

M. en C. Syeda Tauqeerunnisa Begum

Para obtener el grado de

DOCTORA EN CIENCIAS

EN LA ESPECIALIDAD DE FARMACOLOGÍA

Directora de tesis:
Dra. Claudia Pérez Cruz

Ciudad de México Octubre, 2018

CENTRO DE INVESTIGACIÓN Y DE ESTUDIOS

AVANZADOS DEL INSTITUTO POLITÉCNICO NACIONAL

UNIDAD ZACATENCO

DEPARTAMENTO DE FARMACOLOGÍA

“Modulation of gut microbiota released substances by ingestion of bioactive food in a transgenic mouse model of Alzheimer´s disease, and their implications on astrocyte metabolism”

THESIS

Submitted by

Syeda Tauqeerunnisa Begum

In partial fulfilment of the requirements for the award of degree of

DOCTOR IN SCIENCE

SPECIALIZATION IN PHARMACOLOGY

Director of thesis:
Dr. Claudia Perez Cruz

Mexico City October, 2018

ACKNOWLEDGEMENT

There are number of people without whom this thesis might have not been written and to whom I am greatly indebted.

Foremost, I would like to express my sincere gratitude to my thesis supervisor Dra. Claudia Pérez-Cruz for her continuous support, encouragement, motivation, patience, and immense knowledge. I have been extremely lucky to have a supervisor who cared so much about my work, and who responded to my questions and queries so promptly.

My sincere gratitude to all my committee members: Dra. Maria del Carmen García García, Dra. Marcia Hiriart Urdanivia, Dr. Jaime García Mena and Dr. Benjamín Florán Garduño, for their suggestions, constructive comments, and questions, their guidance helped me improve my project.

I would like to thank Dra. Nimbe Torres y Torres, Dr. Armando R. Tovar, Dra. Sofia yolanda diaz Miranda, Dra. Mónica A Torres Ramos and Dr. Felipe Barros for extending their support, suggestions and for providing necessary resources for the project.

I am extremely grateful to the lab auxiliaries (Dra. Jacqueline Acosta, Dra. Maria del Carmen, Dr. Abraham Rosas and Dr. Vicente Sanchez Valle) for their suggestions and help with the experiments. I would also like to acknowledge our lab technician Eduardo Osornio (Lalo) for his assistance during experiments.

I would like to thanks Mónica Sánchez Tapia and Ana Laura Pinedo Vargas for their immense help in the project.

I would like to thanks my friend for their encouragement and for providing a stimulating and fun filled environment in the lab, Daniel, Silvia, Luis, Karina, Erick, Yanahi, Lizabeth, Mariel, Brenda Pérez, Brenda, Sandra, Gabotzin, Carlos, Azalea, Betzy, Hannna, Julieta, Laura Hinte, Laura Wolbeck, Annika, Sima. I would like specially thank Juan for the moral support, encouragement and thank you for the laughs.

My special thanks to my friend Gayathri, for her moral support and encouragement during hard times of my PhD, I would also like to thank Joice, Neeshu, Shiv, Khem Eshwar and Rohini for the support and friendship.

Last but not least I wish to avail myself this opportunity to express a sense of gratitude, love to my dad, mom, Asad and sami, words alone cannot express what I owe them for their inspiration, encouragement and support. This thesis is dedicated to you guys.

Thank you Khairoon, Asma, Najja, Hamed, Ahmed uncle, Raziya aunty and all my family members for your appreciation and love.

Finally, I would like to thanks CONACyT for their financial support for four years during my doctoral study (Scholarship no.339473).

Syeda Tauqeerunnisa begum

INDEX

Table of contents……..

1. Introduction…… 1-25

1.1. Metabolic alterations in Alzheimer´s Disease…….. 4-7

1.1.1. Insulin resistance in Alzheimer´s Disease…… 4-6

1.1.2. Metabolic sensors of cellular energy…… 6-7

1.1.2.1. AMPK in Alzheimer´s Disease…… 6

1.1.2.2. SIRT1 in Alzheimer´s Disease…… 7

1.1.3. Mitochondrial dysfunction…… 8

1.1.3.1. PGC-1α…… 8

1.1.4. Metabolic alterations at cellular level: Neuron vs astrocyte… 8-9 metabolism

1.2. Synaptic hyperactivity in Alzheimer´s Disease……..... 9-11

1.3. Microbiota…… 11-17

1.3.1. Gut microbiota in Alzheimer´s Disease…… 11-14

1.3.2. Lipopolysaccharide…… 15

1.3.3. Short chain fatty acids…….. 15-17

1.3.3.1. SCFAs in astrocytes…… 17

1.4. Diet…….. 17-20

1.4.1. Healthy diet in Alzheimer´s Disease…….. 17-20

1.5. Transgenic model for Alzheimer´s Disease…… 20-25

1.5.1. 3XTg-AD mice…….. 21

1.5.1.2. Pathological alterations in 3XTG AD mice…….. 22-25

2. Justification…… 26

3. Hypothesis…….. 26

4. General Objective…….. 26

5. Particular objectives…… 27

6. Part 1: Bioactive food abates metabolic and synaptic…… 28-62 alterations by modulation of gut microbiota in a mouse model of Alzheimer's disease

6.1. Materials and Methods…….. 29-41

6.1.1. Experimental design…….. 29-31
6.1.2. Cognitive assessment…… 32-33
6.1.3. Tissue Preparation…….. 33
6.1.4. Immunohistochemistry…….. 33-34
6.1.5. Immunofluorescence…….. 34-35
6.1.6. Image acquisition and analysis…….. 36-37
6.1.7. Western blot…….. 37-38
6.1.8. Fecal microbiota analysis…… 38-40
6.1.9. Lipopolysaccharide analysis…… 40
6.1.10. Short chain fatty acids…… 40
6.1.11. Statistical analysis…… 41
6.2. Results…… 41-62
6.2.1. Body weight and behaviour…….. 41-42
6.2.2. Amyloid Beta (Aβ)…… 42-43
6.2.3. Tau phosphorylation…….. 42-44
6.2.4. Inflammation…… 44-46
6.2.5. Metabolic and synaptic proteins…… 45-50
6.2.6. Gut Microbiota…….. 50-59
6.2.7. Propionate level and FFAR3 in brain…… 59-60
6.2.8. Lipopolysaccharide (LPS) levels in plasma…… 59-60
6.2.9. Levels of short-chain fatty acids in feces of TG at different ages…… 60-62
6.3. Conclusion part I…… 62
7. Part 2: Evaluating the differential effect of short-chain fatty acids on the astrocyte-neuron interaction by use of FRET nanosensors…….. 64-74
7.1. Material and methods…… 64-67
7.1.1. Isolation of astrocytes…… 64
7.1.2. Treatment of astrocyte with short chain fatty acid (propionate and butyrate)…… 64-65
7.1.3. Lactate measurement by colorimetry…… 65

7.1.4. Imaging of astrocytes treated with short chain fatty acid…… 65-66
7.1.5. Genetically encoded Förster Resonance Energy Transfer (FRET) sensors……. 66-67
7.1.6. Statistical analysis…….. 67
7.2. Results……. 67-74
7.2.1. Effect of different concentration of propionate on glucose consumption rate and glucose depletion……. 67-69
7.2.2. Effect of different concentration of butyrate on glucose consumption rate and glucose depletion……. 69-70
7.2.3. Glucose consumption rate in astrocytes treated with 2mM propionate, butyrate and β-Hydroxy butyrate……. 70-71
7.2.4. Glucose depletion rate in astrocytes treated with 2mM propionate, butyrate and β-Hydroxy butrate……. 71-72
7.2.5. Glucose clearance in astrocytes treated with 2Mm propionate, butyrate and β-Hydroxy butyrate……. 72-73
7.2.6. Lactate production in in astrocytes treated with 2Mm propionate and butyrate……. 73-74
7.3. Conclusion part II……. 74-75
8. Discussion……... 76-86
9. General conclusion……... 87
10. Perspectives 87
11. References……. 88-111
12. Appendix……. 112-113

FIGURES AND TABLES

Figure1: Hall marks of Alzheimer's disease, amyloid plaques and neurofibrillary tangles…….. 3
Figure 2. Major Bacterial phyla and their representative genera……. 13
Figure 3. Gut microbiota dysbiosis is associated with many disorders… 13
Figure 4. Alzheimer's disease is associated with alterations in gut microbiome composition……. 14

Figure 5: LPS in the brain…….. 15
Figure 6. Insulin signalling in 3xTg-AD mice…….. 25
Figure 7. Schematic diagram of Experimental design…….. 30
Figure 8. Effect of bioactive food on body weight and spatial memory…. 41
Figure 9. Evaluation of amyloid pathology…….. 43
Figure 10. Tau hyper phosphorylation in TG mice…….. 44
Figure 11. Effect of bioactive food on neuroinflammation in 3xTg-AD mice…….. 46
Figure 12: Effect of bioactive food on hippocampal SIRT1 were region specific……. 47
Figure 13. Effect of bioactive food on SIRT1 in GFAP + astrocytes……. 48
Figure 14. Immunoblots of synaptic proteins…….. 49
Figure 15. Protein levels of pGSK-3β/GSK-3β and pAMPK/AMPK in brain cortex…….. 50
Figure 16. Gut microbiota modifications…….. 51
Figure 17. Gut microbiota modifications in transgenic and its restoration by BF ingestion…… 52-53
Figure 18. Bacterial relative abundance at the class level in WT-AIN, TG-AIN, and TG-BF mice……. 54
Figure 19. Bacterial relative abundance at the order level in WT-AIN, TG-AIN, and TG-BF mice……. 54
Figure 20 Bacterial relative abundance at the family level in WT-AIN, TG-AIN, and TG-BF mice……. 55
Figure 21. Bacterial relative abundance at the genus level in WT-AIN, TG-AIN, and TG-BF mice……. 55
Figure 22. Bacterial products in brain and plasma sample…….. 60
Figure 23: Lactate analysis by colorimetry…….. 65
Figure 24: FRET sensor AAV9-GFAP- FLII12Pglu700mΔ6 for glucose detection…….. 67
Figure 25. Changes in intracellular glucose concentration in control and propionate treated cells on exposure to different stimuli…….. 68

Figure 26. Glucose consumption rate and glucose depletion in astrocytes treated with different doses of Propionate ……... 69

Figure 27. Changes in intracellular glucose concentration in control and butyrate treated cells on exposure to different stimuli…… 70

Figure 28. Glucose consumption rate and glucose depletion in astrocytes treated with different doses of Butyrate…… 70

Figure 29. Glucose consumption rate in astrocytes treated with 2mM propionate, butyrate and β-Hydroxy butyrate (BHB)…… 71

Figure 30. Glucose depletion in the presence of Azide in astrocytes treated with 2mM propionate, butyrate and β-Hydroxy butyrate (BHB)…. 72

Figure 31. Glucose clearance in astrocytes treated with propionate, butyrate and β-Hydroxy butyrate…….. 73

Figure 32. Lactate production in astrocytes treated with propionate, butyrate and β-Hydroxy butyrate (BHB)…… 74

Figure 33: Proposed mechanism by which Bioactive food abates AD pathology…… 83

Figure 34: Proposed mechanism for differential effects of propionate and butyrate on astrocyte-neuron interaction…….. 85

Table 1. Pathological alterations reported in 3xTgAD mice…….. 23

Table-2. Composition of experimental diets (g/kg diet)…… 31

Table-3. List of Primary antibodies and secondary antibodies used in the current study…… 35

Table-4. Taxonomic classification of pyrosequences from bacterial communities at the species level…… 56-57

Table-5. Taxonomic classification of pyrosequences from bacterial communities at the Genus level…… 57-59

Table 6: Levels of short-chain fatty acids in feces of TG at different age…… 61

Table-7. Microbial alterations in AD at phylum level…… 80

Table-8. Microbial alterations in AD …… 81

Abbreviations

AD: Alzheimer´s disease

AKT: Ak strain transforming

AMP: Adenosine monophosphate

AMPK: AMP-activated protein kinase

ANOVA: Analysis of variance

APOE: Apolipoprotein

APP: Amyloid precursor protein

Arc: Activity-related cytoplasmic protein

ASD: Autism spectrum disorders

AT100: Phospho-Tau (Thr212, Ser214) Monoclonal Antibody

ATP: Adenosine triphosphate

BACE1: Beta-secretase

BAM-10: Beta Amyloid Antibody (Monoclonal)

BF: Bioactive food

BHB: Beta hydroxyl butyrate

Bp: Base pair

BSA: Bovine serum albumin

°C: Degree centigrade

CA1: Cornu Ammonis1

Ca^{2+}: Calcium

$CaCl_2$: Calcium chloride

C. elegans: Caenorhabditis elegans

CFP: Cyan Fluorescent Protein

CO2: Carbon dioxide

CoA: Coenzyme A

C. pneumonia: Chlamydiophila pneumonia

Cyto B: Cytochalasin B

CNS: Central nervous system

CX: Cortex

DAB: 3'-Diaminobenzidine

DAPI: 4',6-Diamidino-2-Phenylindole, Dihydrochloride

Decosa hexaenoic acid: DHA

Deoxyribonucleic acid: DNA

EDTA: Ethylenediaminetetraacetic acid

Ent.cx: Entorhinal cortex

FBS: Fatal Bovine Serum

FFAR: Free fatty acid receptor

FRET: Förster Resonance Energy Transfer

GSK-3: Glycogen synthase kinase 3

GC: Gas chromatography

GFAP: Glial fibrillary acidic protein

g/kg: Grams per kilograms

GM: Gut microbiota

Glu: Glutamate

Glu-Gln: Glutamate-glutamine

GLUR1: Glutamate Receptor Subunit 1

H_2O_2: Hydrogen peroxide

HCl: Hydrochloric acid

HEPES: 4-(2-hydroxyethyl)-1-piperazineethanesulfonic acid

Iba-1: Ionized calcium binding adaptor molecule 1

IgG: Immunoglobulin G

IL-1β: Interleukin 1 beta

IR: Insulin receptor

lRβ: Insulin receptor beta:

Kcal/g: kilocalories per gram

KCl: Potassium chloride

LPS: Lipopolysaccharides

MDA: Malondialdehyde

MEM: Minimum Essential Medium

$MgCl_{2:}$ Magnesium Chloride

mL/min: Millilitre per minute

mM: Mllimolar

mm^2: Milli meter square

mmol/L: Milimoles per liter

MS: Mass Spectrophotometry

MSD: mass spectrometric detector

NaCl: Sodium Chloride

NAD: Nicotinamide adenine dinucleotide

NADH: Nicotinamide adenine dinucleotide hydrate

$NaHCO_{3:}$ Sodium bicarbonate

NMR: Nuclear magnetic resonance

ORAC: Oxygen radical absorbance capacity

OTUs: Operational taxonomic units

p-IRβ: Phospho insulin receptor beta

p-AKT: Phospho Ak strain transforming

PBS: Phosphate buffered saline

PCoA: Principal coordinate analysis

PDK1: Phosphoinositide-dependent kinase-1

PFC: Prefrontal cortex

PGC-1α: Peroxisome proliferator activator receptor gamma-coactivator-1 Alpha

P-GSK3: Phospho Glycogen synthase kinase 3

PI3-K: Phosphoinositide-3 kinase

PPARγ: Peroxisome proliferator-activated receptor gamma

p-PDK: 1Phospho phosphoinositide-dependent kinase-1

PS1: Presenilin

PSD-95: Postsynaptic density-95 protein

PVDF: Polyvinylidene difluoride

QIIME: Quantitative Insights into Microbial Ecology

SCFAs: Short-chain fatty acids

S.D: Standard deviation

SDS-PAGE: Sodium dodecyl sulfate–polyacrylamide gel electrophoresis

S.E.M: Standard error of the mean

Ser: Serine

SIRT1: Sirtuin 1

SREBP: Sterol regulatory element-binding proteins

St.: Striatum

3xTg-AD: Triple transgenic Alzheimer's disease

T2D: Type 2 diabetes

TBS-T: Tween

TCA cycle: Tricarboxylic acid cycle

TG: Transgenic

TG-AIN: Transgenic group with control AIN diet

TG-BF: Transgenic group with bioactive food

TNF-α: Tumor necrosis factor-alpha

Thr: Threonine

WT: Wild type

WT-AIN: Wild type group with control AIN diet

W/W: Weight by weight

YFP: Yellow fluorescent protein

5Xfad: 5x-Familial Alzheimer's disease

Resumen

Investigaciones recientes resaltan el papel de la microbiota intestinal (MI) en la patogénesis de la enfermedad de Alzheimer (EA). La MI puede modular la salud del hospedero mediante la liberación de sustancias como los lipopolisacáridos (LPS) y los ácidos grasos de cadena corta (AGCC), entre otros. La dieta es capaz de modificar la composición y diversidad de GM, y se ha reportado que la ingesta de una dieta saludable disminuye el riesgo de desarrollar demencia y EA. La ingesta de alimentos funcionales (AF) disminuye la neuroinflamación y el estrés oxidativo en ratas obesas, asociado con cambios en la MI. El objetivo de esta tesis fue delinear el mecanismo de acción de la ingesta de AF en la patología de EA, utilizando un modelo transgénico para la EA. En una primera parte, ratones 3xTg transgénicos (TG) hembra se alimentaron con una combinación de nopal, proteína de soya, aceite de chía y cúrcuma durante 7 meses, seguido de pruebas de memoria y análisis histológicos/bioquímicos. La ingesta con AF mejoró la memoria de trabajo, reduciendo los agregados amiloides y la hiperfosforilación de tau. Se observó una disminución en los niveles de MDA, número de astrocitos y microglia activa, y de proteínas asociadas con la actividad sináptica y metabólica en muestras de cerebro. Así mismo la abundancia de bacterias pro-inflamatorias, LPS y propionato se vió reducida. Dado que el propionato es una sustancia neurotóxica que puede ser utilizada como sustrato energético por los astrocitos, decidimos explorar el efecto de los AGCC sobre el metabolismo astrocítico en un cultivo celular. En una segunda parte, se infectaron cultivos mixtos neurona/astrocito con nanosensores FRET y se incubaron con propionato o butirato. Se observó que el propionato genera un incremento en el aclaramiento, consumo, y agotamiento de glucosa, sin modificar los niveles de lactato. Por el contrario, el tratamiento con butirato disminuye el aclaramiento, consumo y agotamiento de glucosa, además de disminuir los niveles de lactato. En resumen, la ingesta de AF en ratones TG logró disminuir la presencia de marcadores patológicos de la EA. Estos efectos fueron acompañados por cambios en la MI y las sustancias bacterianas (LPS y propionato). Los AGCC modulan de manera diferencial el metabolismo glucolítico. Los datos colectados en esta tesis permiten proponer que la ingesta de AF puede representar una estrategia terapéutica contra la EA al modificar la MI y sustancias neurotóxicas.

ABSTRACT

Recent investigations have demonstrated an important role of gut microbiota (GM) in the pathogenesis of Alzheimer´s disease (AD). GM modulates host's health and disease by production of several substances, lipopolysaccharides (LPS) and short-chain fatty acids (SCFAs), among others. Diet can modify the composition and diversity of GM, and ingestion of a healthy diet has been suggested to lower the risk to develop dementia and AD. Bioactive food (BF) can abate neuroinflammation and oxidative stress in obese rats, an effect associated with GM composition. In this thesis, we aim to delineate the mechanism of action of BF and released substances in AD pathology. In the first part, we fed triple transgenic 3xTg-AD (TG) female mice with a combination of dried nopal, soy protein, chia oil and turmeric for 7 months, followed by behavioral and histological/biochemical examination. We found that BF ingestion in TG mice improved cognition and reduced Aβ aggregates and tau hyperphosphorylation. In addition, BF decreased MDA levels, astrocyte and microglial activation, synaptic and metabolic proteins in brain samples. BF ingestion was able to reduced pro-inflammatory bacteria, LPS and propionate levels to WT values. As propionate is a well-known neurotoxic substance, we aimed to determine if propionate could modify astrocyte metabolism and activation in an *in-vitro* model. In a second part, we evaluated the differential effect of propionate and butyrate on the astrocyte-neuron interaction. We infected mixed neuron/astrocytic culture with FRET sensor. We observed that propionate increased glucose clearance, glucose consumption and glucose depletion in astrocytes, whereas no changes were observed in lactate concentration. On the contrary, butyrate decreased glucose clearance, consumption and depletion, accompanied by reduced lactate production control cells. In summary, ingestion of BF in a TG mice model diminished the pathological markers of AD, reduced neuroinflammation, and improved working memory. Importantly, BF´s effects were accompanied by restoration of GM and their released substances (LPS and propionate). Propionate and butyrate modulated the astrocyte-neuron lactate shuttle differentially, altering glycolysis in astrocytes. Based on the present data we propose that a dietary intervention in early stage of AD is an effective strategy to abate amyloid pathology, metabolic and synaptic alteration by modulating the gut-brain axis, resulting in improved cognition.

INTRODUCTION:

Alzheimer's disease (AD) is a chronic degenerative brain disease and the most common cause of dementia (Wilson et al., 2012). AD is an age related disease, and it is becoming markedly more common with the aging of the world's population. Globally, after the age of 65 years, the incidence rate of AD doubles every 5 years. In 2016, there were more than 46 million people worldwide with dementia, and this number is expected to increase to over 115 million by 2050. Given the heavy economic and social burdens of AD, major emphasis is being placed on understanding its pathogenesis and developing early diagnosis and effective intervention (Sun et al., 2018).

There is no single test for detecting AD. Physicians rely on obtaining a medical and family history, asking a family member about changes in thinking skills and behaviour and conducting cognitive tests, blood tests and brain imaging to find out if the individual has high levels of Aβ (Weller and Budson, 2018). Individuals with AD experience multiple symptoms and the pace at which symptoms advance from mild- to moderate- to severe varies from person to person. In the mild-stage, most people are able to function independently in many areas but are likely to require assistance. In the moderate-stage, individuals may have difficulty performing routine tasks, become confused and start having personality and behavioural changes. In the severe-stage, individuals require help with basic activities of daily living (Alzheimer's Association, 2017).

Women are more at risk to have AD and other dementias. Two thirds of Alzheimer's patients in United States are women. According to 2018 AD Facts and Figures of the 5.7 million people age 65 and older with AD in the United States, 3.4 million are women and 2 million are men. According to the Alzheimer's Association, in population age 71 and older, 16 percent of women have AD and other dementias compared with 11 percent of men (Grabher, 2018).

The pathological hallmark of Alzheimer's are the progressive accumulation of the extracellular senile plaques composed of amyloid-beta peptide (Aβ). Amyloid precursor protein (APP) is cleaved sequentially by β-secretase and γ-secretase to

generate Aβ. The length of Aβ varies at C-terminal according to the cleavage pattern of APP. The Aβ 1–40 isoform is the most prevalent, followed by Aβ 1–42. Aβ assemble and polymerizes into fibrillar, protofibers and polymorphic oligomers (Serrano-pozo et al., 2011; Barage and Sonawane, 2015; Sun et al., 2018). On the one hand, misfolded and aggregated proteins are recognized by astroglia and microglia cells and trigger an innate immune response, characterized by the release of inflammatory cytokines and neuroinflammation, which contribute to disease progression and severity (Clark and Vissel, 2015; Heneka et al., 2015). On the other hand, it has been postulated that soluble Aβ may cause neuronal membrane damage, producing reactive oxygen and nitrogen species (Lauderback et al., 2001). This oxidative damage would alter synaptic membrane structure, causing alterations in dendritic spines with a subsequent cognitive decline. Other hallmark of AD is the intracellular neurofibrillary tangles: it contains hyper-phosphorylated tau protein. Tau proteins are mainly found in neurons. They play an important role in microtubule assembly and stabilization of neuronal microtubules network. The loss of normal tau function affect normal cellular functions of neurons (Serrano-pozo et al., 2011; Barage and Sonawane, 2015; Sun et al., 2018). Under pathological conditions the hyperphosphorylation of tau proteins results in paired helical filaments and straight filaments called neurofibrillary tangles.

AD can be classified into types: Early-onset familial AD and Late-onset sporadic AD. Early-onset familial AD is usually caused by autosomal dominant mutations in the genes for APP, presenilin 1 and presenilin 2. This form of AD accounts for approximately 2–5% of all AD cases. This is a condition characterized by dementia onset at a relatively young age, before 65 years of age (Wu et al., 2012). Late-onset sporadic AD is the most common form of the disease, which happens to people age 65 and older. Majority of AD cases (>93%–95%) are of the sporadic type.

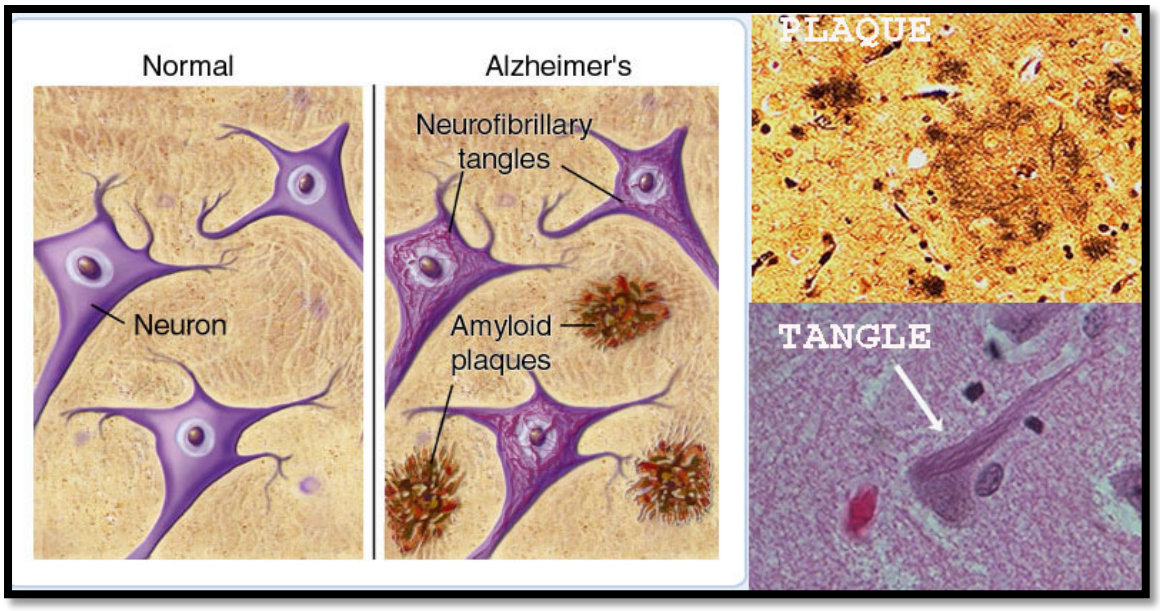

Figure1: Hallmarks of Alzheimer's disease, amyloid plaques and neurofibrillary tangles (Taken from Bright Focus Foundation website)

There are many risk factors associated with Late-onset AD. They can be divided into two categories, modifiable and non-modifiable risk factors. Example of non-modifiable risk factors are age, gender, family history, and genetics. Age is the greatest risk factor for developing Late-onset-AD, while carrying the E4 allele of apolipoprotein (APOE4) is the most important genetic risk factor for this condition (Flamier et al., 2018). ApoE is the major carrier of cholesterol in the CNS and also has important roles in Aβ metabolism, aggregation and deposition. Increased plaque deposition has been observed in APOE e4-positive individuals and in APOE e4 knock-in animal models of cerebral beta-amyloidosis (Zetterberg and Mattsson, 2014). Having a family history of AD is also a non-modifiable risk factor to develop the disease. Individuals who have a parent or siblings with AD are more likely to develop the disease than those who do not have a first-degree relative with Alzheimer's. Those who have more than one first-degree relative with Alzheimer's are at even higher risk (Grabher, 2018).

On the other hand, modifiable risk factors associated with AD are obesity, diabetes mellitus, high total cholesterol, hypertension, asymptomatic cerebral infarction, **diet** and lifestyle. Obesity in the middle age is a risk factor for AD, whereas several analytical studies in the elderly suggested that a significant decrease in BMI was associated with a higher risk of AD in the following 5-6 years (Povova et al., 2012).

Presence of diabetes in middle age or a longer duration of diabetes may play a key role in the development of AD. AD shares many age-related pathophysiological features of type 2 diabetes (T2D). These include insulin resistance and disrupted glucose metabolism in non-neural tissues. Epidemiologic studies shows that AD risk is increased 50%–100% by diabetes including T2D. Of the shared features of AD and T2D, the one most likely to be an etiological factor in AD is insulin resistance. Peripheral insulin resistance promotes AD onset by reducing brain insulin uptake and by raising brain levels of Aβ, tau phosphorylation, oxidative stress, pro-inflammatory cytokines, advanced glycation end products and apoptosis (Talbot et al., 2012).

All this information indicates that pathogenesis of AD is very complex and multifactorial, involving several molecular, cellular and physiological alterations culminating in the aggregation of proteins and neuronal functional impairment.

Current drug development pipelines of most of pharmaceutical companies' targets the alleviation of the main AD pathological hallmark (Aβ aggregation). However, in the following sub-chapters we will describe several metabolic and synaptic alterations observed in AD, even since early stages of the disease can be valid therapeutic targets in drug efficacy studies.

1.1 METABOLIC ALTERATIONS IN ALZHEIMER´S DISEASE

Recently, focus has been paid on the metabolic alterations present since early stages of AD, such as a marked cerebral hypo-glucose metabolism (Tong et al., 2014). Several studies indicate that a reduced brain glucose metabolism correlates with AD symptoms severity. Furthermore, *in vitro* and *in vivo* pre-clinical AD models show deficits in mitochondrial function, metabolic enzyme-expression and -activity before the onset of clinical symptoms (Swerdlow and Khan, 2004; Ding et al., 2013). Here we describe some of these metabolic alterations with more detail.

1.1.1 Insulin resistance

Insulin plays important role in regulating energy metabolism, survival, growth and differentiation of neurons. It participates in synaptic plasticity through activation of phosphoinositide-3 kinase (PI3-K) signalling. Insulin activates the insulin receptor (IR) which is followed by the activation of the IR substrate proteins, which further

activates the PI3-K/Akt and the Ras/mitogen-activated kinase cascades. IR's are widely present in neuronal soma and it is enriched in synaptic terminals of neurons. They regulate neurotransmitter release and receptor recruitment to promote the establishment of long-term potentiation. IR can be detected in hippocampus, hypothalamus, cortex and amygdala (Calvo-ochoa and Arias, 2015).

As described earlier, diabetes is a risk factor for AD. Moreover, insulin resistance is not limited to peripheral tissues in AD patients. Alterations in insulin signalling molecules have been reported in AD cases (Neth and Craft, 2017). In AD, the brain becomes insulin resistant, promoting key pathophysiological events as cognitive deficits, Aβ deposition and tau phosphorylation (Dineley et al., 2014) .

Insulin resistance and glucose metabolism have also been reported in animal model for AD (Chen et al., 2014; Macklin et al., 2016). In APP/PS1 transgenic mice, glucose tolerance and insulin sensitivity are impaired much prior to amyloid plaque pathogenesis and cognitive decline (Macklin et al., 2016).

The findings of impaired brain insulin signalling (Steen et al., 2005; Moloney et al., 2010; Liu et al., 2011; Talbot et al., 2012) and deficient brain glucose metabolism in AD (Hoyer, 2004), suggest that brain insulin deficiency contributes to the pathogenesis of AD. Furthermore, administration of intranasal insulin has been shown to improve memory in AD patients and those at high risk of developing AD (Mild-Cognitive Impairment) (Talbot et al., 2012). However, clinical trials with insulin administration request proven efficacy in early stages of the disease, as once the brain insulin machinery is impaired no beneficial effects can be achieve (Chapman et al., 2018).

Glycogen synthase kinase 3 (GSK3), is a Ser/Thr kinase, and as its name refers it is involved in glycogen metabolism. GSK3 also is involved in the insulin signalling, cell proliferation and neuronal function. Some of the key molecules mediating GSK3 functions are glycogen synthase, tau protein and beta catenin proteins (Rayasam et al., 2009). GSK3 deficiencies have been related to AD, as this an important tau-kinase that induces the hyper-phosphorylation of tau and the formation of neurofibrillary tangles. GSK3 transgenic mice display tau hyper-phosphorylation and neurodegeneration (Hooper et al., 2008). AD patients have been shown to have an increase in GSK3β activity that correlates with an increase in neuronal death

(Maixner and Weng, 2014). In addition, APP/PS1 mice present a decreased p-GSK3β/ GSK3β ratio (Varamini et al., 2013). This body of data indicates that in AD there are important insulin and metabolic alterations as described below (Jolivalt et al., 2016).

1.1.2 Metabolic alterations in Alzheimer´s Disease

Cells adapt to changes in energy status through the modulation of AMP-activated protein kinase (AMPK) and NAD+-dependent deacetylase Sirtuin (SIRT1) pathways so as to maintain energy homeostasis. AMPK and SIRT1functions as a sensor of cellular energy status, and as master regulators of metabolism (Fulco and Sartorelli, 2008). Here we further describe the role of those metabolic sensors in relation to AD.

1.1.2.1 AMPK in Alzheimer´s Disease

AMPK is activated upon alterations in the cellular AMP/ATP ratio. AMPK is a serine/threonine protein kinase composed of a catalytic α subunit, and regulatory β and γ subunits. Increases in AMP/ADP concentration activates AMPK via allosteric regulation. Several upstream kinases, e.g. serine/threonine kinase, Ca2+/calmodulin-dependent protein kinase β and transforming growth factor-activated kinase 1 can activate AMPK by phosphorylating the catalytic β subunit at Thr172 (Vingtdeux et al., 2010).

Many physiological and pathological conditions appear to stimulate AMPK signalling. Activation of AMPK switches on catabolic pathways to produce ATP, while simultaneously shutting down energy-consuming anabolic processes. In order to perform these actions, AMPK regulates metabolic enzymes through a direct phosphorylation (Cantó and Auwerx, 2009). Currently, AMPK is viewed as an important pharmacological target since it is believed that novel AMPK activators may be useful in the therapy of metabolic and neurodegenerative diseases (Salminen and Kaarniranta, 2012). Hippocampal tissue from post-mortem human AD patients showed increased AMPK phosphorylation compared with age-matched controls. Similar results were seen in hippocampal slices from 10- to 12-month-old APP/PS1 mice (Ma et al., 2014). Thus, AMPK dysfunction can be viewed as a marker of metabolic alterations in AD.

1.1.2.2 Sirtuin (SIRT1) in Alzheimer´s Disease

Sirtuin-1 (SIRT1), is one of the seven mammalian homologues belonging to the sirtuin family (Bonda et al., 2011). SIRT1 function as NAD+ dependent protein deacetylase and /or ADP- ribosylases (Sidorova-darmos et al., 2014). It is a regulator of genes and proteins involved in gene transcription (PGC-1), insulin response (IGF-1), anti-inflammatory response (NFκB), antioxidant response (FOXO3) and anti-apoptotic response (p5314 and FOXO3) (Bonda et al., 2011).

SIRT1 increase the activity and production of α-secretase, which is an enzyme responsible for the non-amyloidogenic cleavage of APP. Upregulation of α-secretase reduces pathological accumulation of the toxic Aβ species that results from β- and γ-secretase activity (Tippmann et al., 2009). Aerobic glycolysis involves a gradual decrease of NAD+ reserves in the cell through increased NADH production (Zhang et al., 2007; Nakahata et al., 2012). The reliance of neurons on aerobic glycolysis, inhibits NAD+ dependent SIRT1 activity through the depletion of NAD+ pools and thus results in a shift in APP processing toward an amyloidogenic pathway (Bonda et al., 2011). Reduction of SIRT1 desacetylating action in AD brain could decrease the capacity of acetyl-CoA synthetase to generate acetyl-CoA, a key molecule in cellular metabolism. Significant reduction of SIRT1 has been observed in the parietal cortex of AD patient (Julien et al., 2009). Levels of SIRT1 protein and mRNA were significantly decreased in the brains of the APP/PS1 mice at 6 months and 10 months of age (Dong et al., 2018). Furthermore, transgenic mice that overexpress SIRT1 display improved glucose homeostasis and increased metabolic rates, both this two processes being beneficial in AD (Julien et al., 2009). Therefore, SIRT1 dysregulation may be associated with neuronal dysfunction in AD.

All cells express SIRT1, however, few is known about the roles and modulation of SIRT1 on other brain cells. It has been reported that senescence of microglia is accompanied by reductions in SIRT1 expression (Cho et al., 2015). On the contrary, decreased SIRT1 in astrocytes has been associated with improved neuronal support after treatment with Aβ (Aguirre-Rueda 2015). Thus, content and activity of SIRT1 will affect differently neurons, astrocyte and microglia cells.

1.1.3. Mitochondrial dysfunction in Alzheimer´s Disease

In central nervous system (CNS), mitochondria provides appropriate energetic needs to maintain resting and action potentials, as well as to modulate synaptic plasticity (Dietrich et al., 2008). There is an increased mitochondrial number during synapse formation and in response to local electrical stimulation (Li et al., 2004). Mitochondrial dysfunctions have been widely implicated in the pathogenesis of many neurodegenerative diseases (Riemer and Kins, 2012), and it remains a prominent feature in AD (Swerdlow and Khan, 2004). In AD, there is an abnormal mitochondrial dynamics (mitochondrial fragmentation and abnormal distribution) (Du et al., 2010; Carvalho et al., 2012) and decreased levels of mitochondrial enzymes involved in the oxidative metabolism, such as pyruvate dehydrogenase complex, lactate dehydrogenase and hexokinase (Ding et al., 2013). Peroxisome proliferator activator receptor gamma-coactivator 1 α (PGC-1α), is a transcriptional coactivator that regulates genes involved in energy metabolism and mitochondrial biogenesis (Lin et al., 2002) decreased along with AD severity (Robinson et al., 2014). Here we describe in more detail what is currently known about PGC-1α in AD.

1.1.3.1. Peroxisome proliferator activator receptor gamma-coactivator 1 α (PGC-1α)

PGC- 1α is expressed mainly in mitochondria and in the nucleus of neurons. PGC-1α is involved in the formation and maintenance of synapses in developing hippocampal neurons, as in the maintenance of synapses in the adult hippocampus (Cheng et al., 2012). PGC-1α expression promotes the non-amyloidogenic processing of APP by decreasing the generation of amyloidogenic Aβ peptides (Qin et al., 2009). On the other hand, PGC-1α decreases Aβ generation by activating PPARγ (Katsouri et al., 2016). PPARγ and PGC-1α complex decreases transcription, expression, and activity of BACE1 (Katsouri et al., 2014). A recent study reports changes in the levels of PGC-1α in samples of AD patients according to the severity of the dementia, involving damage to mitochondrial biogenesis (Robinson et al., 2014).

1.1.3.2. Metabolic alterations at cellular level: Neuron vs astrocyte metabolism in Alzheimer´s Disease

Glucose is the primary energy substrate of the adult brain. Glucose can be metabolized by glycolysis and oxidative metabolism in the brain. In glycolysis glucose is processed to pyruvate and then lactate producing two molecules of ATP. Oxidative metabolism is characterized by full oxidation of glucose or of its metabolites, such as pyruvate and lactate, in the mitochondria, resulting in the production of approximately 30–36 molecules of ATP per glucose molecule (Magistretti and Allaman, 2015).

In the brain there are cell - specific metabolic profiles. Early studies in isolated neurons and astrocytes revealed that neurons are more dependent on oxidative metabolism, whereas astrocytes are more dependent on glycolysis (Magistretti and Allaman, 2018). This mean that astrocytes rely primarily on the ATP generated through glycolysis, followed by the release of lactate to the extracellular space. Lactate released from astrocytes is taken up by neurons and serves as a key metabolite for neuronal aerobic metabolism to meet the high energetic demands of neurons (Natarajaseenivasan et al., 2018). This is known as the neuron – lactate – shuttle (Magistretti and Allaman, 2018).

Recent reports indicates that in AD there is a decline in neuronal glucose transport and metabolism followed by decline in mitochondrial function (Ding et al., 2013). Moreover, in diseases with an inflammatory component, astrocytes become activated increasing their own metabolic demand neglecting neuronal metabolism (Natarajaseenivasan et al., 2018). Therefore, alterations in astrocyte function have been associated with metabolic alterations detected since early stages of AD (Haim et al., 2015).

1.2 SYNAPTIC HYPERACTIVITY IN ALZHEIMER´S DISEASE

AD was presumed to be characterized by synaptic failure due to significant decrease in neuronal activity in brain circuits. In prodromal AD states, loss of synaptic contacts is one of the main morphological alterations observed in hippocampus and cortex. However, recent studies revealed a complex picture, characterizing a mix of neuronal hypo- and hyper-activity, leading to cellular defects in various brain regions (Busche et al., 2008; Palop and Mucke, 2010). In addition, data obtained from clinical and preclinical studies have observed the presence of non-convulsive epileptic patterns (Noebels, 2011), as well as cerebral hyperactivity long before

amyloid plaques are detected (Busche et al., 2008). Functional and anatomic magnetic resonance imaging reveal a higher activation in the hippocampus and cortex of human subjects at high risk for developing AD, such as pre-symptomatic carriers of familiar AD-linked genes (Quiroz et al. 2012), APOE-epsilon4 allele carriers (reviewed in Bookheimer and Burggren, 2009), or subjects with mild cognitive impairment (e.g., Bakker et al. 2012, Celone et al., 2006; Dickerson et al., 2004, 2005; Filippini et al. 2009, Kim et al., 2012). Moreover, various studies reported that AD patients are at increased risk of unprovoked seizures (Amatniek et al. 2006; Noebels 2011). Moreover, different animal models of AD also show the presence of non-convulsive epileptic patterns in dentate gyrus (Palop et al., 2005) accompanied by a loss of interneurons in the same region (Palop et al., 2007). Dendritic spines are protrusions from a dendrite's shaft, where neurons form synapses to receive and integrate information. Dendritic spines are the morphologic correlates of excitatory post synapses. A number of specialized synaptic proteins, including scaffolding proteins and ion channels, are clustered at dendritic spines (Dorostkar et al., 2015). As mentioned before, AD is associated with a progressive loss of synapses and neurons. However, animal models indicate that morphological alterations of dendritic spines precede synapse loss. Indicating that alterations in spine morphology could be involved in the early cognitive deficits associated with AD (Androuin et al., 2018).

Postsynaptic density-95 protein (PSD-95), is the major scaffold protein of the dendritic spines that facilitates the anchorage of membrane receptors in the spines, modulates trafficking and localization of adhesion molecules, ion-channels and glutamate receptors (Savioz et al., 2014). PSD-95 is involved in the regulation of the ratio of excitatory versus inhibitory presynaptic contacts through neuroligin-dependent pathways, suggesting that PSD-95 is involved in network activity (Arsenault et al., 2011). Contradictory data have been reported about PSD-95 expression in aging and AD. PSD-95 has been reported to vary according to regions in AD patient versus controls increasing in the frontal cortex in an early stage, and decreasing in the temporal cortex (Savioz et al., 2014). In aged-learning-impaired rats, PSD95 levels were selectively increased (Nyffeler et al., 2007). This increase could be because PSD-95 might be possibly involved in reactive and/or

compensatory mechanisms during aging/AD progression before the occurrence of important synaptic elimination (Savioz et al., 2014).

Pre-synaptic proteins like synaptophysin and post -synaptic proteins like Activity-related cytoplasmic protein (Arc) and GLUR1 have been also reported to be altered in AD (Mucke et al., 2000; Eder et al., 2002; Arsenault et al., 2011; Perez-Cruz et al., 2011a). Arc is involved in the process of long-term memory formation (Bramham et al., 2010) and in the activity-dependent Aβ production (Wu et al., 2011). Enhanced Arc levels are observed in hippocampus of different transgenic mice strains compared to wild-type mice, even before plaque deposition (Perez-Cruz et al., 2011b). Thus, synaptic hyperactivity seems to predominate in early stages of AD, becoming hypoactive as disease progresses.

1.3 MICROBIOTA IN ALZHEIMER´S DISEASE:

Microbiota are all microorganism living in our intestine (Vinolo et al., 2011). Microbiota include all taxonomic domains as fungus, protozoan, virus and bacteria. Gut microbiota (GM) is the microbiota residing in our intestine, and ninety percent of all GM is mainly composed of bacteria (Ursell et al., 2013). GM have important functions on health and disease of the host and alterations in GM have been associated with development of chronic degenerative diseases (i.e. DT2, obesity, etc) (Baothman et al., 2016). Recently, several groups of research have highlighted the fact that AD patients present a high incidence of infectious disease. Infection agents comprised fugal, protozoan, viral and bacterial (Bu et al., 2014). A recent study found a positive association between infection burden and AD (Itzhaki et al., 2017). Increased infectious burden was related to higher serum levels of inflammatory cytokines and serum Aβ markers in AD patients (Miklossy, 2011). These observation leads to suggest a strong link between AD and microbial infections.

1.3.1 Gut microbiota (GM) alterations in Alzheimer´s Disease:

The human gut consists of approximately 1 kg of bacteria, and the number of bacterial genes in the gut is approximately about 9.9 million (Li et al., 2017). Two types of bacteria are present in the healthy human gut, as symbiotic agents with health promoting effects (called commensal bacteria that have no damaging effect on host), and pathobiont bacteria (with negative effect on the host as they may

induce pathology) (Szablewski, 2018). A delicate balance exist in the GM composition, while an imbalance in this composition is commonly known as *dysbiosis* (Yang et al., 2016). Gut dysbiosis leads to pathophysiological consequences such as inflammatory bowel disease, irritable bowel syndrome, coeliac disease, allergy, asthma, metabolic syndrome, cardiovascular disease, and obesity, among others (Carding et al., 2015). The composition of GM depends on various factors, such as the method of delivery, diet, use of drugs, probiotics, prebiotics, as well as age, sex, geographical area, and microflora transplantation (Szablewski, 2018).

GM is very diverse, but it is mainly dominated by four phyla: Firmicutes, Bacteroidetes, Actinobacteria and Proteobacteria (Yang et al., 2016). Firmicutes (60–80%, Gram positive bacteria with more than 200 genera of which the most important are: *Ruminococcus, Clostridium, Eubacterium, Lactobacillus, Faecalibacterium, Roseburia, and Mycoplasma*) and Bacteroidetes (20–30%, Gram-negative bacteria with genera *Bacteroides, Prevotella, and Xylanibacter*) are the main GM phyla. In minor proportions are the following phyla: Actinobacteria (<10%, Gram-negative bacteria with genera *Bifidobacterium*), Proteobacteria (<1%, Gram-negative bacteria with genus *Escherichia, Desulfovibrio, and Enterobacteriacae*), and Verrucomicrobia (with genus *Akkermansia, Fusobacteria, and Cyanobacteria*) (Szablewski, 2018).

Major Bacteria Phyla and Genera Predominating in Human Gut Microbiota

Phyla	Representative genera
Firmicutes (60-80%)	– Ruminococcus – Clostridium – Lactobacillus – Enterococcus
Bacteroidetes (20-30%)	– Bacteroides – *Prevotella* – *Xylanibacter*
Actinobacteria (< 10%)	– Bifidobacterium
Proteobacteria ((< 1%)	– *Escherichia* – *Enterobacteriaceae*

Munoz-Garach A, Diaz-Perdigones C, Tinahones FJ.
Microbiota y diabetes mellitus tipo 2. Endocrinol Nutr. 2016;63:560---568.

Figure 2. Major Bacterial phyla and their representative genera (Taken from Munoz-Garach 2016).

Importantly, recent studies have demonstrated a significant association between GM composition and the structure and function of the enteric and CNS, including human behaviour and brain regulation (Carabotti et al., 2015; Zhu et al., 2017).

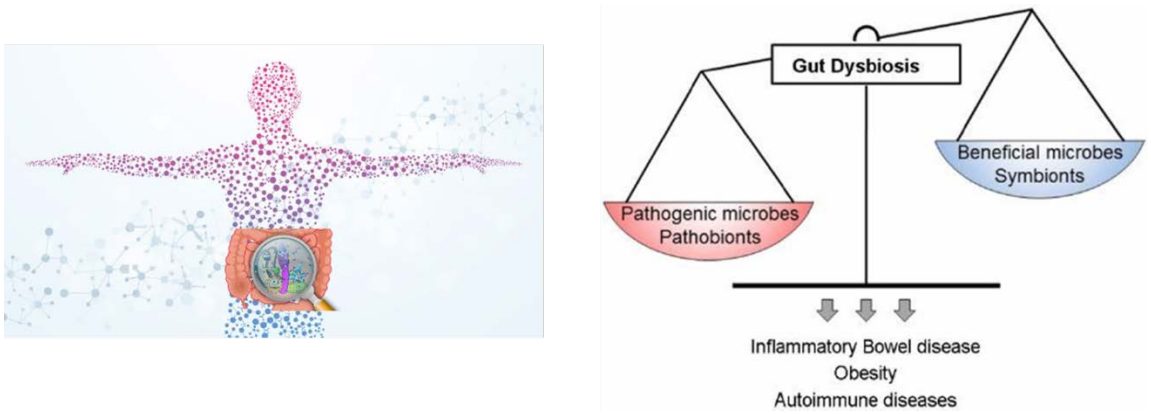

Figure 3. Gut microbiota dysbiosis is associated with many disorders (Taken from brisbanenaturopaths.com)

Moreover, increasing evidence suggests that GM contributes to the physiopathology of AD (Bonfili et al., 2017; Brandscheid et al., 2017; Harach et al., 2017; Vogt et al., 2017; Zhang et al 2017). Moreover, it has been suggested that AD pathology may be modulated by the gut-brain-axis (Jiang et al., 2017).. However, it is still not clear which factors may be associated with this bidirectional communication. More detailed information will be discuss later in Discussion Chapter

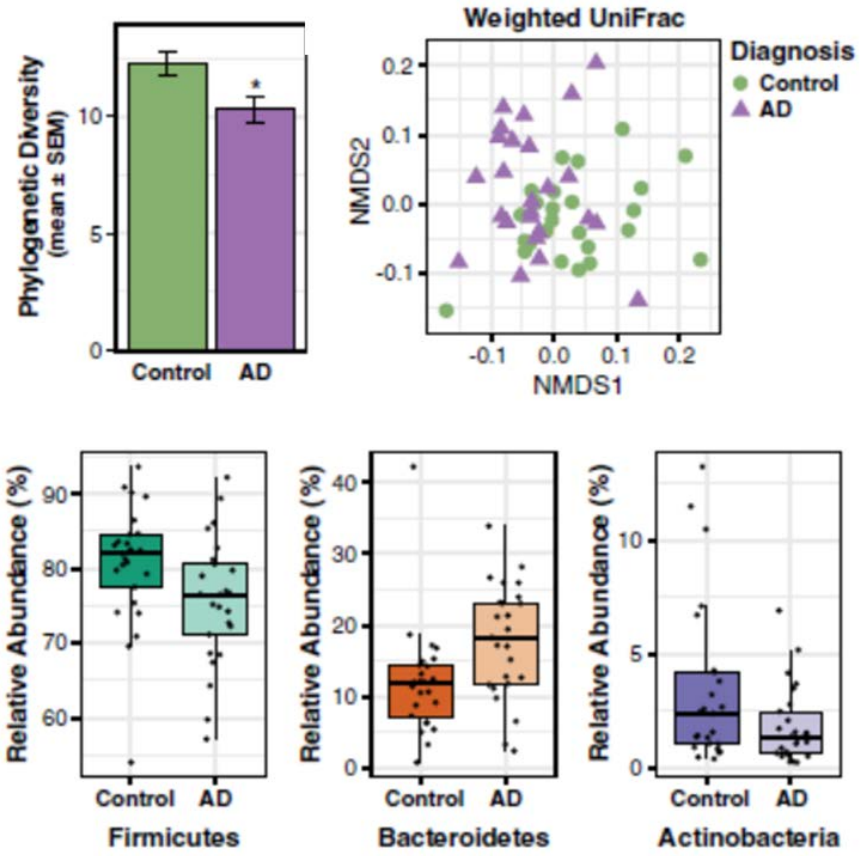

Figure 4. Alzheimer's disease is associated with alterations in gut microbiome composition. (A) Faith's Phylogenetic Diversity is decreased in the microbiome of AD participants. *p<0.05. (**B**) Non-metric multidimensional scaling (NMDS) plot of weighted UniFrac analysis of relative sample OTU composition. NMDS analysis was limited to two dimensions, with a stress measurement of 0.17. Each dot represents a scaled measure of the composition of a given participant, color- and shape-coded by cohort. (**C**) Differential abundance analysis identified 14 OTUs that were increased and 68 OTUs that were decreased in AD relative to Control participants (p < 0.05, FDR-corrected). Each point represents an OTU (taken from **Vogt et al., 2017).**

1.3.2 Lipopolysaccharides (LPS):

LPS are components of the outer membrane of Gram-negative bacteria (Tlaskalová-hogenová et al., 2004). LPS plays key roles in host– pathogen interactions of the innate-immune system (Hill and Lukiw, 2015; Zhao et al., 2015a; Maldonado et al.,

2016) Alterations in GM composition/abundance are associated with enhance plasma levels of LPS (Avila-nava et al., 2016; Sánchez-Tapia et al., 2017) which may result in an exacerbated metabolic endotoxemia, that initiates obesity, insulin resistance and inflammation (Cani et al., 2007). LPS is a well-known neuroinflammatory agent driving the generation Aβ 1-42 (Lee et al., 2008; Asti and Gioglio, 2014; Hill and Lukiw, 2015; Zhao et al., 2015a)

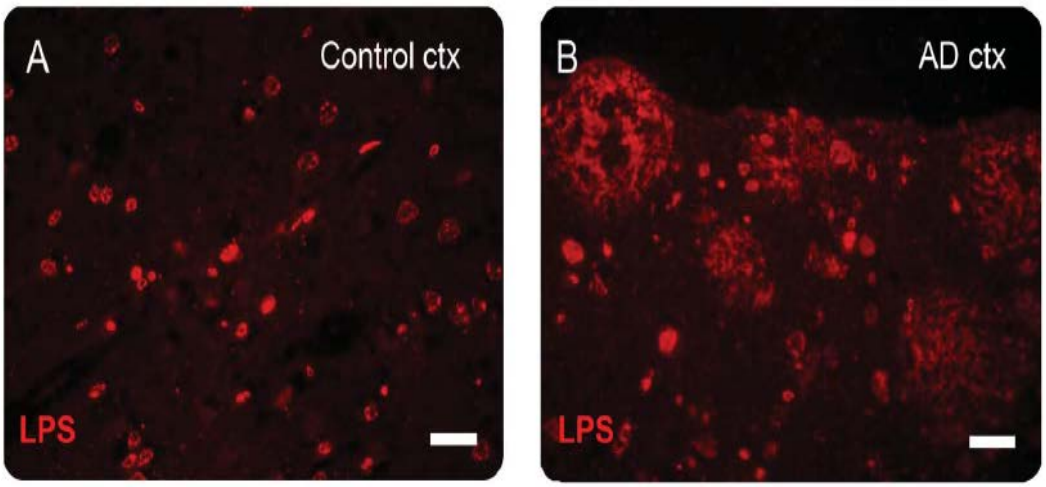

Figure 5: LPS in the brain showed staining in both control (A) and Alzheimer disease (AD) brains (B) in gray matter (GM (taken from Zhan et al., 2016).

LPS administration to mice results in memory impairment, Aβ aggregation and astrocyte activation (Lee et al., 2008). Notably, LPS can be detected in parenchyma and blood vessels of non-demented aged and AD brain samples, but LPS levels were greater in diseased subjects (see Figure 4) (Zhao et al., 2015b, 2017; Zhan et al., 2016).

1.3.3 Short chain fatty acids (SCFAs):

SCFAs are produced by the GM after the degradation of non-digestible polysaccharides, being butyrate, acetate, and propionate the more abundant fermentation products (Wong et al., 2006). Acetate is produced in the highest quantity as a result of fermentation in the large intestine, followed by propionate and butyrate (Hoyles et al., 2018). It has been reported that human GM produces 50–100 mmol/L per day of SCFAs (Duncan et al., 2009). Over 95% of SCFAs produced are absorbed within the colon (Hoyles et al., 2018). To prevent high SCFA concentrations in blood, the liver clears the major part of propionate and butyrate from the portal circulation (Bloemen et al., 2010). In animal studies it has been

demonstrated that SCFAs proportion in cecum is altered depending on diet (Ríos-Covián et al., 2016). When fermentable dietary fibers become limiting in the more distal parts of the large intestine, butyrate-producing bacteria almost completely disappear, and the acetate- and propionate-producing bacteria become dominant. Whereas fiber rich diets increases butyrate concentration decreasing propionate and acetate in a proportion compared to control diet (Walker et al., 2005).

Butyrate is used by the colonocytes as an energy source. It maintains intestinal barrier function through an increase in mucus production (Ríos-covián et al., 2016). SCFAs are avidly taken up also by glia cells in the brain and used as energy substrate (Waniewski and Martin, 1998; Nguyen et al., 2007; Wyss et al., 2011). The majority of studies looking at the role of SCFAs in the gut–brain axis have focused on butyrate, a strong neuroprotective molecule (Govindarajan et al., 2011). Few reports are focused on propionate despite its similar plasma concentration and receptor affinity (Hoyles et al., 2018). Propionate acts as a precursor for gluconeogenesis in the liver and contributes to glucose synthesis (Wiltrout and Satter, 1972). Propionate is converted to propionyl-CoA, which then is converted to succinyl-CoA. Succinyl-CoA enters the tricarboxylic acid (TCA) cycle and is converted to oxaloacetate, the precursor of gluconeogenesis (Frye et al., 2016). Excessive propionate has been shown to alter dopamine, serotonin, and glutamate systems in a manner similar to that observed in autism spectrum disorders (ASD) (El-ansary et al., 2012; Li et al., 2017). In addition ,there are increased mean levels of propionate in stool of ASD children (Wang et al., 2012). Thus, propionate has been described as a neurotoxic agent (Macfabe et al., 2006).

SCFAs activate free fatty acid receptor (FFAR) family of G protein coupled receptors; acetate, propionate and butyrate have affinity in the low millimolar to high micromolar range for FFAR2; propionate and butyrate have mid to low micromolar affinity for FFAR3 (Hoyles et al., 2018).

In AD, different concentrations of SCFAs in feces has been reported that TG mice (Bonfili et al., 2017; Zhang et al., 2017a), and in human brain tissue (Zhang et al., 2017a) compared to controls. Thus, LPS and SCFAs have been widely postulated to modulate the gut-brain axis, but up to now there is no clear evidence of their role in AD pathology.

1.3.3.1 SCFAs in astrocytes

SCFA can be used as metabolic source by different cells, such as colonocites colonocites (Zambell et al., 2003; Wong et al., 2006a) or hepatic (Gonzalez-Manchon et al., 1989; Perry et al., 2016). However, astrocytes are the only brain cell type able to utilize SCFAs as energy substrate. Sodium-Acetate is transported into cells by monocarboxylate mediated transport (MCT) (Wyss et al., 2011). Astrocytes can be avidly take up SCFAs by MCT (Nguyen et al., 2007; Wyss et al., 2011)(Waniewski and Martin, 2004). Propionate is exclusively utilised by astrocytes, although it can be taken up by neurons. The inability of neurons to metabolize propionate may be due to lack of mitochondrial propionyl-CoA synthetase activity or transport of propionyl residues into mitochondria (Nguyen et al., 2007). When glucose is not available astrocytes can utilise alternative sources of energy, such as SCFAs or ketone bodies (Valdebenito et al., 2015). Astrocytes are the only cells able to perform β-oxidation of fatty acids in the brain (Edmond et al., 1987; Schulz et al., 2015) allowing a 20% brain oxidative production (Ebert et al., 2003). Astrocytes utilize SCFAs to supply substrates for the tricarboxylic acid cycle (TCA) (Nguyen et al., 2007) resulting in increased glutamine and glutamate production (Gibbs et al., 2011).

1.4 DIET

Dietary habits, nutritional status and lifestyle factors have a major influence on chronic degenerative diseases, including AD ((Livingston et al., 2017). Currently, there are no effective pharmacological therapies to cure or stop the progression of AD. However, recent reports indicate that lifestyle factors might modulate an individual's risk of developing dementia (Livingston et al., 2017). Particularly ingestion of *healthy* decrease the incidence of dementia and brain atrophy (Scarmeas et al., 2006; Gu et al., 2015; Valls-Pedret et al., 2015; Anastasiou et al., 2017; Wu and Sun, 2017).

1.4.1. Effect of diet on Alzheimer´s Disease incidence

The National Institute on Aging (NIH) and the Alzheimer's Association guidelines for AD and cognitive decline introduced some evidence suggesting a direct relationship between diet and changes in the brain function. In particular, higher adherence to a Mediterranean-type diet has been associated with decreased cognitive decline

(Solfrizzi et al., 2017). Furthermore, combinations of foods and nutrients into certain patterns may act synergistically to provide stronger positive effects on cognition than those conferred by their individual dietary components (Solfrizzi et al., 2017). The mediterranean diet (MED) is characterized by high consumption of fruits, vegetables, legumes and cereals, olive oil as the main added lipid, moderate consumption of alcohol (mainly wine and during meals) and low consumption of red meat and dairy products. Adherence to this kind of diet may affect not only the risk of AD, but also of predementia syndromes and their progression to overt dementia (Giliberto et al., 2010; Gardener et al., 2014; Singh et al., 2014; Zbeida et al., 2014; Morris et al., 2016; Solfrizzi et al., 2017).

Ingestion of MED also contributes to lower hippocampal volume loss and decrease structural connectivity in older individuals (Pelletier et al., 2015; Jacka et al., 2017).

Preclinical studies corroborates that administration of a variety of vitamins or nutraceuticals or plant extracts can significantly decrease appearance of multiple AD´s biomarkers, as well as reduce or delay decline in cognitive performance and behaviour in rodent models. Administration of a combined polyphenolic preparation (grape seed extract, resveratrol and Concord grape juice extract) improved long-term potentiation deficits induced in hippocampal slices following treatment with oligomeric Aβ (Wang and BiW, Cheng A, 2014). Cocoa extracts interfered with Aβ oligomerization and impaired signalling in murine hippocampal slices (Wang J, Varghese M, Ono K, 2014), while quercetin showed significant anti-inflammatory and antioxidant properties and in cell cultures has been shown to attenuate Aβ production (Creegan et al., 2015).

It is not clear the mechanism of action of ingestion of MED and similar diets. However, it has been postulated that content of bioactive food (BF) may play an important role on their beneficial effects. BF is food that besides its nutritional value offers additional benefits against a disease condition (Weaver, 2018). We have previously demonstrated that ingestion of BF was able to modify GM, restoring glucose levels, oxidative stress in liver and brain, reducing LPS plasma levels, neuroinflammation, and causing improved cognitive abilities in obese rats (Avila-nava et al., 2016; Sánchez-Tapia et al., 2017).

In the present study we used combination of BF which includes chia seed oil, dehydrated nopal, soy protein and turmeric root. We have used a combination of these foods because they may create a synergistic effect (Allès et al., 2012; Nichols

et al., 2015). Chia seed (Salvia hispanica) has high amount of omega-3 fatty acids; quercetin, kemperin, and fiber). Chia seed regulates the expression of PPARα, PGC-1α and CPT1, resulting in an increased fatty acid oxidation (Tovar et al., 2011; Guevara-cruz et al., 2012). Decosahexaenoic acid (DHA) is the most well-known omega-3 fatty acid in chia. Dietary administration of DHA reduced the amyloid burden from Aβ infused brains, with concurrent increases in DHA levels in the cortico- hippocampal tissues (Hashimoto and Hossain, 2011). There are no reports regarding the effect of chia seed in AD-mouse model.

Nopal (*Opuntia cacti*) is rich in soluble fibers (mucilage and pectin), insoluble fiber (cellulose, hemicellulose, lignin), β-carotenes, polyphenols and vitamin C, showing strong antioxidant activity (Sanchez-Tapia et al., 2017). Nopal is reported to be a pre- and pro-biotic due to is important metabolic effects in patients with metabolic syndrome or obesity (Guevara-cruz et al., 2012). Moreover, it regulates GM by increasing probiotic microorganisms (Bacteroidetes, Lactobacillus, Akkermancia, Bifidobacterium) and decreasing Firmicutes (Sanchez-Tapia et al., 2017). Sanchez-Tapia et al shown that ingestion of nopal improve cognition in obese rats (Sanchez-Tapia et al., 2017). There are no reports on effect of nopal consumption in AD patients nor in transgenic mice.

Soy (glycine max), contains flavonoids (genistein and daidzein) and it is able to regulate expression of PPARα, PGC-1, SREBP-1, and SREBP-2 having a negative effect on lipogenesis and insulin secretion (Ascencio et al., 2004; Tovar et al., 2005; Guevara-cruz et al., 2012) but there is a lack of information about the effects of soy in AD.

Turmeric (*Curcuma long*) contains principle bioactive compound curcumin. It has antioxidant, anti-inflammatory and anti-cancer properties. Curcumin inhibits inflammatory cytokine secretion in experimental systems (Chandra et al., 2001). Furthermore, curcumin was shown to reduce Aβ level *in-vivo* (Wang et al., 2010) and *in-vitro* AD models (Zhang et al., 2010). Epidemiological studies performed in India (where Turmeric is highly consumed) show that AD incidence is the lowest among the World population associated with the high amount of curcumin in the diet (Chandra et al., 2001). However, so far there are few reports regarding the effect of the whole turmeric on the cellular metabolism or cognitive decline in AD-model.

Turmeric

Nopal

Chia

Soy protein

1.5 TRANSGENIC MICE MODEL OF ALZHEIMER´S DISEASE

Transgenic (TG) models mimic a range of AD–related pathologies. Although none of the models fully replicates the human disease, TG models have contributed significant insights into the pathophysiology of AD. They have also been widely used in the preclinical testing of potential therapeutic modalities and have played a pivotal role in the development of immunotherapies for AD that are currently in clinical trials. *Caenorhabditis elegans* (*C. elegans*) and *Drosophila melanogaster* are TG useful model to study common and fundamental toxic mechanisms underlying human neurodegenerative diseases. They both offers advantages in terms of the high degree of experimental control and the relatively short life span of the organisms. Unfortunately, although the *C. elegans* genome includes genes encoding proteins related to human APP, these genes do not possess the region encoding the neurotoxic Aβ (Carlo, 2012). Drosophila model of AD generates an aberrant species of Aβ with an additional N-terminal glutamine residue (Allan et al., 2014). Thus, despite being commonly used model of AD, *C. elegans* and *D. melanogaster* generates different Aβ peptides than present in human and other invertebrates. TG mice are commonly used as models for neurodegenerative diseases, because they have comparable, not identical, brain networks and neurobiological processes with humans. Numerous TG mouse models harbouring single or combinations of familial AD-associated mutations are used in research. TG AD models have greatly contributed to the advancement of AD research, and based on the unique properties of each mutation, they remain highly useful to study specific aspect of the disease process.

Over expression of mutant APP is the most common strategy to generate a TG mouse model of AD, and it has been widely used to develop PDAPP, Tg2576 mice,

APP23 and TgCRND8 transgenic mice, among others. Over-expressions of mutant presenilins (PS) have been used to develop PS1 or PS2 transgenic mice. Overexpression of mutant APP and PS have been used to develop APPPS1 mice and 5X FAD mice. Tau (P301L) mutation was used to develop TG mouse called JNPL3 (Elder et al., 2010; Kitazawa et al., 2012). TG mice overproducing mutant APP develop a pathology similar to the human AD brain; Aβ plaques found in the brains of AD transgenic mice are structurally similar to those found in the human brain (Laferla and Green, 2012).

However single expression of mutant APP, PS1 or tau gene in mice does not trigger the other pathology. To overcome this issue, mouse model have been developed that successfully exhibits both hallmark pathologies in AD: 3xTg-AD mouse is one such model (Kitazawa et al., 2012).

1.5.1 Triple transgenic mouse model (3xTg-AD):

The 3xTg-AD mouse is one of many mouse models of AD, it harbours three transgenes: a human APP associated with familiar AD (APPswe); a mouse PS1 gene carrying a human mutation also associated with familiar AD (PS1M146V); and a human gene associated with tau pathology (TauP301L). This mouse, was created by Salvatore Oddo, in the laboratory of Frank LaFerla, in California. 3xTg-AD mouse was created by adding the tau and APP mutations to a mouse with the PS1M146V mutation. This model mimic major pathological hallmarks of human AD (Aβ load and tau hyperphosphorylation) and develop an age-dependent cognitive decline (Oddo et al., 2003a, 2003b). It has been shown that the accumulation Aβ and tau proteins increases gradually with age in 3xTg-AD mice (Ontiveros-Torresa et al., 2016). According to Oddo et al. (2003a) this mouse presents intra-neuronal Aβ between 3 and 4 months of age in the CA1 region of the hippocampus, and extracellular deposits are evident at 6 months in the frontal cortex (layers 4 to 5) but they can be seen more frequently at 12 months old. However Mastrangelo and Bowers, 2008 reported that intra-neuronal Aβ occurs at 6 months and extracellular deposits are present until 15 months of age in CA1, suggesting that the discrepancies may be due to the type of antibodies used (Mastrangelo and Bowers, 2008). 3xTg-AD mice show behavioral phenotype similarities as observed in patients, such as cognitive deficiencies (Billings et al., 2005)(Guzmán-Ramos et al., 2012), the loss of episodic

memory (Davis et al., 2013), circadian changes, anxiety, and agitation (Sterniczuk et al., 2010). It also has deficiencies in learning and spatial memory as well as

emotional disturbances since the age of 4 months (Cañete et al., 2015).

1.5.1.2 PATHOLOGICAL ALTERATIONS IN 3xTg-AD MICE

3xTg-AD mice exhibit a broader spectrum of AD pathologies. It has been reported to have metabolic, synaptic and GM alteration described earlier in the introduction

GM alterations have been reported in 3xTg-AD mice also. Principal component analysis revealed significant differences in GM structure between the wild type and 3xTg-AD mice, while probiotic formulation restored GM composition and this was associated with improvement in cognition (Bonfili et al., 2017).
3xTg-AD mice also showed episodic-like memory deficit that could be due to the development of an abnormal hyper-excitable state in the hippocampal formation (Davis et al., 2014).

Table 1. Pathological alterations reported in 3xTgAD mice

Age (months-old)	Marker	Outcome	Reference
Male mice			
8, 12, 18 and 24-weeks-old	GM composition	Altered	Bonfili et al., 2017
4 – 6, 13 months-old	Episodic and spatial memory	Decreased	Davis et al., 2014 Morin et al., 2016
4 - 6, 10, 13 months old	Synaptic activity	Increased	Davis et al., 2014;Morin et al., 2016;Arsenault et al., 2011
7 months-old	Neuronal glycolysis	Increased	Sancheti et al., 2014
8 months-old	Lactate in plasma	Increased	Piquet et al., 2018
8 months-old	p- GSK3β/GSK3β	Decreased	Zhang et al., 2017
8 months-old	p-AMPK	Decreased	Zhang et al., 2017
12 months-old	SIRT in hippocampus	Decreased	Rodriguez-ortiz et al., 2014
Female mice			
3 months-old	Mitochondrial respiration	Decreased	Yao et al., 2009
4 - 6 months-old	Memory (episodic)	Decreased	Davis et al., 2014
6, 14 months-old	Glucose tolerance	Decreased	Giménez-Llort et al., 2010; Vandal, et al. 2017
6, 14 months-old	Weight	Increased	Giménez-Llort et al., 2010; Vandal, et al. 2014
8 months-old	Lactate in plasma	Increased	Piquet et al., 2018
8 months-old	p- GSK3β/GSK3β	Decreased	Zhang et al., 2017
8 months-old	p-AMPK	Decreased	Zhang et al., 2017
9 months-old	Insulin signalling	Altered	Chen et al., 2014

Synaptic hyperactivity has been reported in 3xTg-AD mice. Patch-clamp recording revealed that 3xTg-AD mice entorhinnal cortex neurons displayed loss of cell capacitance, increase of firing rate and overactivation of glutamatergic synapses (Arsenault et al., 2011). Pascal et al reported that the basal percentage of Arc-expressing cells in 10-month-old 3xTg-AD mice was higher than wild type in CA3 (Morin et al., 2016b).

Regarding metabolic alterations in this mouse strain, a nuclear magnetic resonance (NMR) study reported increase in neuronal glycolysis in 7-months old 3xTg-AD mice (Sancheti et al., 2014), and a recent metabolomic study revealed higher lactate plasma level in 8-months old 3xTg-AD mice, that could result from a higher neuronal glycolytic flux (Piquet et al., 2018). Mitochondrial functional analyses in female 3xTg-AD mice revealed decreased mitochondrial respiration and decreased pyruvate dehydrogenase protein level and activity and increased oxidative stress. Moreover, embryonic neurons derived from 3xTg-AD mouse hippocampus exhibited significantly decreased mitochondrial respiration and increased glycolysis (Yao et al., 2009). In the hippocampus and cortex of 3xTg-AD mice the ratio of p-GSK3β/GSK3β significantly decreased compared with WT mice (Zhang et al., 2017b), while p-AMPK is reported to significantly decreased in the cortex of 3xTg-AD mice compared with WT mice (Zhang et al., 2017b). SIRT-1 levels have been reported to be significantly lower in the hippocampus of twelve-month old 3xTg-AD mice (Rodriguez-ortiz et al., 2014). Furthermore, female 3xTg-AD mice showed decreased glucose tolerance as compared to non-Tg mice after intraperitoneal injection of glucose (Giménez-Llort et al., 2010; Do et al., 2018). Twelve-month Female 3xTg-AD mice showed glucose hypo-metabolism in hippocampus, frontal and temporal cortices (Sanguinetti et al., 2018).

Brain insulin signalling was also deregulated in the 3xTg-AD mice, as significant decrease in the levels of IRβ, p-IRβ, PI3K, PDK1, AKT, and p-AKT, and an increase level of p-PDK1 was found in brain samples compared to WT control mice. Intranasal insulin treatment for seven days, resulted in restoration of insulin signalling and 50% reduction of the Aβ 40 level in 3xTg-AD mice (Figure 6)(Chen et al., 2014).

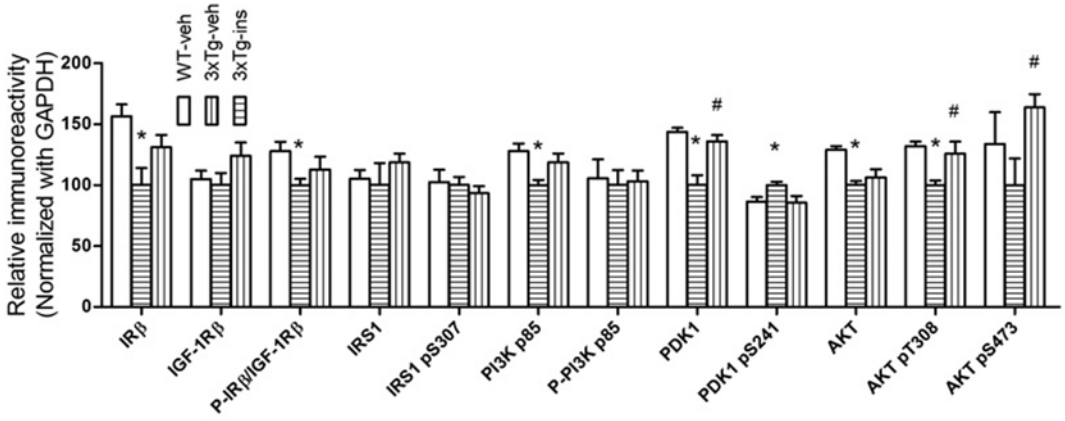

Figure 6. Insulin signalling in 3xTg-AD mice: Homogenates of the rostral halves of brains from mice sacrificed after intranasal administration of insulin (ins) or saline (veh) for seven days were analyzed by Western blots developed with the indicated antibodies. Taken from Chen et al., 2014

Female 3xTg-AD mice are reported to be heavier than non-Tg mice (Gim´enez-Llort et al., 2010; Arsenaul et al, 2011). In addition, female 3xTg-AD mice showed decrease in corticosterone levels and thymus weight and increase in fat as compared to non-Tg mice (Gim´enez-Llort et al., 2010).

The pathological hallmarks are also more prominent in female 3XTg-AD mice, as amyloid plaques, neurofibrillary tangles, neuroinflammation, and spatial cognitive deficits are greater than males (Yang et al., 2018). Furthermore, female 3xTg-AD mice exhibited greater cognitive deficits compared to age-matched male 3xTg-AD mice (Clinton et al., 2007).

Thus, 3xTg-AD mice resemble all the pathological markers observed in AD patients (see Table 1), and we consider it is an ideal model to assess brain and GM alterations after ingestion of BF.

2. JUSTIFICATION

AD is an age-related disease becoming markedly more common as the world's population ages. In 2016, there were more than 46 million people worldwide with dementia, and this number is expected to increase to over 115 million by 2050. Given the heavy economic and social burdens of AD, major emphasis is being placed on understanding its pathogenesis and developing early diagnosis and effective intervention. AD pathogenesis is a multifactorial disease that conveys different mechanistic pathways. This may explain the fact that currently, there are no effective pharmacological therapies to cure or stop the progression of AD. However, non-pharmacological approaches, such as ingestion of healthy diet or pro/pre-biotic supplementation ameliorates AD progression.

GM composition differs in AD patients and TG mice compared to their controls. GM modulates amyloid aggregation and neuroinflammation. However, it is not clear what factor(s) might be involved in this bidirectional gut-brain axis.

Bioactive food ingestion can modify GM composition and reduces neuroinflammation. However, it has not been evaluated whether BF may impact synaptic and metabolic alterations present in AD pathology, and which factors may be involved on this modulation.

Thus, we aimed to reveal whether the mechanism of action of ingestion of BF depends on modulation of GM and its released substances in a TG mice model.

3. HYPOTHESIS

- Bioactive food ingestion will alleviate the course of Alzheimer´s pathology by modulation of the gut-brain axis.
- Butyrate will decrease glycolysis while propionate will increase it in astrocyte/neuronal mixed culture.

4. GENERAL OBJECTIVE:

I. To describe the impact of ingestion of bioactive food on Alzheimer´s pathology with special focus on synaptic and metabolic alterations and the modulation of the gut-brain axis in a TG mice model.

II. To evaluate the effect of short-chain fatty acids treatment on astrocyte metabolism in primary mixed culture by using FRET sensors.

5. PARTICULAR OBJECTIVES:

1) Part 1.- Transgenic mice fed with bioactive food:

I.I) Evaluate memory performance.

I.II) Evaluate markers of Alzheimer´s pathology (Aβ load and Tau hyper-phosphorylation).

I.III) Determine the levels of synaptic proteins.

I.IV) Determine the levels of proteins involved in cellular metabolism.

I.V) Analyse markers related to neuroinflammation.

I.VI) Analyse gut microbiota diversity, quantify lipopolysaccharides levels in plasma, and propionate concentration in the brain.

2) Part II.- Mixed neuron/astrocyte cell culture treated with propionate or butyrate.

II) Evaluate the effects of propionate and butyrate on astroctye metabolism.

II.I) Evaluate the effect of propionate, butyrate and beta-hydroxybutyrate in astrocyte glycolytic rate.

I.III) Evaluate the effect of propionate, butyrate and beta-hydroxybutyrate on lactate production.

6. PART 1

Bioactive food abates metabolic and synaptic alterations by modulation of gut microbiota in a mouse model of Alzheimer's disease

(Manuscript accepted for publication in Journal of Alzheimer´s Disease)

6.1. Experimental design: Female 3XTg-AD transgenic mouse (TG) (RRID: MMRRC_034830-JAX) harbouring the APPSWE and TauP301L transgenes on a PS1M146V knock-in background (homozygous mutant APPSWE, PS1M146V, and TauP301L), and female wild type (WT) B6129SF1/J (RRID:IMSR_JAX:101043) from same genetic background as PS1M146V knock-in mice, but harbouring the endogenous wild-type mouse PS1) (both Jackson Laboratory, Bar Harbor, ME, USA) were used for the study. All mice were housed with access to food (Purina RodentChow5001) and water *ad libitum*, and under optimal vivarium conditions (12 h/12 h light–dark cycle, 20 ˚C, and 40–50% relative humidity). Animal management was supervised by a licensed veterinarian in accordance with the principles set forth in the NIH guide for the care and use of laboratory animals, and was approved by the Bioethics Committee of the Instituto de Neurobiología, UNAM. This work was carried out in accordance with the EU Directive 2010/63/EU for animal experiments and the ICMJE Uniform Requirements for manuscripts submitted to biomedical journals.

Once animals reached two months of age, they were housed individually and feed with two types of diet: 1) **Control diet** (TG-AIN, n=7; WT-AIN, n=9), prepared according to the American Institute of Nutrition recommendations (Reeves, 1997); 2) **Bioactive Food diet** (TG-BF, n=10), with similar composition as AIN-93 diet, except that cellulose was exchanged by dried nopal (5%), casein by soya protein (19.4%), soy oil by chia seed oil (9%), adding 0.1% turmeric (Table 2) (see Figure 7 for experimental design)

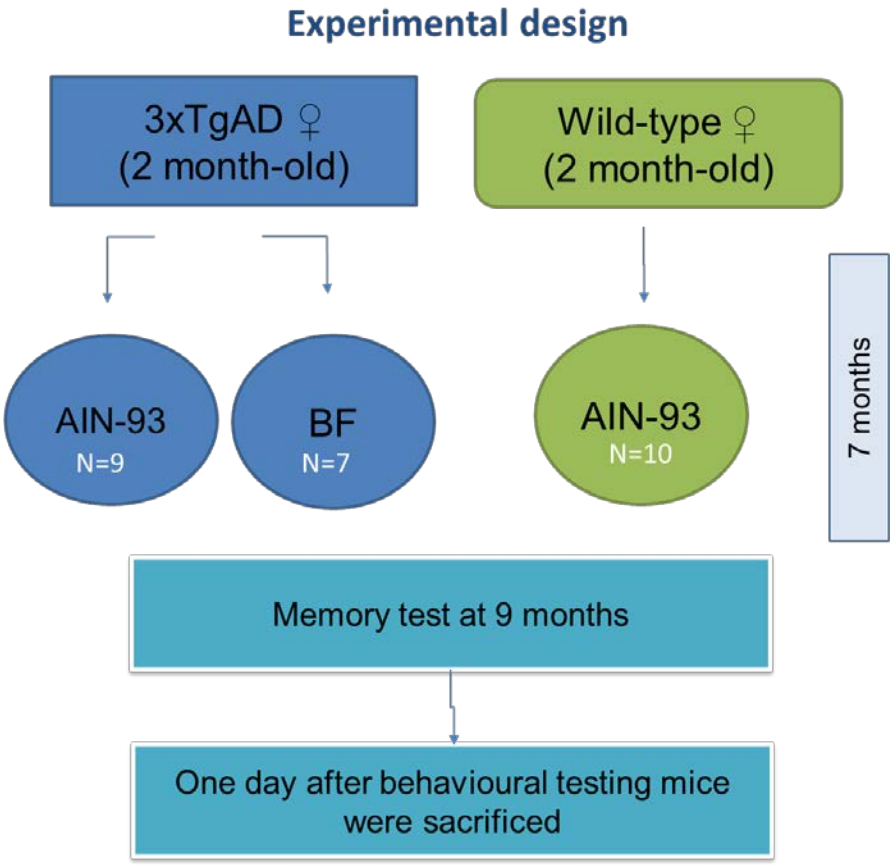

Figure 7. Schematic diagram of Experimental design

Both diets offer equal nutritional requirements and same calories/g, but BF diet had stronger antioxidant activity versus AIN93 by the ORAC method (Table 2). Diets were administered in a dry form (5 g/day, per animal) during 7 months. In average, animals ate both diets without any preference, with an average of 2.2 g/day. Body weight and food intake was monitored over the course of the protocol.

TABLE-2: Composition of experimental diets (g/kg diet)

CONTROL (AIN-93)		BIOACTIVE FOOD (BF)	
Ingredients	**g/kg**	**Ingredients**	**g/kg**
Cornstarch	397.486	Cornstarch	373.30
Casein	200	Soy protein	194
Maltodextrin	132	Maltodextrin	132
Sucrose	100	Sucrose	100
Soy oil	70	Chia seed oil	90
Cellulose	50	Nopal	50
Mineral mix	35	Mineral mix	35
Vitamin mix	10	Vitamin mix	10
L-Cysteine	3	L-Cysteine	3
Choline	2.5	Choline	2.5
TBHQ	0.014	TBHQ	0.014
		Turmeric	1
Energy (Kcal/g)	3.9		3.9
Anti-oxidant activity (Equivalent Trolox: µm/g of sample)	166.4 ± 34.61		1540 ± 110.2***

6.2. Cognitive assessment

Spatial and short-term working memory was evaluated by the T-maze (Deacon and Rawlins, 2006). It is an ideal test to examine differences in the cognitive outcome of behavioural tasks without stress components (i.e. water maze) even in early stages of AD pathology (Davis et al., 2017). T-maze performance is affected by lesions to the hippocampal system and other brain areas, such as the prefrontal cortex (PFC) (Gerlai, 1998), whereas the hippocampus is a region heavily affected in AD. Three days before finalizing dietary intervention, behavioural testing was performed. In order to habituate the animals for the behavioural test, animals were placed in the behavioural room during 1 hour, one day before testing.

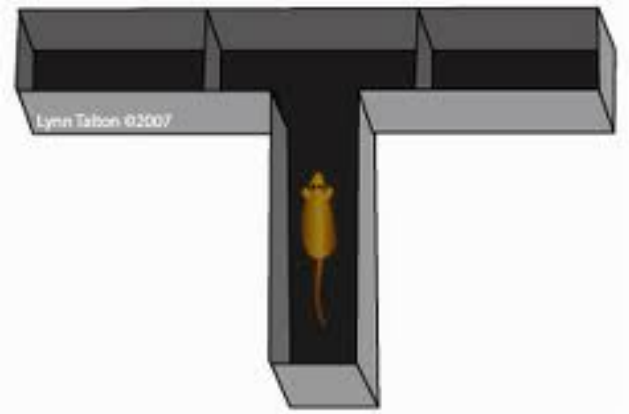

T - MAZE TEST

Briefly, a T-shaped maze Plexiglas apparatus with starting arm (8.5 × 10.5 × 33.0 cm), and the two choice arms (8.5 × 10.5 × 30.0 cm) was used as previously described (Deacon and Rawlins, 2006). T-maze consisted of two phases: 1) Sample phase: animals were placed at the start arm, and allowed to choose between one of the two choice arms. A central divider was inserted into the start arm to create a start box. Once animals have chosen an arm, they are confined there for 30 seconds, thereafter the door was reopened and allow mice to return to the start arm. Animals were finally removed and returned to their cage. 2) Choice phase: Two minutes later, animals were placed again in the start arm, but without the central divider, and allowed them to choose an arm**.** If the animal choose two different arms in both phases, this is counted as spontaneous alteration. Two hours later the procedure

was repeated. Three trials were given on each day, during two days, with a total of 6 trials per animal. Percentages of spontaneous alternations were calculated from total of correct arm entries. Experiments were recorded with a Sony DCR TRV280 camera, which was connected to a computer equipped with in-house develop software to track animals trajectory.

6.3.Tissue Preparation

One day after behavioural testing mice were sacrificed by cervical decapitation, plasma and brain were immediately collected for further analysis. Brain was divided into two halves. Right hemisphere was dissected out and PFC and cortex (CX) were separated. Tissues were snap frozen in liquid nitrogen and stored at -70°C until processing for Western blot and SCFAs analysis. Left hemisphere was post fixed in 4% paraformaldehyde for 48 hours at 4°C for immunohistochemistry and immunofluorescence analysis. For this, brain tissue was cryoprotected by immersion in 30% sucrose/PBS for 4 days. Coronal brain slices (40 µm thickness, from Bregma -2.18 mm to Bregma -2.54 mm) were obtained with a sliding microtome (Leica Jung histoslide 2000R). All sections were immersed in cryoprotectant solutions for light microscopy and immunofluorescence, as described previously (Rodriguez-Callejas et al., 2016), and stored at -20°C until use.

6.4.Immunohistochemistry:

Detection of hyperphosphorylated tau was achieved by use of AT-100 antibody (1:250), and Iba-1 antibody (1:100) for microglia detection. Briefly, sections were thoroughly washed with PBS, and permeabilized with 0.2% Triton in PBS (0.2% PBS-triton) for 20 min. Endogenous peroxidases were inhibited by incubation in 0.3% H_2O_2 in PBS for 10 min. Tissue sections were washed three times for 10 min each, in 0.2% PBS-triton. Non-specific binding was done by incubation in 5% bovine serum albumin (BSA, Sigma) in PBS for 5 min. Subsequently, sections were incubated with primary antibodies, all diluted in 0.2% PBS-triton, washed and incubated with respectively secondary peroxidase-conjugated antibodies (Table 3) in 0.2% PBS-triton for 2 h at room temperature. Hydrogen peroxide (0.01%) and 3,30-diaminobenzidine (DAB) (0.06%) in 0.2% PBS-triton was used to develop the horseradish peroxidase enzymatic reaction. The enzymatic reaction was stopped with 0.2 % PBS-triton and then sections were mounted on glass slides and left to dry

overnight. To evaluate the presence of amyloid aggregates, we used BAM-10 antibody that recognized Aβ 1-40 peptide. We also tested an anti-Aβ 1-42 antibody, however, we could not detect immunoreactivity in TG mice, probably due to the early stage of the pathology. Dry sections were cover slipped with mounting medium Entellan (Merck). For amyloid beta staining, tissue sections were washed three times in PBS during 5 min, then incubated in formic acid (89.8%) for 10mins, followed by three times washing in PBS for 5 min each. Sections were incubated in solution of H_2O_2 (30%) + Methanol (10%) for 30 mins followed by washing in PBS and then incubated in 0.1% PBS-tween for 15mins, followed by incubation in 5% goat serum (Vector) in PBS-triton for 30mins. Thereafter, sections were incubated with BAM-10 (1:1500) in 5% goat serum in PBS-triton for 18 hrs at 4°C. After washing in PBS, sections were incubated with secondary antibody (Table 3) in 0.2% PBS-triton for 2 hrs at room temperature. Subsequently, sections were washed and incubated with the avidin-biotin complex (ABC Kit; Vector Laboratories) in 0.2% PBS-triton for 2 hrs according to the manufacturer's instructions. Finally, antibody binding was visualized with the chromogen DAB (DAB Peroxidase Substrate Kit; Vector Laboratories) 0.025%, with 0.01% H_2O_2 as a catalytic agent. Sections were washed with PBS, dehydrated by serial dilution in ethanol, and mounted with Eukit (Fluka). Control sections for all antibodies were processed without the primary antibody.

6.5. Immunofluorescence:

For immunofluorescence staining, sections were washed in PBS and pre-treated with citrate buffer 20X (Sigma), at 94°C for 10 min, and then permeabilized with 0.2% PBS-triton for 20 min. Thereafter, sections were treated with 5% BSA for 5 min, and incubated with primary antibodies (Table 3): anti-Glial Fibrillary Acidic Protein (GFAP, 1:500), anti-Sirtun-1 (SIRT1, 1:500) (Table 3), all diluted in 5% horse serum (Vector Laboratories, S-2000) during 48 hrs at 4°C. Then, tissue was washed with 0.2% PBS-triton, and incubated with respective secondary antibodies (Table 3) in 0.2% PBS-triton. All sections were co-incubated with DAPI (4',6-Diamidino-2-Phenylindole, Dihydrochloride, Invitrogen) in 0.2% PBS-triton for 30 min, washed and mounted on glass slides. After drying they were cover slipped with mounting medium Vecta shield (Vector Laboratories). Control sections were processed without the primary antibody.

TABLE-3: List of Primary antibodies and secondary antibodies used in the current study

Primary antibodies			
Antibody	**Host/Isotype**	**Brand**	**Catalog number**
Anti p- AMPK	Rabbit/ IgG	Santacruz biotechology	sc-33524
AMPK	Rabbit/ IgG	Santacruz biotechology	sc-74461
ARC	Mouse/IgG	Santacruz biotechology	sc -17839
AT100	Mouse/IgG	Jackson ImmunoRes	111-175-166
BAM-10	Mouse/IgG	Sigma	A3981
FFAR 3	Rabbit/ IgG	My biosource	MBS7003084
GFAP	Mouse/IgG	Cell Signaling	3670
GLUR1	Rabbit/ IgG	GeneTex	GTX 61101
p-Gsk3-β	Rabbit/IgG	Cell signalling	9331
Gsk3-β	Rabbit/IgG	Santacruz biotechology	sc-9166
Human Tau	Mouse/IgG	Thermo scientific	MN1000
Anti-Iba-1	Rabbit/IgG	Wako Chemicals	019-19741
PGC-1α	Rabbit/IgG	Abcam	ab54481
PSD 95	Mouse/IgG	Thermo scientific	7E3-1B8
SIRT1	Rabbit/IgG	Santacruz	sc -15404,
Synaptophysin	Rabbit/IgG	Abcam	ab32127
Tau 231/AT180	Mouse/IgG	Thermo scientific	MN1040
Secondary antibodies			
Peroxidase-conjugated anti-mouse	Goat/IgG	Jackson ImmunoRes	115-035-146
Peroxidase-conjugated anti-rabbit	Goat/IgG	Jackson Immuno Research	111-035-144
Biotinylated anti-rabbit	Horse/IgG	Vector Laboratories	BA-1100
Cy3-conjugated anti-rabbit	Donkey/ IgG	Jackson ImmunoRes	711-165-152
Cy5-conjugated anti-mouse	Goat/ IgG	Jackson ImmunoRes	115-175-166
ALEXA488-conjugated anti-mouse	Goat/IgG	Jackson ImmunoRes	115-545-166
ALEXA488-conjugated anti-mouse	Donkey/IgG	Jackson ImmunoRes	715-545-150
ALEXA647-conjugated anti-goat	Donkey/IgG	Jackson ImmunoRes	705-605-147

6.6.Image acquisition and analysis:

Leica DMI6000 inverse microscope was used to acquire bright-field images under 40x objective for BAM-10, AT100 and iba-1. For fluorescent labeling, a laser scanning microscope (Leica TCS-SP8) with argon (488 nm), and helium/neon (543 nm) lasers and with optimized pinhole diameter was used. For GFAP and SIRT1 we used a 20X objective (SIRT zoom 4), whereas for double labeling of SIRT1 and GFAP, a 40X objective was used. Images were obtained by using system optimized z-stacks parameter (10 stacks, each stack 1.385 µm) in Z axis, projected and analyzed in a two-dimensional plane. Stacks were superimposed as a single image by using the Leica LAS AF 2.6.0 build 7268 software.

Iba-1+ cells located in the *striatum (st.) radiatum* from CA1 hippocampal region were quantified based on their morphological characteristics, according to previous reports (Streit et al., 2004, 2009; Rodriguez-Callejas et al., 2016). Microglia cells were classified as: inactive (displaying a slight ramified morphology and small rounded soma), or active (hypertrophic soma and with extensively thick and branched processes). Number of astrocytes labeled with GFAP were quantified in *st. radiatum, st. oriens* of CA1 hippocampal region, and layers I-V from entorhinal cortex (Ent. cx). We have differentiated in sub-areas of CA1 region because previous reports indicate *stratum*-specific alterations in hippocampus of TG mice (Perez-Cruz et al., 2011a).

Brightfield images were acquired at the same exposure light, and tissue background staining was subtracted from optical density values from fiber tracts within the same section, e.g., corpus callosum (Perez-Cruz et al., 2011a). Threshold was determined by identifying best signal-to-noise ratio from at least 4-5 images, and averaging threshold values from those images. All images were analyzed with that averaged threshold (Herline et al., 2018). Immunoreactive signal was evaluated by using the plugin "*measure"* in Image J 1.49v (NIH, open access) as previously reported (Rodriguez-Callejas et al., 2016).

Immunoreactivity against BAM-10 showed scarce amyloid aggregates (i.e. plaques) in subiculum (Fig. 2). BAM-10 staining was mainly as intracellular aggregates (Fig. 2). Thus, images obtained from subiculum were used to quantify number of plaques, while *st. pryramidale* of CA1 region of the hippocampus, and Ent. cx (layers III-V) were used for quantification of intracellular aggregates.

For BAM-10 and AT100, percentage of area stained was calculated in a determined area (BAM-10: 0.00614357142 mm^2 in CA1, and 0.0933945 mm^2 in cortex; AT100: 0.001314 mm^2). The percentage of area stained was calculated as the sum of areas with aggregates divided by the total area analyzed, and multiplied by 100.

For quantification of microglia cells and astrocytes, the total number of iba1+ and GFAP+ cells were measured as number of cells / number of images x single image area (Iba1: 0.089355 mm^2; GFAP: 0.0338578125 mm^2).

SIRT1 immunofluorescence was evaluated in hippocampal region. We used the plug-in "*Analyse particles"* of Image J 1.49v (NIH, open access) adjusting size and circularity of particles immunereactive to SIRT1. We summed the total number of particles quantified per area (*st. radiatum*: SIRT; 0.00185165 mm^2; *st. oriens*: SIRT:0.0015mm^2) in at least 3 images per animal. For detection of SIRT1 in GFAP+ cells, we first located SIRT1 immunoreactivity in the nucleus of GFAP+ cells labeled with DAPI in *st. radiatum* of CA1 hippocampal region. Then, SIRT1 signal intensity was analyzed by Image J plugin "*measure*" only in the nucleus, as described above. In all staining, one image (with 20x objective) or two images (with 40x objective) per slice, 3 slices per animal, and at least 5 animals per group were analyzed, yielding 5 values for statistical analysis.

6.7. Western blot:

Cortex was homogenized in RIPA buffer (150 mM sodium chloride, 1.0% NP-40 or Triton X-100, 0.5% sodium deoxycholate, 0.1% sodium dodecyl sulphate, 50 mM Tris, pH 8.0) (10% weight/volume). Homogenates were centrifuged at 13000 rpm for 15 min at 4 °C. The purified total protein was quantified by the Lowry assay (Bio-Rad DC Protein Assay Kit) method. Samples (40 μg proteins) were separated on SDS-PAGE (10%–12%) and then transferred onto a polyvinylidene difluoride (PVDF) membrane. Blots were blocked with 5% blotting grade non-fat dry milk (Bio-Rad, Hercules CA, USA) or with 1% casein (C3400, Sigma) for p-AMP, p-GSK 3β, p-Tau231, for 1 hour at room temperature and incubated overnight at 4 °C with the primary antibodies as described in table 3: ARC (1:250), GLUR1 (1:500), PSD 95 (1:1000), Synaptophysin (1:1000), AMPK (1:1000), p-AMPK (1:1000), Gsk3-β (1:250), p-Gsk3-β (1:500), FFAR 3 (1:250), Human Tau (1:250), Tau 231/AT180 (1:250), Malondialdehyde (MDA) (1:1000). Membranes were washed with TBS-T (TBS +0.05% Tween20), and then incubated with a horseradish peroxidase linked to

secondary antibody (Table 3). As loading control we used α-Actin (1:1000). Immunoreactive bands were visualized by enhanced chemiluminescence ECL for routine immunoblotting (Mruk and Cheng, 2011) using Chemidoc (Bio rad XRS+SYSTEM). The western blots were performed at least 3 times using independent blots. Densitometry analysis was performed using NIH image J software. Values were normalized with actin and expressed as fold increase.

6.8. Microbiota analysis by real time PCR:

DNA isolation and sequencing. Fecal samples were collected for each animal during the habituation day (three days before sacrifice). Animals were placed during 20 min in a Plexiglas arena (50 cm x 50 cm) previously cleaned and disinfected. At least 100 gm of feces pellets were collected per animal, immediately frozen and stored at −70 °C until use. Bacterial DNA was extracted using the QIAamp DNA Mini Kit (Qiagen, Valencia, CA, USA) according to the manufacturer's instructions. MiSeq platform was used for the sequencing of the samples and then genomic libraries of the regions V3 and V4 of the 16S gene were generated, using primers for those regions that also contained an overhang adapter specified by Illumina (F: 5′-TCGTCGGCAGCGTCAGATGTGTATAA GAGACAGCCTACGGGNGGCWGCAG-3′ and R: 5′-GTCTCGTGGGCTCGGAGA TGTGTATAAGAGACAGGACTACH VGGGTATCTAATCC-3′). The amplicons of the V3 and V4 regions were generated by PCR reactions containing genomic DNA (5 ng/μL in 10mM Tris pH 8.5), high Fidelity DNA polymerase 2× KAPA HiFi HotStart ReadyMix and primers (1μM). This mixture was placed into the thermal cycler and run through the following program: 3 min at 95 °C, followed by 25 amplification cycles consisting of denaturation (30 s at 95 °C), alignment (30 s at 55 °C) and elongation (30 s at 72 °C). The final elongation consisted of 5 min at 72 °C. The amplicons were purified using AMPure XP beads and their size was verified on capillary electrophoresis in the Agilent 2100 Bioanalyzer (Agilent Technologies, Santa Clara, California, USA), with an approximate size of 550 bp. Once passed the quality control, the samples were indexed using the Illumina Nextera XT Index Kit (v.2, Set A). For this process 5 μL of the first PCR product, High Fidelity DNA polymerase 2× KAPA HiFi HotStart ReadyMix and primers (Index) were mixed and returned to the thermocycler, using the following program: 3 min at 95 °C, followed by 8 amplification cycles which

consisted of denaturation (30 s at 95 °C), alignment (30 s at 55 °C) and extension (30 s at 72 °C). The final extension consisted of 5 min at 72 °C. This product was purified and the integrity was analyzed. The amplicons had an approximate size of 610 bp. The concentration of double-stranded DNA was determined by fluorometry (Qubit fluorometer 3.0, high sensitive kit). The final library was mixed equimolarly and sequenced on the Illumina MiSeq platform (MiSeq Reagent Kit V.3, 600 cycles) following the supplier's instructions. Sequence Analysis: For taxonomic composition analysis, Custom C# and python scripts, as well as python scripts in the Quantitative Insights into Microbial Ecology (QIIME) software pipeline 1.9 were used to process the sequencing files. The sequence outputs were filtered for low-quality sequences (defined as any sequences that are 620 bp, sequences with any nucleotide mismatches to either the barcode or the primer, sequences with an average quality score of 0). Sequences were chimera checked with Gold.fa, and chimeric sequences were filtered out. Analysis started by clustering sequences within a percent sequence similarity into Operational taxonomic units (OTUs). 91% of the sequences passes filtering, resulting in 83,906 sequences/sample with a 97% similarity threshold. Operational taxonomic units (OTUs) picking was performed using tool set Qiime-tools, using Usearch method. OTUs were picked against the Green Genes 13.9. 97% OTUs reference database. After the resulting OTU results files were merged into one overall table, taxonomy was assigned based upon the gg v13.9 reference taxonomy. Thus, 99.76%, 99.69%, 99.64%, 86.8%, 50.48% and 10.86% of the reads were assigned to the phylum, class, order, family, genus and specie level, respectively. Species richness (Observed, Chao1) and alpha diversity measurements (Shannon) were calculated, and we estimated the within-sample diversity at a rarefaction depth of >17351 reads per sample. Weighted and unweighted UniFrac distances were used to perform the principal coordinate analysis (PCoA). Microbial sequence data were pooled for OTUs comparison and taxonomic abundance analysis but separated by batch in principle coordinates analysis (PCoA) to have clear PCoA figures. For even sampling, a depth of 17,351 sequences/sample was used. PCoAs were produced using Emperor. Community diversity was determined by the number of OTUs and beta diversity, measured by UniFrac unweighted and weighted distance matrices in QIIME. ANOSIM, a permutational multivariate analysis of variance was used to determine statistically significant clustering of groups based upon microbiota structure distances.

6.9.Lipopolysaccharide analysis: Lipopolysaccharide content in plasma was determined by ELISA kit (CEB526Ge, Cloud-Clone Corp) according to manufacture instructions.

6.10.Short chain fatty acids: Short-chain-fatty acids (SCFA) content in feces and brain samples were analyzed by gas chromatography (GC). We collected fecal samples from WT-AIN, TG-AIN shortly before finalizing the experiment, and from WT and TG mice of 3-, 6-, and 11-months of age (WT, n=3 each age; TG, n=4 each age) for the ontogeny study. Feces samples were immediately frozen and stored at −70°C until analysis. Fifty mg of feces was suspended in 5 mL of water and homogenized to get fecal suspension. The pH of the suspension was adjusted to 2–3 by adding 5M HCl, and then kept at room temperature for 10 min with occasional shaking. The suspension was centrifuged for 20 min at 5000 rpm and the supernatant was collected. The internal standard, 2-Ethylbutyric acid solution (1mM in formic acid), was spiked into the supernatant. Supernatant was injected in GC (Agilent technologies-6850 series 11, Agilent, Santa Clara, CA, USA) with flame ionization detection (Agilent), by using Agilent J&W DB-225ms column as previously described (Zhao et al., 2006).

To evaluate the levels of propionic acid in brain we used GC-Mass Spectrophotometry (MS) using an Agilent Intuvo 9000 gas chromatography system coupled to an Agilent 5977B mass spectrometric detector (MSD, Agilent Technologies, Santa Clara, CA). No sample preparation was required as Thermal separation Probe accessory (5990-8715EN Thermo Sep Probe.indd - Agilent) was used for introduction of the sample into GC-MS. Briefly, samples were weighed and loaded into the vial for propionic acid extraction at the inlet, followed by the standard GC analysis. Propionic acid was separated using an Agilent Column (part number 122-7033UI-INT: Serial number US16460202), phase DB-WAX_UI (Dimensions 30 m x 250 µm x 0.5 µm). 0.4µl of derivatives was injected in split mode with a ratio of 20:1, and the solvent delay time was set to 6 min. Helium was used as a carrier gas at a constant flow rate of 1 mL/min. The initial oven temperature was held at 60 °C for 0.05 min, ramped to 250 ˚C at a rate of 900 °C/min, and finally held at this temperature for 3 min. Data analysis was performed using MassHunter Quantitative software. (Agilent Technologies, Santa Clara, California, USA).

6.1.11.Statistical analysis: Data are expressed as the mean ± S.E.M. for body weight and microbiota analysis at species and genus level, otherwise we expressed data as mean ± S.D. For analysing BAM-10, AT100 TAU231, and propionate concentration in feces we used an un-paired t-test. To assess body weight changes we used a two-way repeated measures analysis of variance (ANOVA) followed by Bonferroni´s post-hoc test. One-way ANOVA followed by Newman-Keuls post-hoc test was used for T-maze data, and Tukey´s test for the rest of the analysis (GFAP, iba1, SIRT1, SIRT1 in GFAP, GluR-1, PSD-95, Arc, synaptophysin, pGSK-3β/GSK-3β, pAMPK/AMPK, microbiota, propionate level and FFAR3 in brain and LPS levels) as recommended by the Software (GraphPad v.6). All results were considered statistically significant at $p<0.05$.

6.2. Results Part I:

6.2.1. Body weight and Behaviour: We observed that TG groups had significantly higher body weight compared to WT mice (Figure 8A). However, BF ingestion by TG mice did not modify food intake, nor weight gain with respect to the control group. Body weight changes in TG mice have been associated with glucose intolerance (Giménez-Llort et al., 2010; Vandal et al., 2014).

Spatial and working memory were assessed using a T- maze test (Figure 8B). Percentage of spontaneous alterations decreased in TG-AIN compared to WT-AIN mice, but BF ingestion for 7 months significantly improved cognition in TG-BF mice (Fig. 8B).

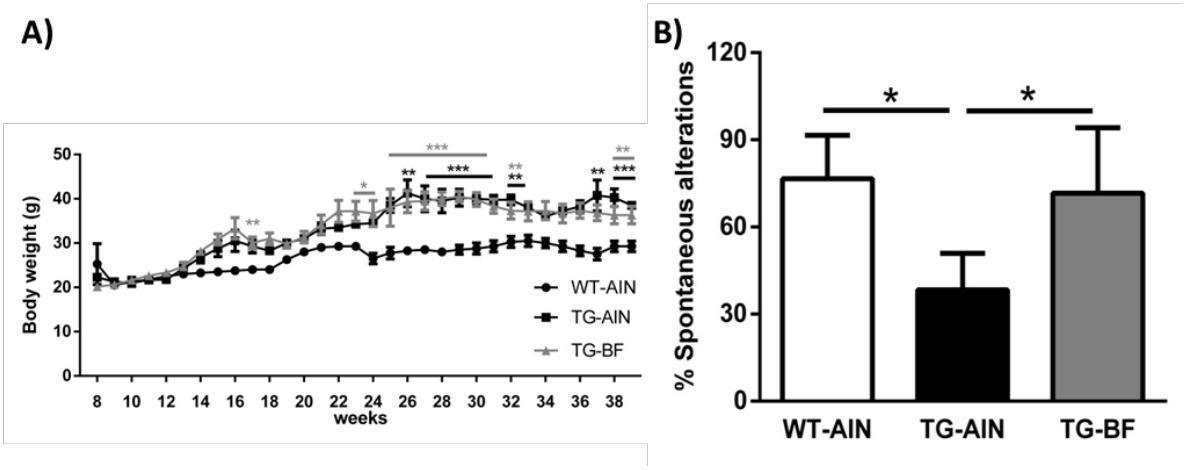

Figure 8: Effect of bioactive food on body weight and spatial memory. A) Body weight (g) in TG-AIN, TG-AIN and TG-BF mice. TG mice gained more body weight compared to WT-AIN mice starting from the 17th experimental week (black asterisk: WT-AIN vs TG-AIN; grey asterisk: WT-AIN vs TG-BF). At the end of experiment, WT-AIN mice gained less body weight (9.66 ± 0.66 g),

compared to TG-AIN (16.25 ± 1.03 g) ($p < 0.001$) and TG-BF mice (16.16 ± 2.71 g) ($p < 0.01$), but there were no differences in final weight gain among TG mice. **B) Working memory and spatial learning.** Spontaneous alterations were recorded during 2 days-test on the T-maze. TG-AIN mice alternated less than WT-AIN mice ($p > 0.05$), while TG-BF showed same values as control mice ($p < 0.05$ vs TG-AIN). Data in A are expressed as the mean ± S.E.M., in B as mean ± S.D. *$p< 0.05$, **$p < 0.01$, ***$p< 0.001$.

6.2.2. Amyloid Beta: We analyzed Aβ load using BAM-10 antibody. At 9 months of age, only a few amyloid plaques were observed in the subiculum of 3xTg-AD mice. We did not detect a significant effect of BF on the number of plaques in TG mice (Fig 9A-B). However, intracellular Aβ was readily identified in neurons from the hippocampal region and Ent.cx. No significant differences in the degree of intracellular Aβ aggregation were detected in the CA1 subfield of the hippocampus as a function of diet. In Ent. cx, however, TG-BF mice had fewer aggregates than the TG-AIN group ($p < 0.001$) (Fig. 9A-B).

6.2.3. Tau phosphorylation: Tau pathology was analysed by immunohistochemistry (AT100) and immunoblot (TAUp231). AT-100 staining in pyramidal layer of CA1 region decreased in TG-BF compared to TG-AIN mice (Figure 10A and c). Moreover, protein levels of p-TAU231/TAU in the cortex correlated to those changes, as p-TAU231 decreased significantly in TG-BF compared to TG-AIN mice, resulting in a lower ratio p-TAU231/TAU in TG-BF mice (Fig. 10c).

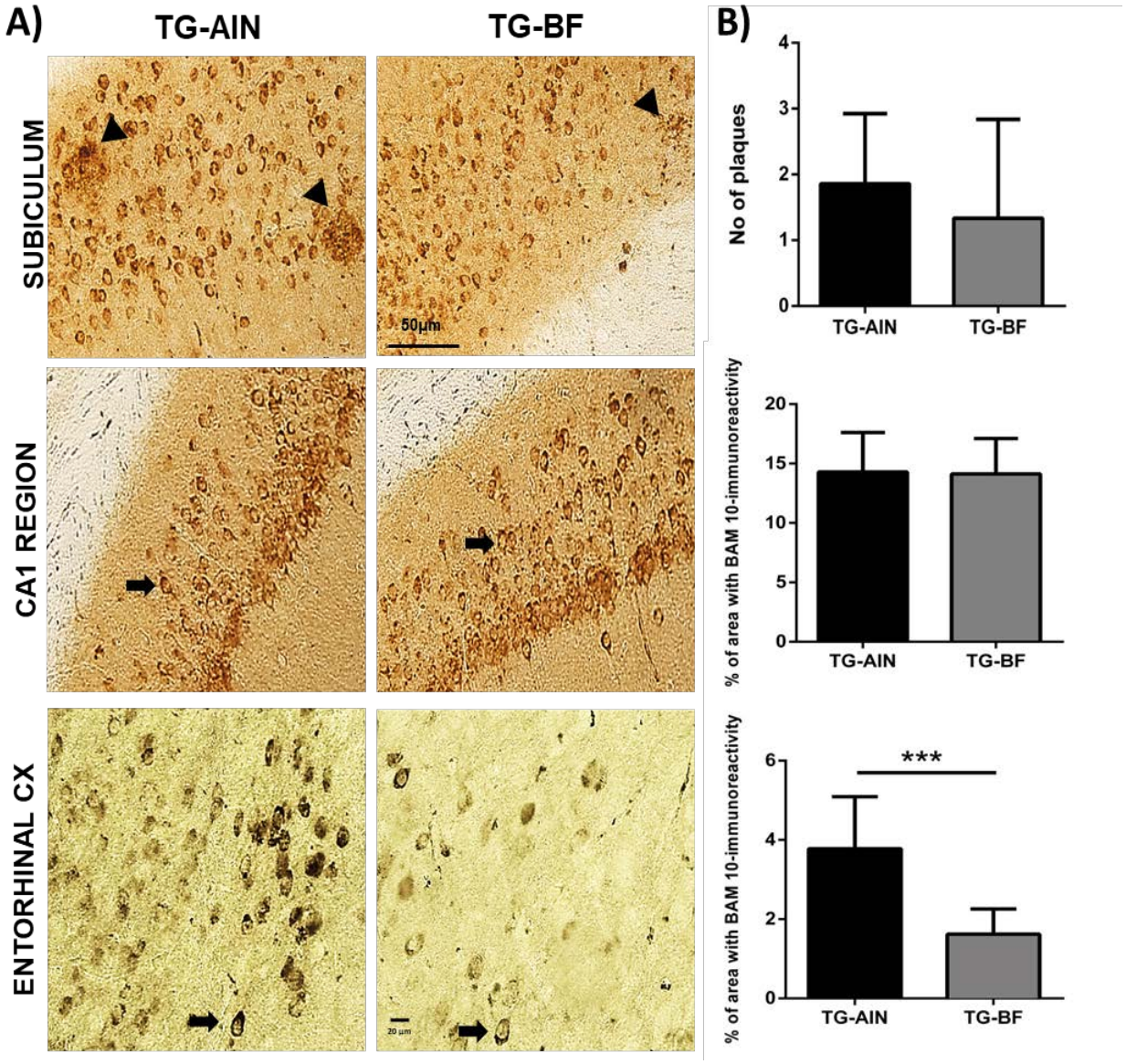

Figure 9. Evaluation of amyloid pathology. A) Representative images of BAM10 staining in hippocampus and Ent.cx. Scale bar 50 µm (hippocampus) and 20 µm (cortex). B) Quantification of BAM10 staining: Upper panel, in subiculum there were few large aggregates with no differences between groups. Middle panel, in CA1 region there were no differences between groups. Lower panel, in Ent.cx TG mice treated with BF showed a decreased BAM10 staining compared to TG-AIN mice ($p<0.001$). Data are expressed as the mean ± SD. ***, $p>0.001$

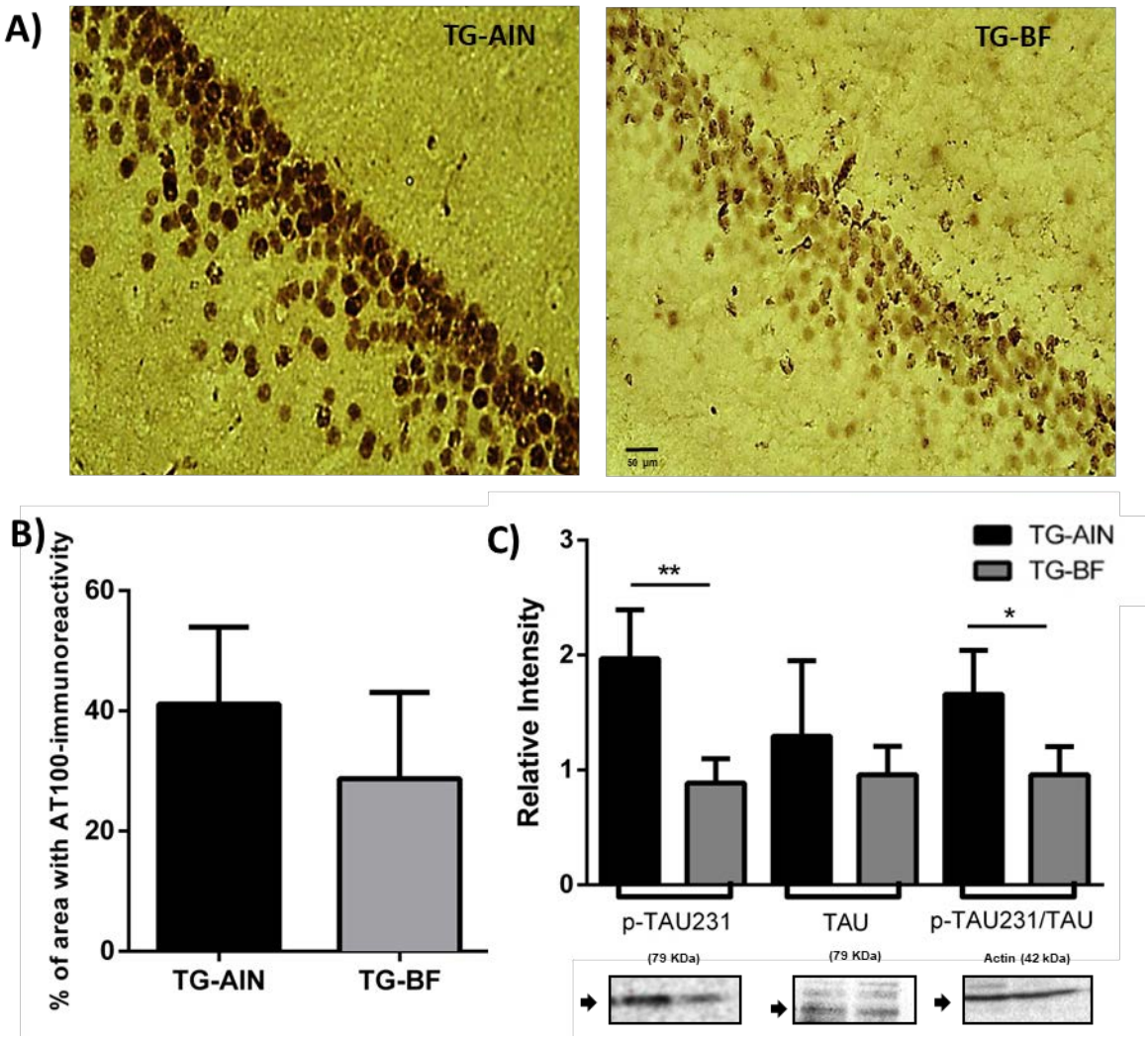

Figure 10. Tau hyperphosphorylation in TG mice. A) Representative photomicrographs of AT100 staining in CA1 hippocampal region. B) Quantification of AT100 indicates a reduction in the percentage of area occupied by tau aggregates in TG-BF mice compared to TG-AIN ($p < 0.05$). C) Western blot analysis of brain cortex corroborates that tau hyperphosphorylation (p-TAU231) decreased in TG-BF mice compared to TG-AIN ($p < 0.01$). Blot were normalized with α-actin. Images below graphs are representative blots for each protein done by quadruplicate in pool samples. Scale bar 50 µm. Data represents mean ± S.D. *$p < 0.05$, **$p < 0.01$

6.2.4. Inflammation: Glial cells were labeled with iba1 and GFAP antibodies. We classified the microglia phenotype as inactive or active, according to previous reports (Streit et al., 2009; Rodriguez-Callejas et al., 2016). Representative images of the microglia are shown in Fig. 11A. The quantification of microglia in *st. radiatum* showed more activated cells in TG-AIN compared to WT-AIN mice, while the inclusion of BF abated those increases. The number of inactive microglia did not differ between any of the three groups (Fig. 11B. Left panel). Astrocytes labeled with GFAP were quantified in hippocampus (*st. radiatum* and *st. oriens*) and in Ent.cx;

representative images are shown in Fig. 11A. We observed that TG-AIN mice had more GFAP+ astrocytes in both *strata* and Ent. cx compared to WT-AIN mice. Contrastingly, the ingestion of BF resulted in a lower number of astrocytes in both *strata* from hippocampus, but there was not a significant recovery in Ent. cx in TG-BF mice (Fig. 11B. Right panel).

6.2.5. Metabolic and synaptic proteins: To evaluate if the anti-inflammatory effect of BF could be associated with changes in cellular metabolism, we analysed SIRT1, GSK-3β and AMPK proteins in brain tissue. We evaluated the immunoreactivity against SIRT1 in *st radiatum* and *oriens* (Fig. 12). In *st. radiatum*, a layer with an increased number astrocytes and microglia cells, SIRT1 was higher in TG-AIN mice compared to WT-AIN mice, while TG-BF group showed decreased values compared to TG-AIN (Fig. 12B, right panel). No differences were observed in *st. oriens* (Figure 11B, right panel). To evaluate if SIRT1 levels in *st. radiatum* were associated with the increased number of astrocytes in same layer, we used double immunofluorescence (SIRT1 and GFAP). We observed that nucleus of GFAP + astrocytes had increased SIRT1 labelling in TG-AIN mice compared to WT-AIN and TG-BF mice. SIRT1 in nucleus of GFAP + cells also decreased in TG-BF compared to TG-AIN mice (Figure 13).

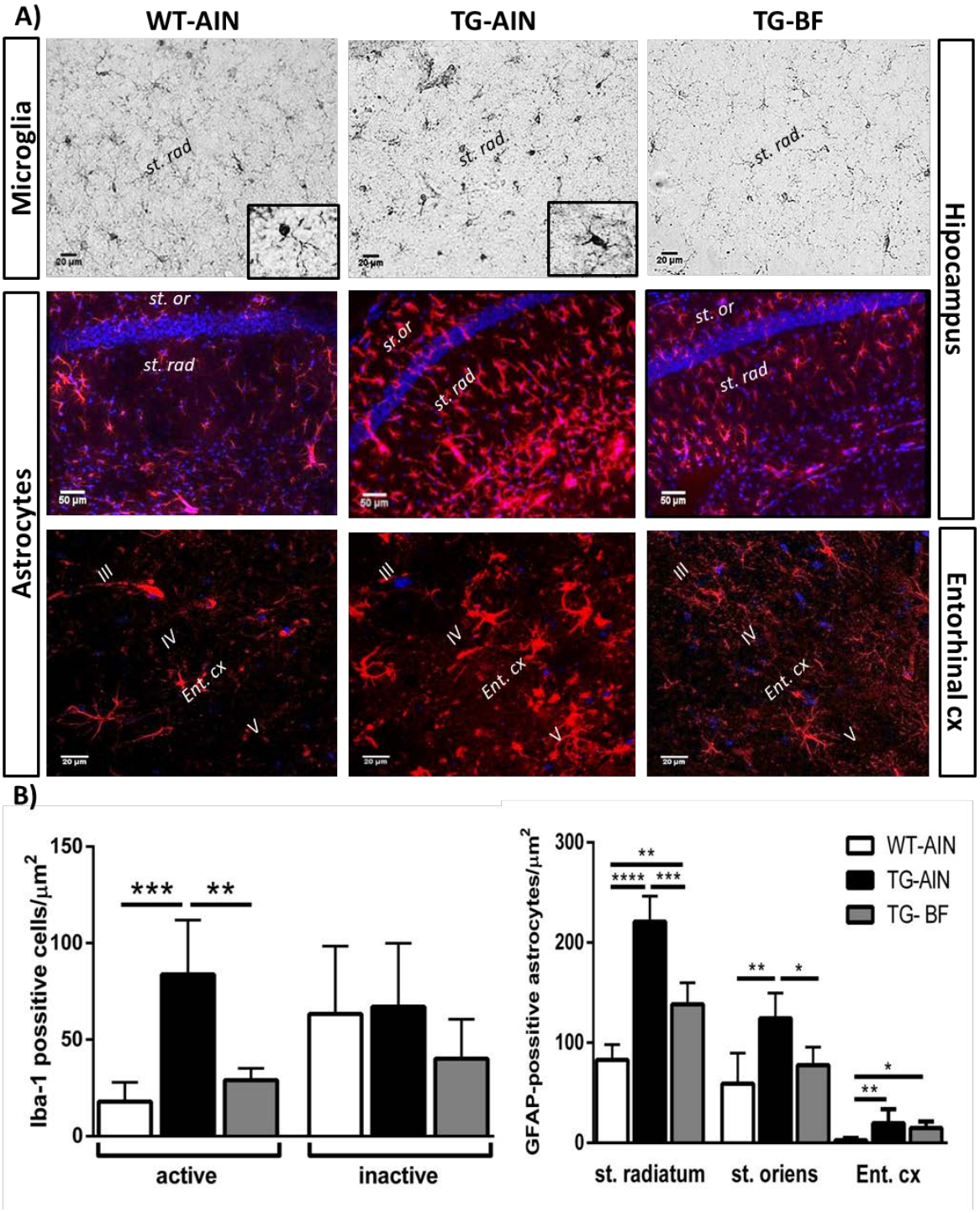

Figure 11. Effect of BF on neuroinflammation in 3xTg-AD mice. **A)** Representative images of microglia labeled with iba1 in *st. radiatum* of CA1 hippocampal region (scale bar 20µl), and reactive astrocytes labeled with GFAP in *st. radiatum, st. oriens* (scale bar 50µl) and Ent. cx (scale bar 20µm). Iba + cells in WT-AIN mice presented mainly an inactive phenotype (insert, WT-AIN), while in TG-AIN mice, abundant activated microglia was detected (insert, TG-AIN). **B)** Left panel: Quantification of microglia cells in *st. radiatum* showed an increased number of activated microglia in TG-AIN compared to WT-AIN mice, while TG-BF mice showed similar values as controls ($p<0.001$ and $p<0.01$, respectively). Number of inactive microglia did not showed differences between groups. Right panel: GFAP+ astrocytes increased in *st. radiatum, st. oriens* and Ent. cx in TG-AIN compared to WT-AIN mice ($p < 0.0001$, $p < 0.01$, $p < 0.01$, respectively), while TG-BF mice had a reduced number of astrocytes in *st. radiatum* and *st. oriens* ($p < 0.001$ and $p < 0.05$). Note that more active astrocytes

were observed in *st. radiatum* compared to *st. oriens* in TG-AIN mice. In Ent cx there was a slight recovery in TG-BF compared to TG-AIN as number of astrocytes was not so abundant compared to WT-AIN ($p<0.05$), but it did not reach significance. Data represents mean ± SD. *$p<0.05$, **$p<0.01$, ***$p<0.001$, ****$p< 0.0001$

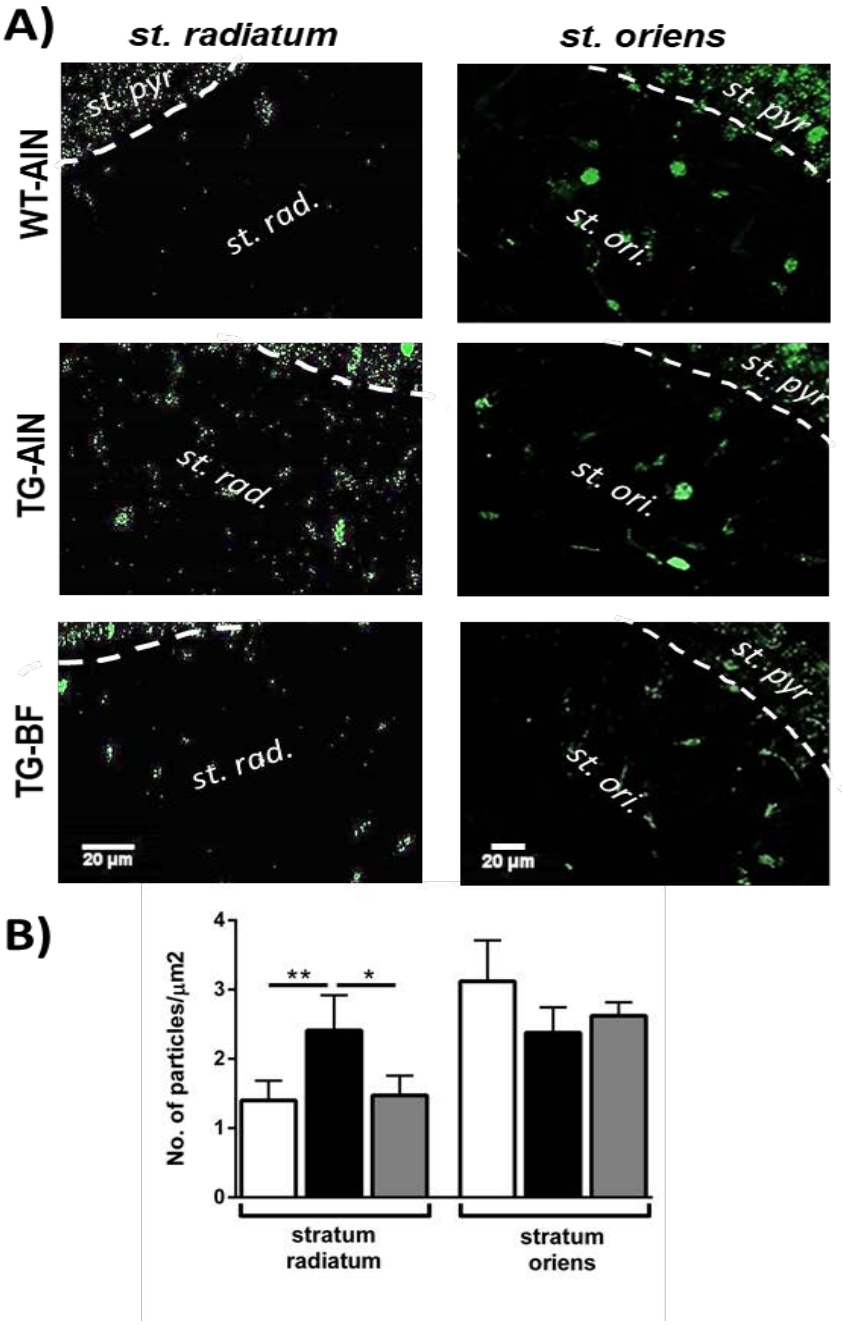

Figure 12: Effect of bioactive food on hippocampal SIRT1 were region specific. A) Representative images of SIRT1 labelling in st. *radiatum* and *st.oriens*. Scale bar 20 µm. B) Quantification of SIRT labelling in *st. radiatum* and *st. oriens*. In *st. radiatum,* TG-AIN mice had more number of SIRT1 particles compared to WT-AIN ($p< 0.01$) and TG-BF ($p<0.05$). No differences between groups were observed in *st. oriens*. Data are expressed as the mean ± S.D. *$p <0.05$, **$p < 0.01$

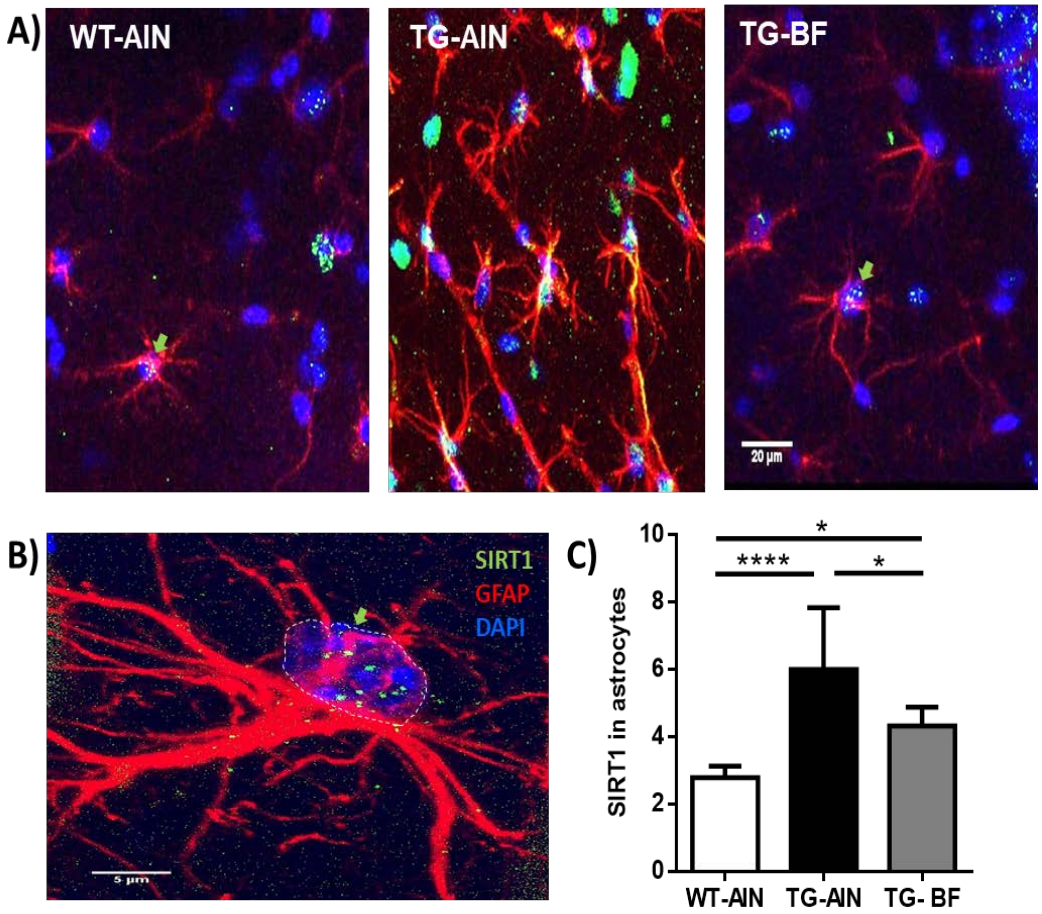

Figure 13. Effect of bioactive food on SIRT1 in GFAP + astrocytes. A) Representative images of GFAP + astrocytes (red) located in *str. radiatum* of CA1 hippocampal region co- labelled with SIRT1 (green), and counterstained with DAPI (blue). Scale bar 20 µm. B) Magnification of an astrocyte where nucleus was selected to analyse SIRT1 particle intensity. Scale bar 5 µm. C) Quantification of SIRT1 in nucleus of astrocytes indicates that TG-AIN mice had more SIRT1 than WT-AIN ($p<0.0001$) and TG-BF mice ($p<0.05$). Moreover, TG-BF mice showed increase SIRT1 compared to WT-AIN ($p<0.05$). Data are expressed as the mean ± SD. $p<0.05$, ****$p<0.0001$.

We analyzed GluR-1 (an integral membrane protein belonging to the glutamate-gated ion channel family), PSD-95 (Post-synaptic density protein 95), Arc (Activity-regulated cytoskeleton-associated protein), and pre-synaptic synaptophysin protein levels in brain cortex. We observed that TG-AIN mice had more GluR-1, PSD-95, and Arc when compared to WT-AIN mice, indicating synaptic hyperactivity. Synaptophysin levels were lower in TG-BF compared to WT-AIN and TG-AIN mice ($p < 0.01$, both). TG-BF mice showed significant decreases in all those synaptic proteins (GluR-1, PSD-95, Arc and synaptophysin) compared to TG-AIN mice (Fig. 14 A-B).

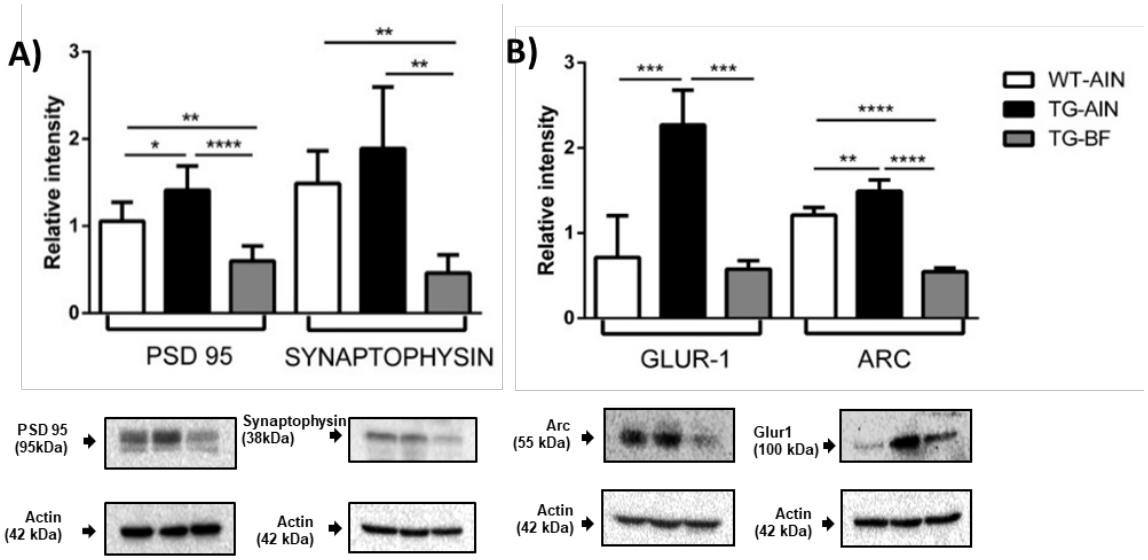

Figure 14. Immunoblots of synaptic proteins. . PSD95, synaptophysin, GluR-1, and Arc protein levels were evaluated in brain cortex. **A)** PSD95 levels were higher in TG-AIN compared to WT-AIN and TG-BF mice ($p < 0.05$ and $p < 0.0001$, respectively), while in TG-BF mice PSD95 levels were even lower than WT-AIN ($p < 0.01$). Synaptophysin levels were lower in TG-BF compared to WT-AIN and TG-AIN mice ($p < 0.01$, both). **B)** GluR-1 levels were higher in TG-AIN compared to WT-AIN and TG-BF ($p < 0.001$, both), while content of Arc protein was higher in TG-AIN mice compared to WT-AIN ($p < 0.01$) and TG-BF ($p < 0.0001$), but in TG-BF there were lower values compared to WT-AIN ($p < 0.0001$). Images below graphs are representative blots for each protein done eight (PSD95), four (Arc and GluR-1) or five (synaptophysin) times, in pool samples. Data represents mean ± S.D. *p< 0.05; **p <0.01, ***p < 0.001; ****p < 0.0001.

We also evaluated GSK-3β and p-GSK-3β protein content in the brain cortex by western blot. We observed that BF ingestion induced a significant increase in p-GSK-3β compared to WT-AIN and TG-AIN, with no changes in total GSK-3β. Therefore, the ratio p-GSK-3β/GSK-3β increased in TG-BF mice compared to the other groups (Fig. 15A). We also observed a decrease in p-AMPK in TG-BF compared to WT-AIN and TG-AIN, while the total AMPK increased in TG-AIN compared to WT-AIN. Therefore, the ratio pAMPK/AMPK decreased in TG-AIN and TG-BF compared to WT-AIN (Fig. 15B).

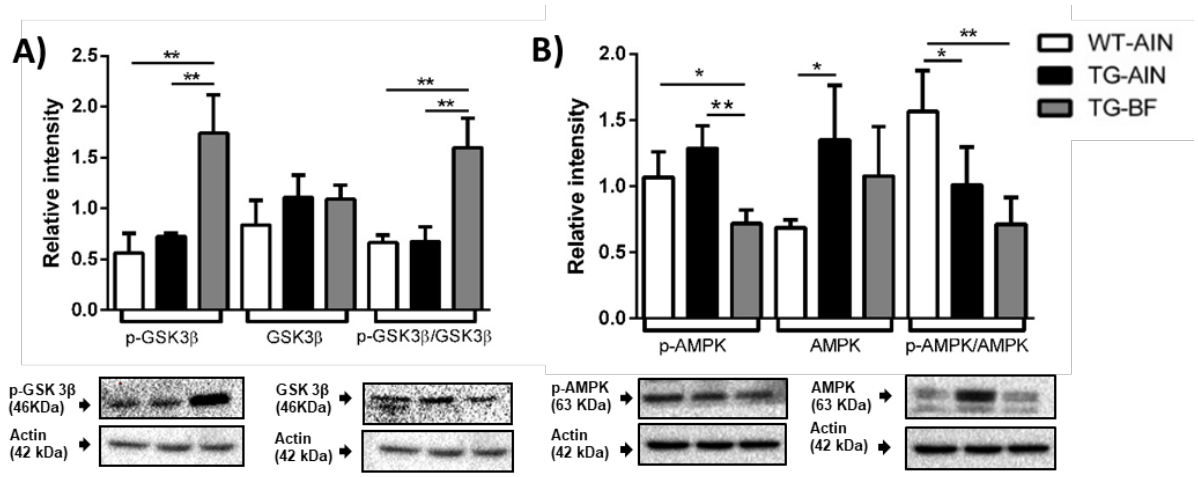

Figure 15. Protein levels of pGSK-3β/GSK-3β and pAMPK/AMPK in brain cortex. . A) Due to an increase level of pGSK- 3β in TG-BF mice compared to the other two groups (both, $p < 0.01$), there was increase in the ratio p-GSK-3β/GSK-3β in TG-BF mice compared to the other groups (both, $p < 0.01$). B) p-AMPK was decreased in TG-BF compared to WT-AIN ($p < 0.05$) and TG-AIN ($p < 0.01$) mice. AMPK increased in TG-AIN compared to WT-AIN ($p < 0.05$). Thus, ratio pAMPK/AMPK decreased in TG-AIN and TG-BF compared to WT-AIN ($p < 0.05$ and $p < 0.01$ respectively). Blots were normalized with α-actin. Images below graphs are representative blots for each protein done by quintuplicate (GSK3) or triplicate (AMPK) in pool samples. Data represents mean ± S.D. *$p < 0.05$;**$p < 0.01$.

6.2.6. Gut Microbiota: We analyzed the microbiota composition and diversity in feces of TG and WT mice. Alpha diversity was estimated by observed Shannon indexes. WT-AIN group showed the highest diversity followed by TG-BF group, whereas the TG-AIN group had the lowest bacterial diversity (Fig. 16A). Clustering the bacterial communities using principal component analysis (PCoA) revealed that GM in TG-AIN and TG-BF was different to that of the wild type **(Fig.16B)**.

At the phylum level, TG-AIN showed increased abundance of Bacteroidedetes($p < 0.01$) and Firmicutes ($p < 0.01$), whereas decreased abundance of Cyanobacteria($p < 0.0001$), Deferibacteres ($p < 0.0001$), Proteobacteria($p < 0.01$), TM7($p < 0.0001$), Tenericutes($p < 0.0001$), Verrucomicrobia($p < 0.0001$) compared to WT-AIN mice (Figure 16A) . After ingestion of BF there was an increased relative abundance of Actinobacteria ($p < 0.05$), Bacteroidedetes ($p < 0.01$), but decreased of Cyanobacteria($p < 0.0001$), Deferibacteres ($p < 0.0001$), Proteobacteria ($p < 0.001$), TM7($p < 0.0001$), Tenericutes ($p < 0.0001$), Verrucomicrobia ($p < 0.0001$) in TG versus WT-AIN mice (Fig 17A).

In TG mice, supplementation of BF caused an increase in the relative abundance of Tenericutes ($p < 0.05$) and Verrucomicrobia ($p < 0.0001$) compared to AIN diet

(Figure 17A). Accordingly, there were microbial alterations at the class, order, family, and genus level (Figure. 18,19,20,21 Table 5.

At species level there were important differences between TG-AIN and WT-AIN. TG-AIN presented more abundance of pro-inflammatory bacteria (Prevotella copri, Lactobacillus ruminis, Streptococcus anginosus, Actinobacillus parahaemolyticus and Haemophilus parainfluenzae), while with ingestion of BF they all were reduced. Furthermore, BF ingestion increased the relative abundance of anti-inflammatory bacteria (Bacteroides uniformis, Faecalibacterium prausnitzii and Akkermansia miciniphila) in TG mice (see Fig. 18B and Table. 4).

Those GM alterations in TG-mice let us to evaluate the levels of LPS in plasma samples. In addition, due to the dramatic increased in *Prevotella copri* in TG-AIN mice, a bacteria known as propionate producer, were evaluated propionate content and its SCFA´s receptor (FFAR3) in brain tissue.

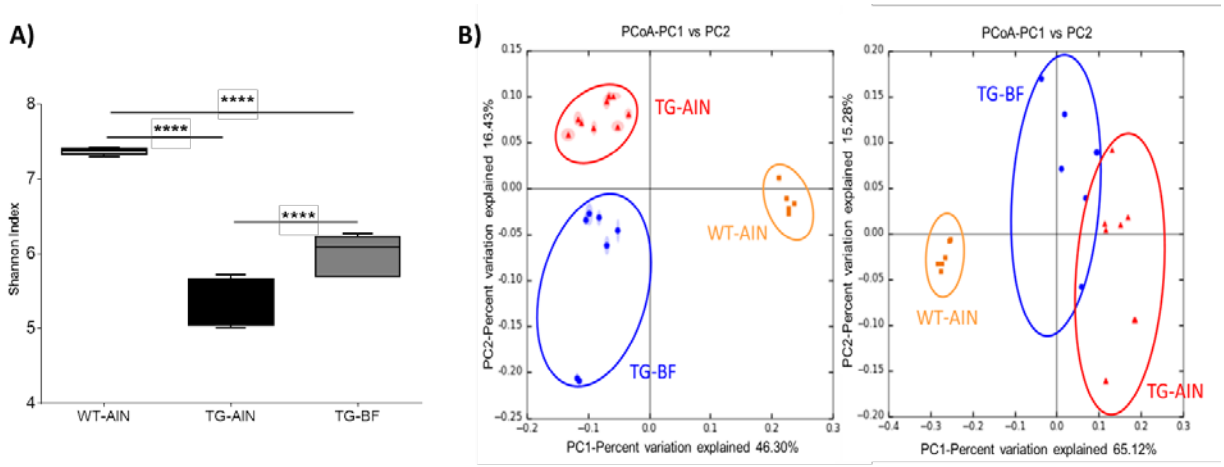

Figure 16: Gut microbiota modifications (A) Alpha diversity by Shannon Index in the tree groups studied showed statistical differences between WT-AIN and TG-AIN mice, and between TG-AIN and TG-BF mice (all, p< 0.0001) . B) Principal components analysis (PCoA) of unweighted (left) and weighted variables (right) by ANOSIM: unweighted: R=0.8836, p < 0.001; weighted: R= 0.8326, p =0.001.

A)

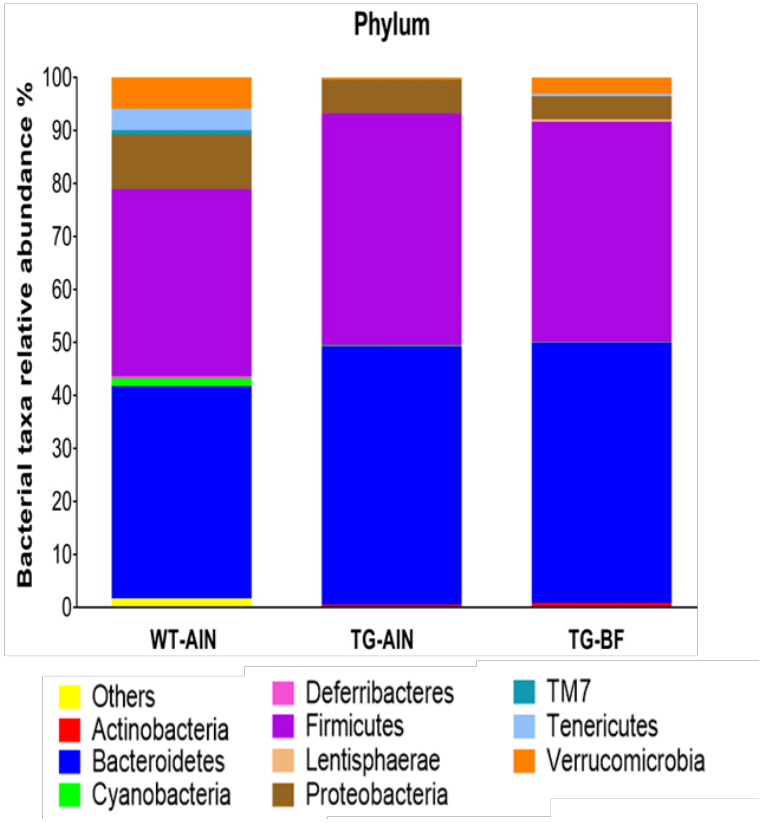
Phylum
Bacterial taxa relative abundance %
100
90
80
70
60
50
40
30
20
10
0
WT-AIN
TG-AIN
TG-BF
Others
Actinobacteria
Bacteroidetes
Cyanobacteria
Deferribacteres
Firmicutes
Lentisphaerae
Proteobacteria
TM7
Tenericutes
Verrucomicrobia

B)

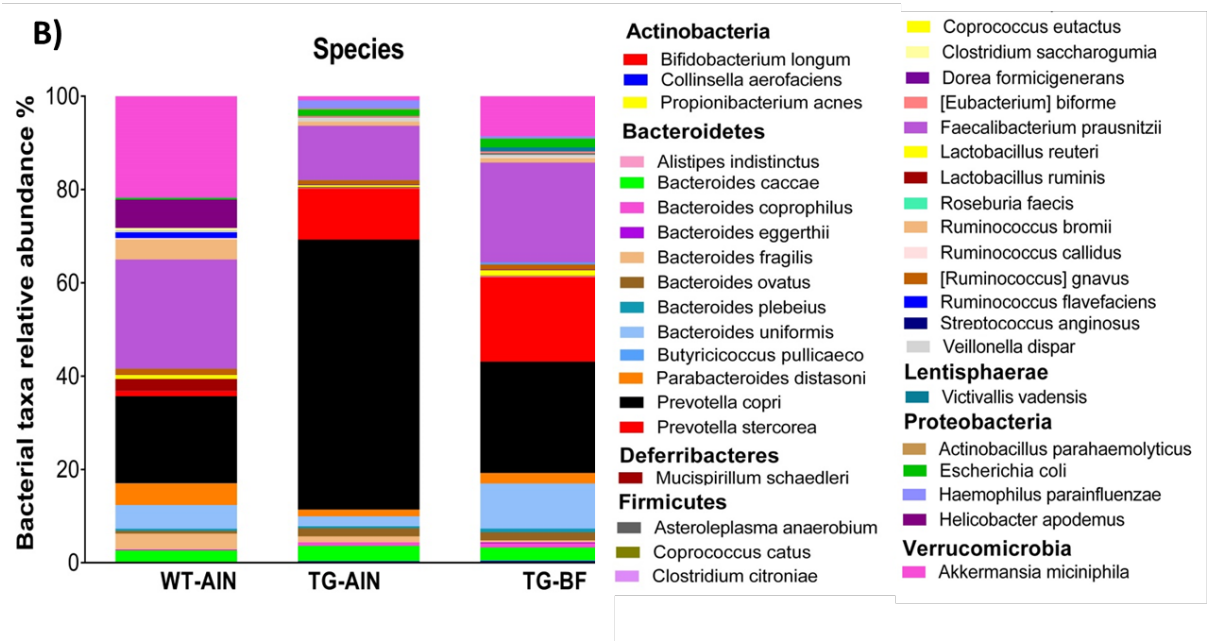
Species
Bacterial taxa relative abundance %
100
80
60
40
20
0
WT-AIN
TG-AIN
TG-BF
Actinobacteria
Bifidobacterium longum
Collinsella aerofaciens
Propionibacterium acnes
Bacteroidetes
Alistipes indistinctus
Bacteroides caccae
Bacteroides coprophilus
Bacteroides eggerthii
Bacteroides fragilis
Bacteroides ovatus
Bacteroides plebeius
Bacteroides uniformis
Butyricicoccus pullicaeco
Parabacteroides distasoni
Prevotella copri
Prevotella stercorea
Deferribacteres
Mucispirillum schaedleri
Firmicutes
Asteroleplasma anaerobium
Coprococcus catus
Clostridium citroniae
Coprococcus eutactus
Clostridium saccharogumia
Dorea formicigenerans
[Eubacterium] biforme
Faecalibacterium prausnitzii
Lactobacillus reuteri
Lactobacillus ruminis
Roseburia faecis
Ruminococcus bromii
Ruminococcus callidus
[Ruminococcus] gnavus
Ruminococcus flavefaciens
Streptococcus anginosus
Veillonella dispar
Lentisphaerae
Victivallis vadensis
Proteobacteria
Actinobacillus parahaemolyticus
Escherichia coli
Haemophilus parainfluenzae
Helicobacter apodemus
Verrucomicrobia
Akkermansia miciniphila

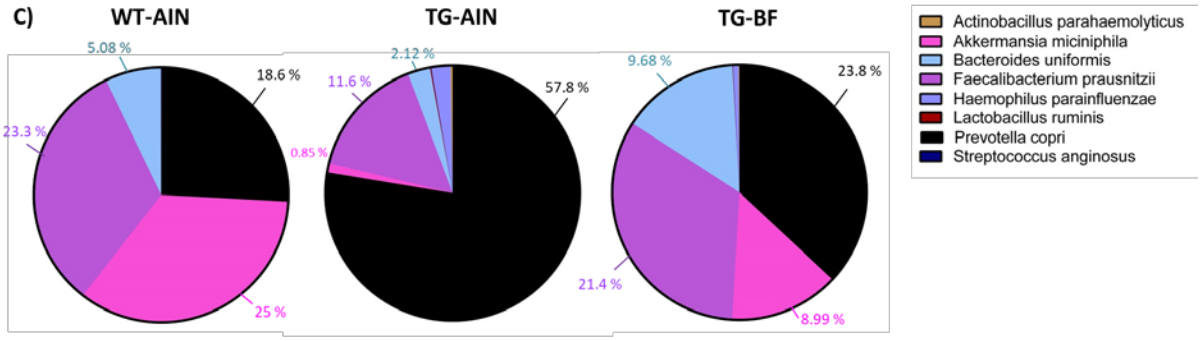

Figure 17. Gut microbiota modifications in transgenic mice, and its restoration by BF ingestion. (A) Relative abundance of bacteria at the phylum level in all the groups (significant differences are described in the main text). **(B)** Relative abundance of bacteria at the species levels. **C)** Pie chart of main bacterial species that showed significant changes between WT-AIN and TG-AIN compared to TG-BF mice. Relative abundances (%) are represented in the figure according to the color code of each species. Significant differences (increase or decrease) were as follow: *Actinobacillus parahaemolyticus* was not detected in WT-AIN, thus it increased by 20 % in TG-AIN, whereas TG-BF showed a decrease of 67 % compared to TG-AIN; *Akkermansa munciphila* showed a high relative abundance in WT-AIN mice (25% from all GM bacteria identified). In TG-AIN mice, *A. munciphila* decreased by 97 % compared to WT-AIN, but it increased up to 958 % in TG-BF mice; *Bacteroides uniformis* decreased by 42% in TG-AIN compared to WT-AIN mice, while it increased up to 90 % in TG-BF compared to WT-AIN mice, and 356 % in TG-BF compared to TG-AIN mice; *Faecalibacterium prausnitzii* decreased by 50 % in TG-AIN compared to WT-AIN, but it increased 85 % in TG-BF compared to TG-AIN; *Haemophilus parainfluenzae* increased by 2346 % in TG-AIN compared to WT-AIN, but decreased by 75 % in TG-BF compared to TG-AIN; *Lactobacillus ruminis* was not detected in WT-AIN mice, thus in TG-AIN increased by 9 % compared to WT-AIN, and decreased by 67 % in TG-BF compared to TG-AIN; *Prevotella copri* had 25% of relative abundance in WT-AIN mice, but in TG-AIN it increased up to 210% compared to WT-AIN, but it decreased by 59 % in TG-BF compared to TG-AIN; *Streptococcus anginosus* was not detected in WT-AIN, so it increased 3 % in TG-AIN, but in TG-BF mice it showed a decrease of 59 % compared to TG-AIN. Statistical differences can be found in Table 4.

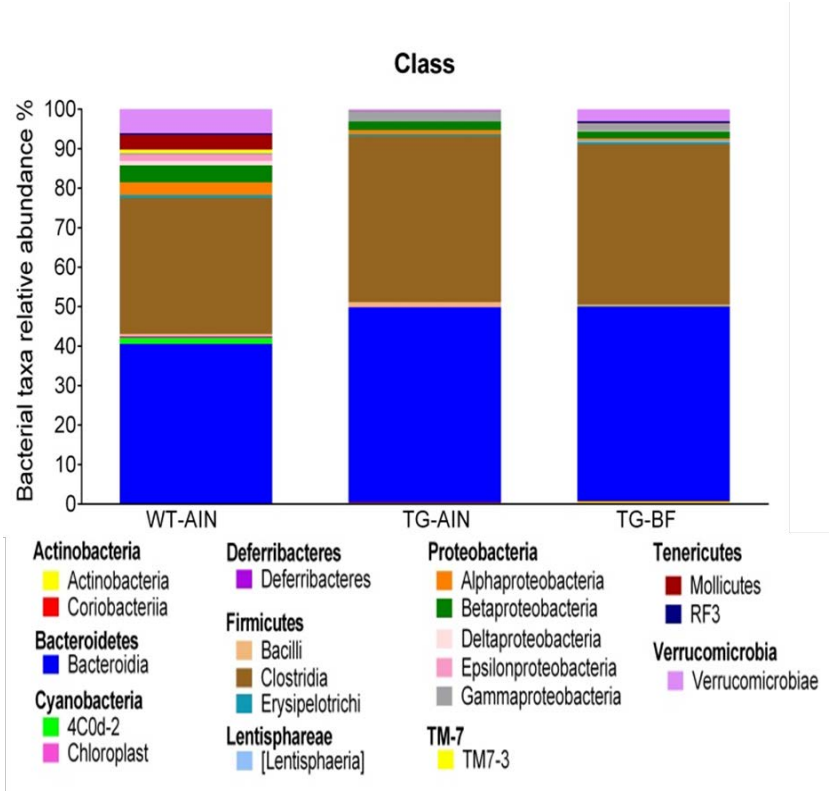

Figure 18. Bacterial relative abundance at the class level in WT-AIN, TG-AIN, and TG-BF mice.

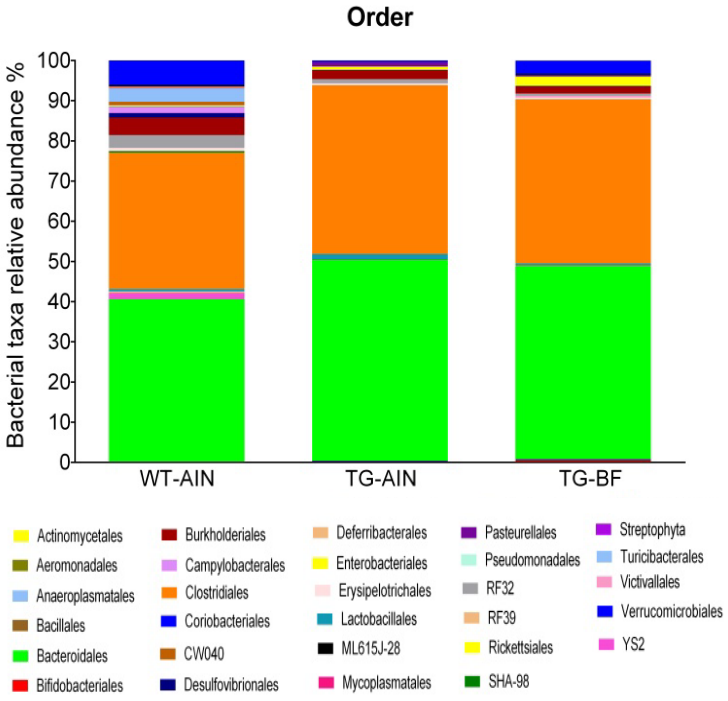

Figure 19. Bacterial relative abundance at the order level in WT-AIN, TG-AIN, and TG-BF mice.

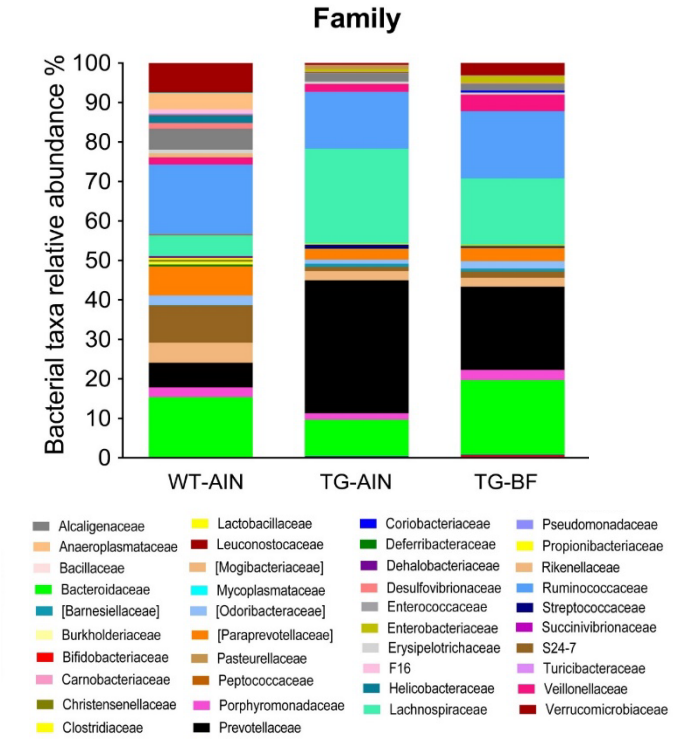

Figure 20. Bacterial relative abundance at the family level in WT-AIN, TG-AIN, and TG-BF mice.

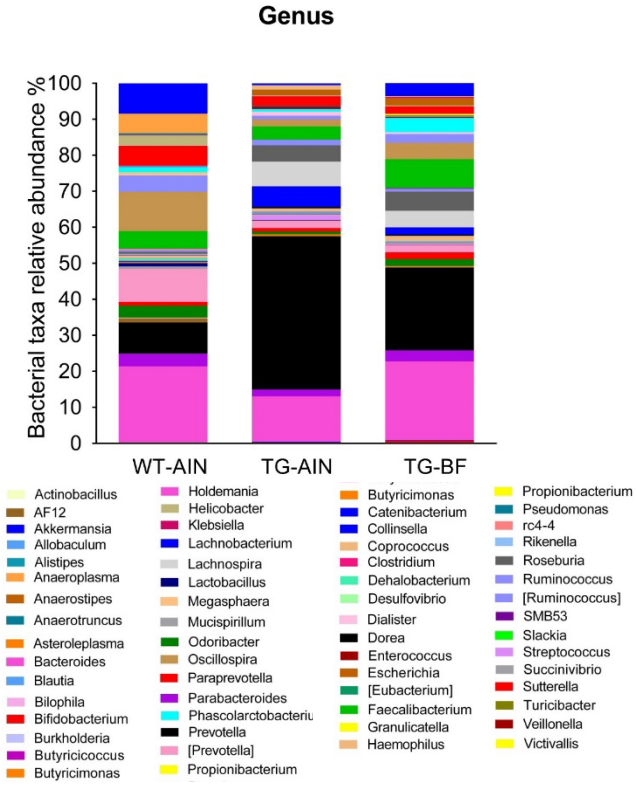

Figure 21. Bacterial relative abundance at the genus level in WT-AIN, TG-AIN, and TG-BF mice. Values and statistical differences are shown in Table 5

TABLE-4: Taxonomic classification of pyrosequences from bacterial communities at the species levels.

Species	WT-AIN	TG-AIN	TG-BF
Propionibacterium acnes	0.050±0.024	0.0167±0.005	0.006±0.002
Bifidobacterium longum	0	0.05±0.017	0.0904±0.030*
Collinsella aerofaciens	0	0.275±0.1718	0.321±0.101
Bacteroides caccae	2.596±0.157	3.274±1.507	2.825±0.747
Bacteroides coprophilus	0.088±0.032	0.761±0.710	0.922±0.833
Bacteroides eggerthii	0.105±0.0118	0.013±0.001	0.230±0.171
Bacteroides fragilis	3.425±0.187	1.285±0.566**	0.413±0.168***
Bacteroides ovatus	0.582±0.070	1.767±0.555	1.750±0.318
Bacteroides plebeius	0.473±0.059	0.409±0.355	0.777±0.750
Bacteroides uniformis	5.085±0.367	2.122±0.670	9.681±1.380*****
Parabacteroides distasonis	4.642±0.230	1.407±0.645**	2.238±0.599*
Prevotella copri	18.66±0.567	57.88±3.157 ****	23.86±2.791****
Prevotella stercorea	1.107±0.0209	10.95±1.199	18.13±5.677**
Alistipes indistinctus	0.015±0.0012	0.068±0.0422	0.129±0.060
Mucispirillum schaedleri	2.572±0.256	0.001±0.003****	0.001±0.003****
Lactobacillus reuteri	0.457±0.108	0.047±0.050****	0.015±0.0064*****
Lactobacillus ruminis	0	0.091±0.014***	0.030±0.011**
Streptococcus anginosus	0	0.034±0.007**	0.014±0.006*
Clostridium citroniae	0	0.018±0.007	0.017±0.005
Coprococcus catus	0.016±0.010	0.01±0.021*	0.086±0.021
Coprococcus eutactus	0.39±0.048	0.37±0.126	1.158±0.392
Dorea formicigenerans	0.014±0.009	0.175±0.015***	0.166±0.040**
Roseburia faecis	0	0.033±0.009*	0.0104±0.003
[Ruminococcus] gnavus	1.335±0.172	0.864±0.323	1.054±0.344
Butyricicoccus pullicaecorum	0.031±0.013	0.067±0.025	0.445±0.211
Faecalibacterium prausnitzii	23.35±0.177	11.59±1.337**	21.42±3.404**
Ruminococcus bromii	4.358±0.358	0.885±0.387****	0.966±0.444****
Ruminococcus callidus	0.269±0.059	0.036±0.006**	0.132±0.072
Ruminococcus flavefaciens	1.220±0.107	0.001±0.004****	0.007±0.002****
Veillonella dispar	0.393±0.032	0.824±0.211	0.591±0.163
Asteroleplasma anaerobium	0.006±0.007	0.051±0.007	0.330±0.316
Clostridium saccharogumia	0.503±0.092	0.001±0.001****	0.007±0.003****

[Eubacterium] biforme	0.034±0.012	0.295±0.044*	0.369±0.090**
Victivallis vadensis	0.01364±0.008640	0.002±0.001	0.8707±0.580
Helicobacter apodemus	6.051±0.337	0.008±0.00242****	0.008±0.003****
Escherichia coli	0.368±0.048	1.333±0.73	1.836±1.129
Actinobacillus parahaemolyticus	0.0	0.208±0.021****	0.0694±0.023***
Haemophilus parainfluenzae	0.074 ±0.017	1.810±0.271****	0.457±0.1225***
Akkermansia miciniphila	25.05±1.073	0.850±0.305****	8.998±0.688*****,***

Significances between WT-AIN vs TG-AIN are reported in black; WT-AIN vs TG-BF are reported in red, TG-AIN vs TG-BF are reported in green. Data represents mean ± S.E.M. *p < 0.05; **p < 0.01; ***p < 0.001; ****p < 0.0001

TABLE-5: Taxonomic classification of pyrosequences from bacterial communities at the Genus levels.

GENUS	WT-AIN	TG-AIN	TG-BF
Propionibacterium	0.0107±0.005	0.01±0.002	0.002±0.001
Bifidobacterium	0	0.289±0.034	0.736±0.297*
Collinsella	0	0.170±0.109	0.161±0.050
Slackia	0	0.013±0.006	0.018±0.012
Bacteroides	21.37±0.648	12.57±1.227**	21.86±2.206***
Parabacteroides	3.507±0.131	1.918±0.893	3.057±0.489
Prevotella	8.69±0.684	42.53±1.775****	23.00±3.709****, **
AF12	1.153±0.112	0.010±0.001****	0.003±0.002****
Alistipes	0.004±0.002	0.040±0.026	0.059±0.03
Rikenella	0.115±0.018	0.0002±0.0002****	0.001±0.0008****
Butyricimonas	0.121±0.009	0.529±0.115*	0.371±0.106
Odoribacter	3.255±0.121	0.726±0.127*	1.921±1.106
Paraprevotella	1.095±0.030	0.961±0.377	1.886±0.686
[Prevotella]	9.166±0.126	2.099±0.447****	1.940±0.832****
Mucispirillum	0.647±0.075	0.006±0.002****	0.0007±0.0007****
Granulicatella	0	0.013±0.003*	0.003±0.002
Enterococcus	0.023±0.009	0.02±0.018	0.035±0.021

Lactobacillus	0.889±0.126	0.148±0.011****	0.043±0.011****
Streptococcus	0.034±0.010	1.433±0.245****	0.354±0.070***
Turicibacter	0.063±0.011	0.0002±0.0002****	0****
Clostridium	0.147±0.013	0.072±0.029	0.109±0.026
SMB53	0.383±0.032	0.062±0.022****	0.022±0.02****
Dehalobacterium	0.631±0.047	0.006±0.002****	0.002±0.001****
Anaerostipes	0.016±0.003	0.036±0.020	0.083±0.03
Blautia	0.104±0.008	0.660±0.290	0.431±0.145
Clostridium	0	0.010±0.004	0.007±0.002
Coprococcus	0.809±0.052	0.927±0.108	1.531±0.420
Dorea	0.044±0.005	0.423±0.038***	0.333±0.093**
Lachnobacterium	0.141±0.028	5.7101±0.341****	1.99±0.298****,**
Lachnospira	0.206±0.02	6.8±0.340***	4.661±1.631*
Roseburia	0.612±0.020	4.593±0.312***	5.321±1.03***
[Ruminococcus]	0.481±0.055	1.516±0.271**	0.752±0.153*
rc4-4	0.343±0.043	0.002±0.001****	0.003±0.001****
Anaerotruncus	0.056±0.009	0****	0****
Butyricicoccus	0.008±0.003	0.040±0.016	0.187±0.080*
Faecalibacterium	4.810±0.053	3.706±0.561	7.999±0.531****,**
Oscillospira	10.92±0.243	1.915±0.303****	4.583±0.738**,****
Ruminococcus	4.502±0.135	1.033±0.265****	2.381±0.406*,***
Dialister	0.123±0.023	1.094±0.314*	0.590±0.149
Megasphaera	0.785±0.131	0.001±0.0005****	0****
Phascolarctobacterium	1.457±0.083	0.737±0.464	3.971±1.010**,*
Veillonella	0.098±0.008	0.492±0.130*	0.288±0.084
Allobaculum	0.112±0.019	0.001±0.0006****	0.001±0.001****
Asteroleplasma	0.002±0.002	0.030±0.005	0.129±0.123
Catenibacterium	0.01±0.008	0.112±0.013***	0.047±0.019*
Clostridium	0.126±0.023	0.0007±0.0004****	0.003±0.001253*** *
Holdemania	0.019±0.005	0.011±0.005	0.001±0.002

[Eubacterium]	0.009±0.003	0.175±0.029**	0.182±0.05**
Victivallis	0.003±0.002	0.001±0.0004	0.431±0.311
Sutterella	5.560±0.265	2.758±0.336****	2.083±0.386****
Burkholderia	0.005±0.002	0.025±0.009	0.026±0.011
Bilophila	0.050±0.012	0.028±0.005	0.078±0.011**
Desulfovibrio	0.088±0.014	0.015±0.008	0.134±0.07
Helicobacter	2.585±0.091	0.025±0.005****	0.008±0.003****
Succinivibrio	0.144±0.015	0.135±0.134	0
Escherichia	0.09±0.010	1.597±0.501	2.060±1.031
Klebsiella	0.073±0.011	0.043±0.008	0.339±0.179
Actinobacillus	0	0.123±0.014****	0.031±0.010****
Haemophilus	0.018±0.004	1.073±0.170****	0.206±0.057***
Pseudomonas	0.375±0.044	0.027±0.009****	0.024±0.009****
Anaeroplasma	5.452±0.219	0.008±0.002****	0.003±0.002****
Akkermansia	8.438±0.561	0.49±0.162****	3.501±0.274****,*** *

Statistical differences between groups: WT-AIN vs TG-AIN are reported in black, WT-AIN vs TG-BF are reported in red, TG-AIN vs TG-BF are reported in green. Data represents mean ± S.E.M. *p < 0.05; **p < 0.01; ***p < 0.001; ****p < 0.0001;

6.2.7. Propionate level and FFAR3 in brain: As prefrontal cortex (PFC) is an area related to T-maze working memory performance, and we have observed working memory impairments in TG mice, we evaluated levels of propionate in this brain region. Propionate levels were larger in TG-AIN mice compared to WT-AIN and TG-BF mice in PFC (Figure 22A). We also quantified SCFAs receptor FFAR3/GPR41 in same brain cortex. FFAR3 has a high affinity for propionate. We observed that FFAR3 was more abundant in TG-AIN mice compared to WT-AIN mice, whereas BF ingestion decreased those values in TG mice (Figure 22B).

6.2.8. Lipopolysaccharide (LPS) levels in plasma: LPS levels in plasma were larger in TG-AIN compared to WT-AIN mice ($p<0.01$), while BF ingestion lower LPS concentration in TG mice ($p<0.05$) (Figure 22C).

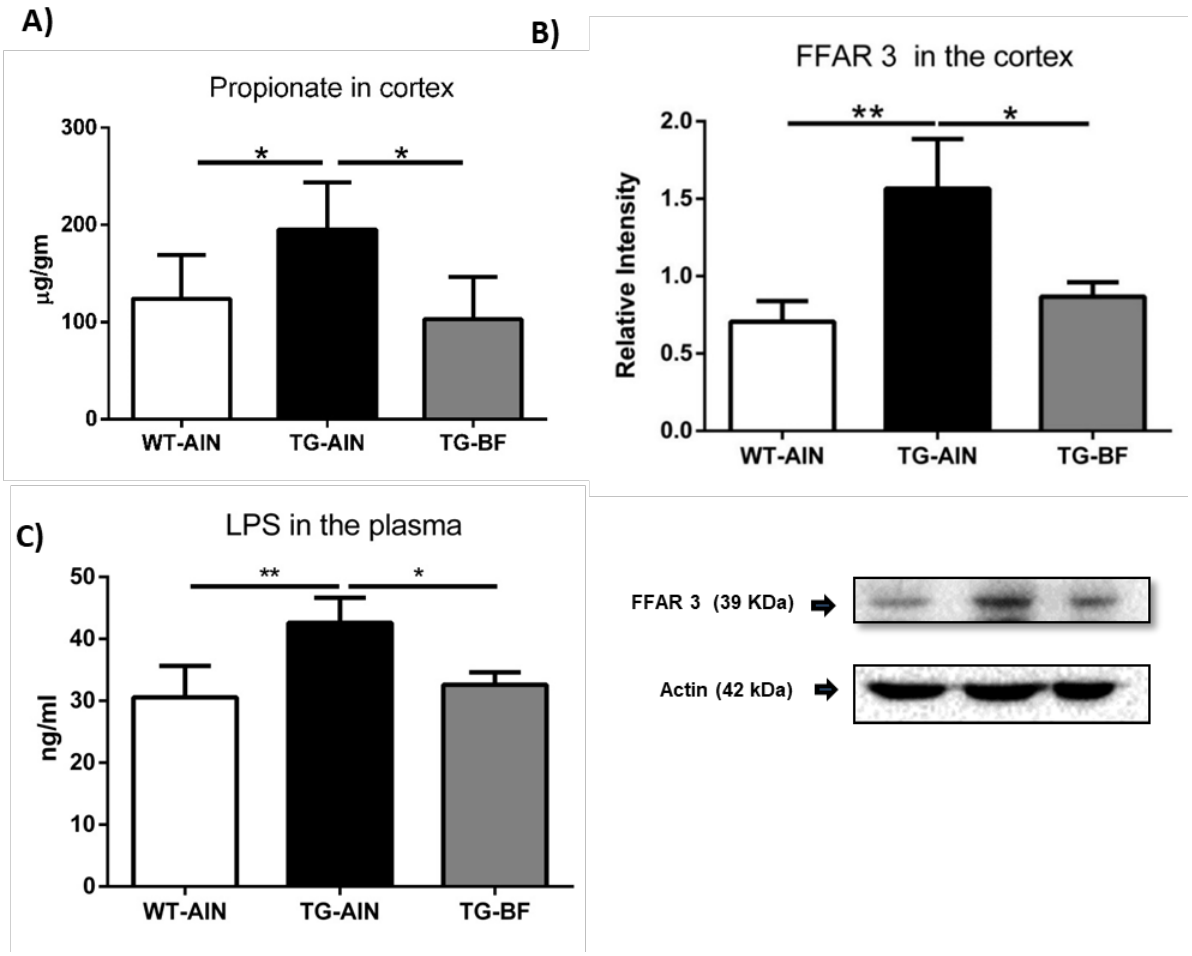

Figure 22. Bacterial products in brain and plasma samples. A) Propionate levels in PFC were larger in TG-AIN compared to WT-AIN mice ($p<0.05$) and ingestion of BF reduced those levees ($p<0.05$). B) FFAR3 receptor levels were higher in TG-AIN mice compared to WT-AIN and TG-BF mice ($p<0.01$ and $p<0.05$, respectively). C) LPS plasma levels were higher in TG-AIN compared to WT-AIN and TG-BF mice ($p<0.01$ and $p<0.05$, respectively).). Images below graphs are representative blots for each protein done by quadruplicated in pool samples. Data represents mean ± S.D. $^{**}p < 0.01$;$^{*}p < 0.05$.

6.2.9. Levels of short-chain fatty acids in feces of TG at different ages: Acetate, butyrate, and propionate are the most abundant SCFAs produced by GM (Ríos-Covián et al., 2016). We observed an increase in propionate producing bacteria in TG-AIN mice compared to WT-AIN mice, an effect accompanied by increased propionate in brain tissue. Propionate is a potent neurotoxic agent. Then, we sought to evaluate whether propionate levels increased in an age-dependent manner according to the progression of the pathology. SCFAs levels (acetate, butyrate and propionate) were measured in feces from WT and TG mice along the ontogeny (3-, 6- and 11-month-old). In WT mice, total SCFA concentration decreased at 6- and 11-months of age in comparison to 3-months of age (both, $p < 0.05$), whereas in TG

Table 6 Levels of short-chain fatty acids in feces of TG at different ages

	ACETATE (µg/gm)		PROPIONATE (µg/gm)		BUTYRATE (µg/gm)		TOTAL SCFA (µg/gm)	
11months	42010 ± 2546[a]	38019 ± 1723	13153 ± 2252	18176 ± 2481	14447 ± 2246[b,c]	13014 ± 1646[b]	58954 ± 7321[b]	67054 ± 4139[b]
6 months	25487 ± 2703[b]	26329 ± 2862	**12617 ± 4305**	**32602 ± 5448***	25810 ± 10376[b]	37989 ± 5396[a]	78941 ± 28372[b]	164245 ± 16849[a]
3 months	36009 ± 4069[b]	37705 ± 5457	24661 ± 12851	29740 ± 5248	58617 ± 8349[a]	32125 ± 6289[a]	185533 ± 19064[a]	172838 ± 29217[a]
GENOTYPE	**WT**	**TG**	**WT**	**TG**	**WT**	**TG**	**WT**	**TG**

In WT mice, total SCFA concentration decreased at 6- and 11-months of age in comparison to 3-months of age (both a>b, $p<0.05$), whereas in TG mice the total SCFA concentration decreased at 11 months of age compared to 3- and 6-months-old mice (both a>b, $p<0.01$). Acetate concentration increased in WT mice at 11 months-of age compared to 6 months-of age (a>b, $p<0.05$). Butyrate decreased in WT mice at 6 and 11months in comparison to 3months (a>b, $p<0.05$, and a>c, $p<0.01$). In TG mice, butyrate decreased at 11 months in comparison to 3 months and 6 months (a>b, 3 months vs 11 months, by $p<0.05$; 6 months vs 11 months, $p<0.01$). Regarding genotype effect, we observed that propionate concentration increased in TG compared to WT mice at 6 months of age (*$p<0.05$). Data represents mean ± S.EM.

mice the total SCFA concentration had a age delay, as it decreased only in 11 month old mice compared to 3- and 6–month-old mice (both, $p < 0.01$). Regarding acetate concentration in WT, we observed an increase in 11-month-old mice compared to the 6-month-old group ($p < 0.05$). No changes in acetate concentration were observed in TG mice. Butyrate in WT mice decreased at 6- and 11-months of age in comparison to 3-months-old animals ($p < 0.05$ and $p < 0.01$, respectively). Notably, in TG mice, the decrease in butyrate was not as early as in WT, since differences were observed between 11- and 6-month-old mice versus 3-month-old group ($p < 0.05$ and $p < 0.01$, respectively). Regarding the genotype effect, we observed that propionate concentration increased in TG compared to WT mice at 6 months of age ($p < 0.05$) (Table 6).

CONCLUSION PART I.

In study, we observed that female TG mice presented intracellular Aβ aggregates in cortex and tau hyperphosphorylation in cortex and hippocampus, along with increased astrocyte activation and SIRT1, synaptic and metabolic brain alterations compared to WT mice. Those events were accompanied by gut microbiota alterations, increased LPS and propionate concentration in feces and brain samples. An ontogeny study revealed that butyrate concentration in feces decreased, while propionate levels increased with aging. SCFAs can be taken up by astrocytes as metabolic substrates, and we observed an increased SIRT1 in astrocytes, suggesting that these glial cells in TG mice have a preference for a mitochondrial metabolism. Therefore, we aimed to determine whether this propionate/butyrate ratio impact astrocyte metabolism by use of a mix cell-culture transfected with nanosensors-FRET to assess glycolytic metabolism, and lactate production. The results from this experiments are described in Part II.

PART 2

7. Evaluating the differential effect of short-chain fatty acids on the astrocyte metabolism by use of FRET nanosensors.

7.2 Methodology:

Mixed F1 male mice (C57BL/6J) were used in this study. All experiments were approved by the Centro de Estudios Científicos animal Care and Use Committee, Chile. Mixed cortical cultures of neuronal and glial cells were prepared from 1- to 3-day old neonatal mice**.**

7.2.1. Isolation of astrocytes:

Cover slips were immersed in alcohol, flamed to remove alcohol and were put in culture plate. Approximately 0.5 ml of Poly-Lysine was added on the cover slip and incubated for 15 minutes inside the hood. Poly-lysine was removed from the cover slip and recovered for reuse. Plates were washed with 2 ml of sterile ultra-pure water two times. Plates were left with water in an oven at 37 ° C until the next day.

Mouse was decapitated and brain was isolated. Two hemispheres of the brain were separated. Meninges, hippocampus and ventricle remnants were removed. Dissected cortex was placed in falcon tube with 2ml Hank's solution. To the Hank's solution and cortex, 2 ml of Trypsin-EDTA 1X was added and incubated for 5 min in a water bath at 37 °C. After 5 minutes, trypsinization was stopped by adding approximately 4 ml minimum essential medium (MEM) with 10% Fatal Bovine Serum (FBS). Medium was discarded and then 800µl of MEM with 10% FBS was added, then with a P1000 micropipette tips, the cortex was disintegrated by gently pipetting 50 times and avoiding foam. Volume is made up to 2 ml with MEM 10% FBS. Disintegrated tissue was let to decant for 3-5 minutes then with a filter tip, material that was not disintegrated, was removed from the bottom of the tube (remnants of meninges, etc.). Then volume was made up to 4 ml (for two cortical hemisphere) with MEM 10% FBS. 1.5 mL of MEM 10% FBS and 500 µl of cell suspension was added to each poly-lysine coated covers slip. So that final volume is 2 ml of MEM 10% FBS. Coverslips were incubated for one hour in an incubator at 37 °C, 5% CO2. Medium was changed with Neuro basal B27 without FBS and Coverslips were placed in an incubator at 37 °C, 5% CO2. Medium was changed every 3rd day.

7.2.2. Treatment of astrocyte with short chain fatty acids (propionate and butyrate):

Cultures were maintained at 37°C in a humidified atmosphere of 5% CO2. 7 day old astrocytic culture was infected with FLII12Pglu700mΔ6 overnight. Next morning medium was changed and the culture was treated with different concentration of propionate (0.25 mM, 0.5 mM and 2mM), butyrate (0.125mM and 2mM) or β hydroxyl-butyrate (2mM), as positive control, for 3 days. On 11th day fluorescence imaging is done (see 7.2.4 and 7.2.5).

7.2.3. Lacatate measurement by Colorimetry: Lactate was measured in the culture medium of the cells. Lactate was measured by an end point enzymatic method that uses lactate dehydrogenase to convert lactate to pyruvate with the concomitant reduction of NAD to NADH, which is then measured at 340 nm (Buttery et al., 1985).100 µl of the medium from primary culture treated with propionate and butyrate was collected and left in an Eppendorf tube at room temperature for 15-20min. 2.8ml of the glycine-hydrazine buffer, 0.6ml of NAD^+ and 0.2ml of water are placed in a well of 96 well plate and used as a blank. 2.8ml of the glycine-hydrazine buffer, 0.6ml of NAD^+ (0.02M), 0.2ml of sample or standard was added. 0.4ml of lactate dehydrogenase (2mg / ml) was added to the each well, the mixture was left to incubate at 40 °C for 1 hour and then its absorbance was determined at 340nm.

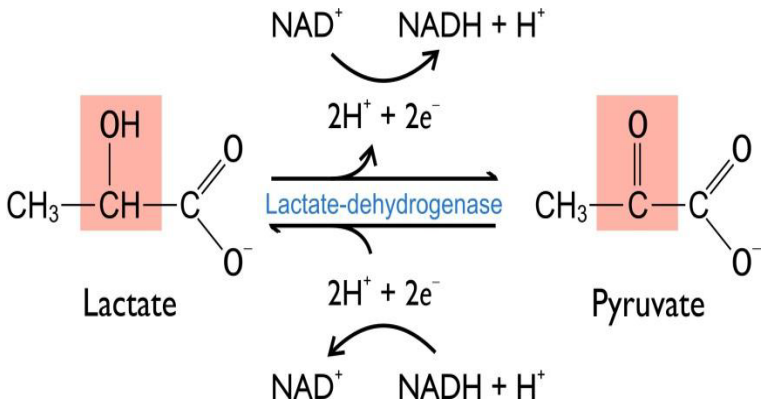

Figure 23: Lactate analysis by colorimetry: Lactate was analysed based on principle of conversion lactate and pyruvate by lactate dehydrogenase with the concomitant reduction of NAD to NADH, which is then measured at 340 nm.

7.2.4. Imaging of astrocytes treated with short chain fatty acid

Cultured cells treated with SCFA were imaged with with Olympus IX70 or BX51 microscopes equipped with Optosplits and a Hamamatsu Orca camera. Cells were superfused at room temperature with a 95% air and 5% CO2-gassed solution of the

following composition (mM): 112 NaCl, 3 KCl, 1.25 CaCl2, 1.25 MgCl2, 2 glucose, 1 Na-lactate, 10 HEPES and 24 NaHCO3, pH 7.4 (Valdebenito et al., 2015). During imaging we exposed astrocytes to zero glucose (no glucose on the medium), Cytochalasin B (20 µM) and Azide (5mM) solutions. We recorded changes in fluorescence intensity on exposure to this stimuli, florescence was then converted to glucose concentration.

7.2.5. Genetically encoded Förster Resonance Energy Transfer (FRET) sensors:

Genetically encoded intracellular fluorescent sensors are used to image intracellular concentration of many molecules. FRET sensors report changes in energy transfer between a donor and a acceptor fluorescent protein that occur when an attached sensor domain undergoes a change in conformation in response to ligand binding. The FRET efficiency depends not only on the distance and the relative orientation, but also on the overlap between the donor's emission and the acceptor's absorption spectra (Lindenburg and Merkx, 2014).

We used the FRET sensor AAV9-GFAP- FLII12Pglu700mΔ6 (Addgene 17866) for live intracellular glucose measurement in astrocytes. It has Cyan Fluorescent Protein (CFP) and Yellow fluorescent protein (YFP) and domain for glucose/galactose-binding, glucose serves as the ligand. Glucose binding to glucose/galactose-binding protein causes a conformational change and consequently fluorophores move closer increasing FRET, which can be seen as increase in fluorescence intensity (Muhič et al., 2015). As the concentration of glucose changes in the cell, there will be changes in the fluorescence. In order to deliver sensor intracellularly adenovirus was used, and for astrocytic specific delivery it has GFAP promoter which is specific for astrocytes. Adenoviral vectors showed a very high selectivity for astrocytes over neurons, with a ratio >100.

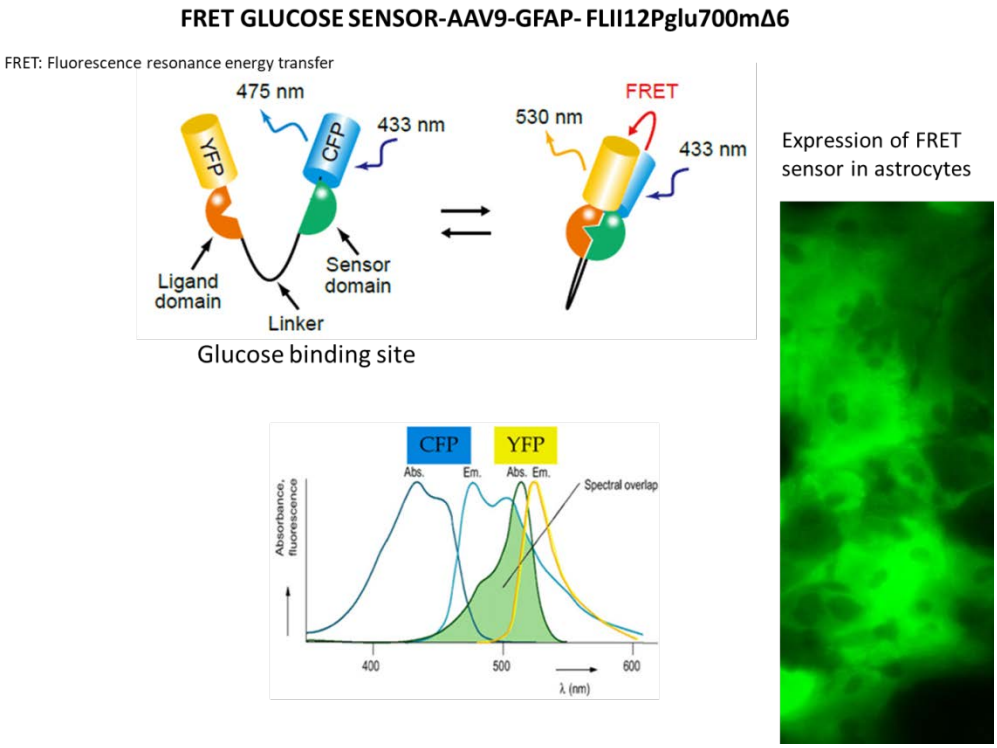

Figure 24: Structure and principle of working of FRET sensor AAV9-GFAP- FLII12Pglu700mΔ6 for glucose detection. Expression of FRET sensor in astrocyte.

7.2.6. Statistical analysis Data are expressed as the mean ± S.D. One-way ANOVA followed by Tukey´s test analysis as recommended by the Software (GraphPad v.6). All results were considered statistically significant at $p<0.05$.

7.3 RESULTS

7.3.1. Effect of different concentration of propionate on glucose consumption rate and glucose depletion:

We calculated glucose consumption rate by blocking glucose transporter with Cytochalasin B (Cyto B), a specific glucose transporter (GLUT1) blocker (Fig. 25). GLUT1 transport glucose into and out of astrocytes, therefore, when GLUT1 is blocked there is no entry or exit of glucose from the cell. Under this condition, the decreased intracellular glucose concentration is due to consumption by the cell. The rate at which glucose concentration decreased was considered as glucose consumption rate.

Glucose depletion rate was defined as rate the decrease in glucose concentration when mitochondrial oxidative phosphorylation is blocked. We blocked mitochondrial oxidative phosphorylation with Azide (chemical anorexia due to inhibition of

mitochondrial function (Ishii et al., 2014). (Fig. 25). When oxidative phosphorylation is blocked, there is compensatory increase in glycolysis that leads to further decrease in intracellular glucose concentration. The rate at which glucose concentration decreases was considered as glucose depletion rate.

We first perform a dose-response curve to assess the optimal dose of propionate to effect glucose consumption rate and glucose depletion. We used 0.25mM, 0.5mM and 2mM of propionate**.**

Glucose consumption rate was significantly higher in cells treated with 0.25mM, 0.5mM and 2mM propionate compared to control cells ($p < 0.0001$, for all) (Fig. 26A). Glucose depletion rate was significantly higher in cells treated with 2mM Propionate compared to control cells ($p < 0.0001$) and compared to 0.25mM, 0.5mM propionate treated cells ($p < 0.01$, $p < 0.05$**) (Fig. 26B).** Thus, we define 2 mM propionate as optimal dose to induce changes in glycolytic and oxidative metabolism.

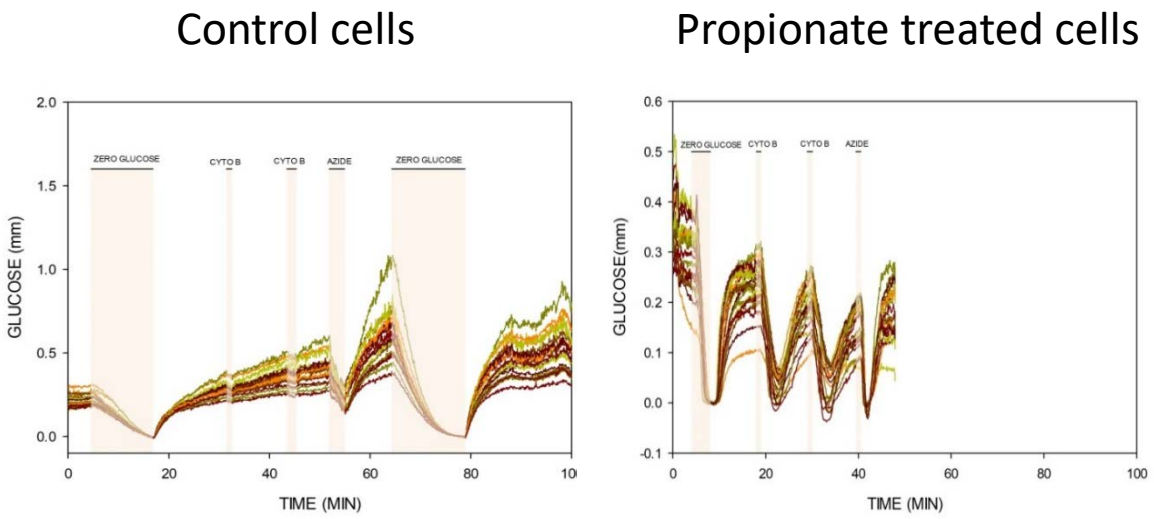

Figure 25. Changes in intracellular glucose concentration in control and propionate treated cells on exposure to different stimuli. Changes in intracellular glucose concentration under zero glucose condition, in CYTO-B,Azide and Propionate treated cells. Each line represents data from individual astrocytes. We run 4 experiments for each condition, and 10-15 cells were used for analysis.

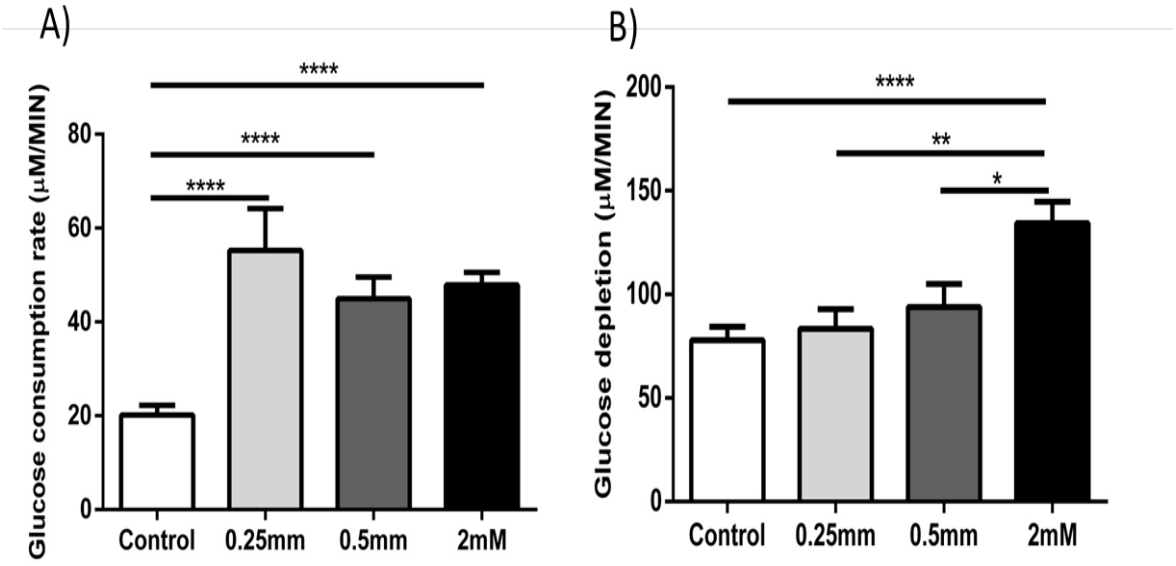

Figure 26: Effect of different concentrations of propionate on glucose consumption rate and glucose depletion: (A) Glucose consumption rate was significantly higher in cells treated with 0.25mM, 0.5mM and 2mM Propionate compared to control cells ($p < 0.0001$, for all), (B) Glucose depletion was significantly higher in cells treated with 2mM Propionate compared to control cells ($p < 0.0001$),and compared to 0.25mM, 0.5mM propionate treated cells ($p < 0.01$, $p < 0.05$). Data are expressed as the mean ± S.D. Statistical analysis was performed using one-way analysis of variance (ANOVA) with a post-hoc Tukey's multiple comparison test (GraphPad). All results were considered statistically significant at $p<0.05$, ****$p < 0.0001$ **$p < 0.01$,*$p < 0.05$.

7.3.2. Effect of different concentration of butyrate on glucose consumption rate and glucose depletion:

We first run a dose-response curve to set the optimal dose of butyrate the glucose consumption rate and glucose depletion. We used 0.125mM and 2mM of butyrate. Glucose consumption rate was significantly lower in cells treated with 0.125mM and 2mM butyrate compared to control cells ($p < 0.0001$, for both) (Fig. 27, 28A). Glucose depletion was significantly lower in cells treated with 2mM butyrate compared to control cells ($p < 0.0001$) and compared to 0.125mM butyrate treated cells ($p < 0.001$) (Figure 27, 28B).

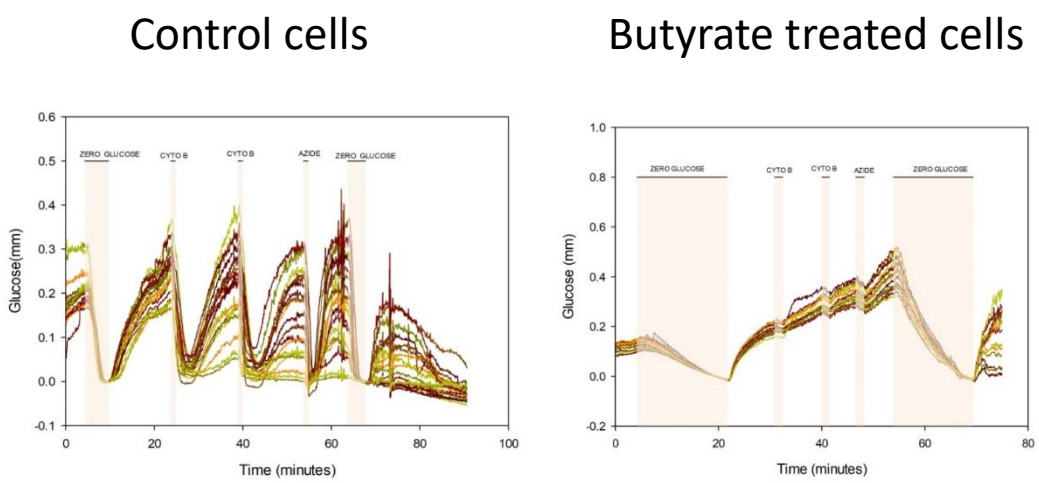

Figure 27. Changes in intracellular glucose concentration in control and butyrate treated cells on exposure to different stimuli. Changes in intracellular glucose concentration on exposure to zero glucose condition, CYTO-B and Azide in A) Control cells B) Butyrate treated cells. Each line represents data from a individual astrocytes. N for each condition was 4, 10-15 cells were used in each experiment.

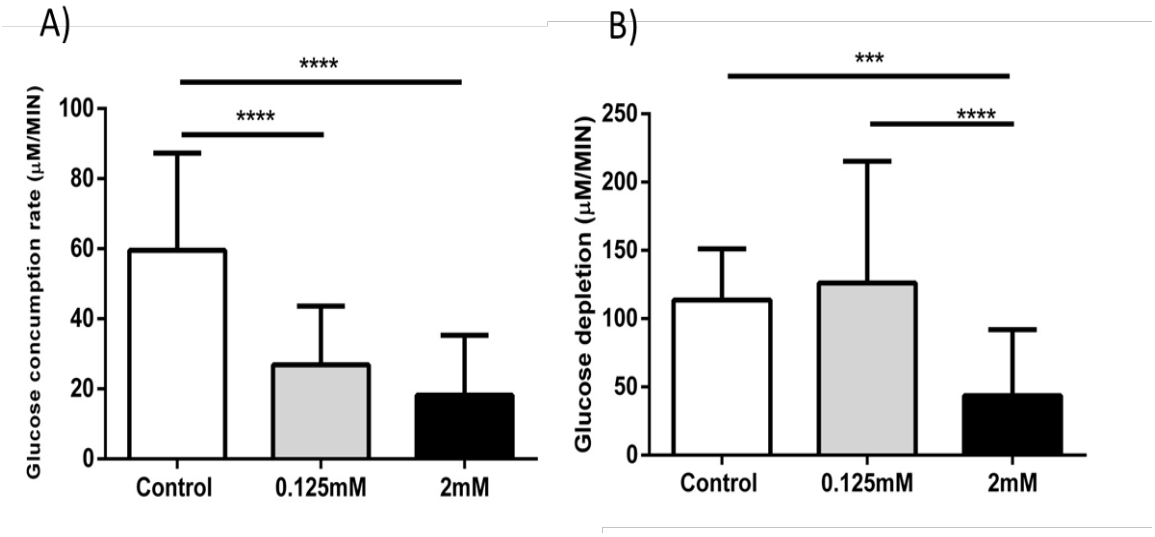

Figure 28: Effect of different concentration of butyrate on glucose consumption rate and glucose depletion: (A) Glucose consumption rate was significantly lower in cells treated with 0.125mM and 2mM Butyrate compared to control cells ($p < 0.0001$ for both), (B) Glucose depletion was significantly lower in cells treated with 2mM Butyrate compared to control cells ($p < 0.0001$) and compared to 0.125mM Butyrate treated cells ($p < 0.001$). Data are expressed as the mean ± S.D. Statistical analysis was performed using one-way analysis of variance (ANOVA) with a post-hoc Tukey's multiple comparison test (GraphPad). All results were considered statistically significant at $p< 0.05$, ****$p < 0.0001$ ***$p < 0.001$.

7.3.3. Glucose consumption rate in astrocytes treated with 2mM propionate, butyrate and β-Hydroxy-butirate: β-hydroxy butyrate (BHB) has been reported to decreases glucose consumption rate in astrocytes, as it is utilized as alternative metabolic energy source (Valdebenito et al., 2015). We used BHB as reference control in the following experiments.

We use 2mM BHB, as at this dose propionate and butyrate caused changes in glucose consumption rate and glucose depletion in our previous experiments, and at this dose BHB alters glycolytic rate in similar mixed neuron/astrocyte culture (Valdebenito et al., 2015).

In cells treated with 2mM propionate, glucose consumption rate was significantly higher than control ($p<0.001$) (Fig.29A), whereas 2mM of butyrate and BHB results in lower consumption rate compared to control ($p < 0.05$ for both) (Fig.29B).

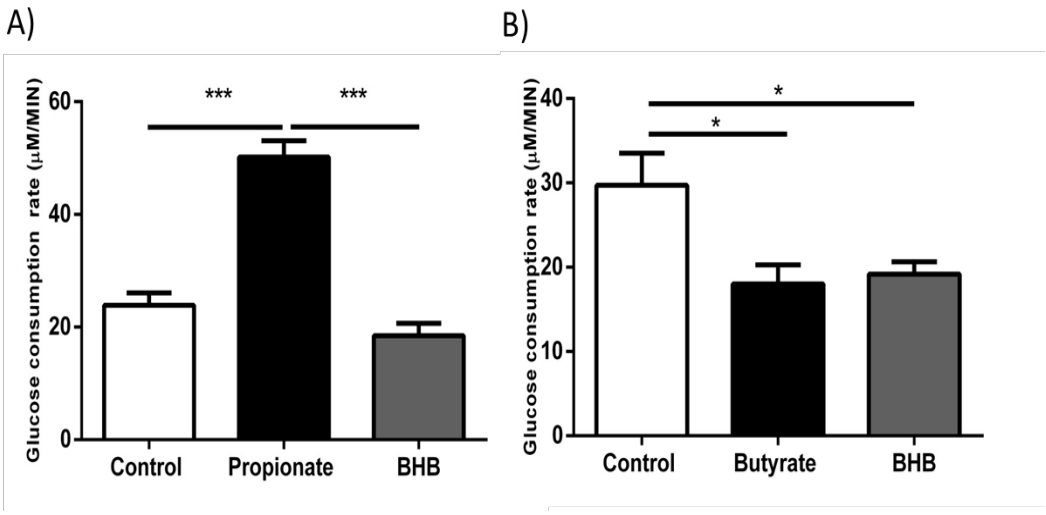

Figure 29: Glucose consumption rate in astrocytes treated with propionate, butyrate and β-Hydroxy butyrate. (A) Glucose consumption rate was significantly higher in propionate compared to control cells ($p < 0.001$) and BHB treated cells ($p < 0.001$). (B) Glucose consumption rate was significantly lower in butyrate treated cells compared to control cells and BHB treated cells (both, $p < 0.05$). Data are expressed as the mean ± SD. Statistical analysis was performed using one-way analysis of variance (ANOVA) with a post-hoc Tukey's multiple comparison test (GraphPad). All results were considered statistically significant at $p < 0.05$, ***$p < 0.001$;*$p < 0.05$.

7.3.4. Glucose depletion rate in astrocytes treated with 2mM propionate, butyrate and β-Hydroxy butrate:

We assess glucose depletion rate in cells treated with 2 mM propionate, butyrate or BHB. Glucose depletion rate was significantly higher in propionate than control cells ($p < 0.001$) and butyrate ($p< 0.05$) treated cells, indicating that astrocytes pre-treated with propionate were more dependent on oxidative phosphorylation than those pretreaed with BHB or butyrate (Fig. 30A, 30B),

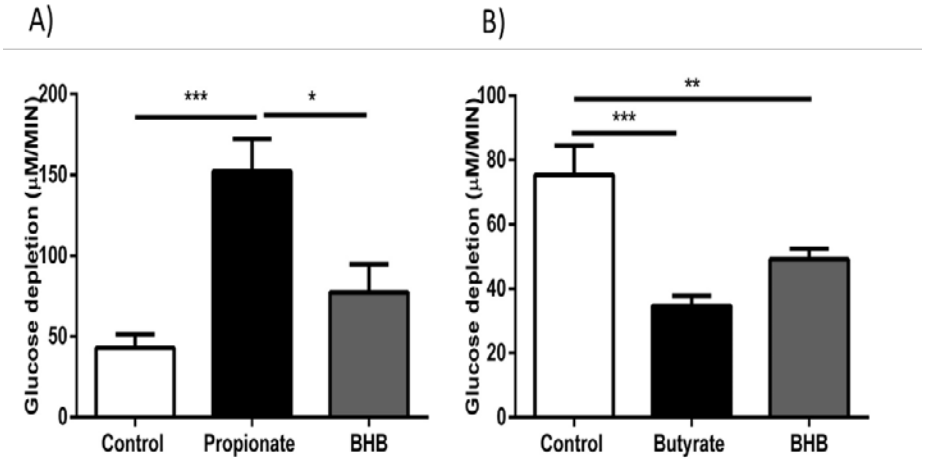

Figure 30: Glucose depletion in astrocytes treated with propionate, butyrate and β-Hydroxy butyrate. (A) Glucose depletion was significantly higher in Propionate treated cells compared to control ($p < 0.001$) and BHB treated cells ($p< 0.05$). (B) Glucose depletion was significantly lower in butyrate ($p < 0.001$) and BHB ($p < 0.01$) treated cells compared to control cells. Data are expressed as the mean ± S.D. Statistical analysis was performed using one-way analysis of variance (ANOVA) with a post-hoc Tukey's multiple comparison test (GraphPad). All results were considered statistically significant at $p < 0.05$, ***$p < 0.001$;**$p < 0.01$;*$p < 0.05$.

7.3.5. Glucose clearance in astrocytes treated with 2mM propionate, butyrate and β-Hydroxy butrate: To calculated glucose clearance rate we removed glucose form the perfusion solution (Fig. 25 and 27). When glucose is removed from the perfusion solution, the intracellular glucose concentration decreases either due to consumption or due to extracellular transport to equilibrate the concentration. The rate at which glucose concentration decreases was considered glucose clearance. In cells treated with propionate, glucose clearance was significantly higher than control ($p < 0.001$) and BHB treated cells ($p < 0.001$). Moreover, BHB treated cells showed lower glucose clearance rate than control situation ($p < 0.05$) (Fig. 31A). Similarly, cells treated with butyrate showed a lowerglucose clearance compared to control ($p < 0.001$) (Fig. 31B).

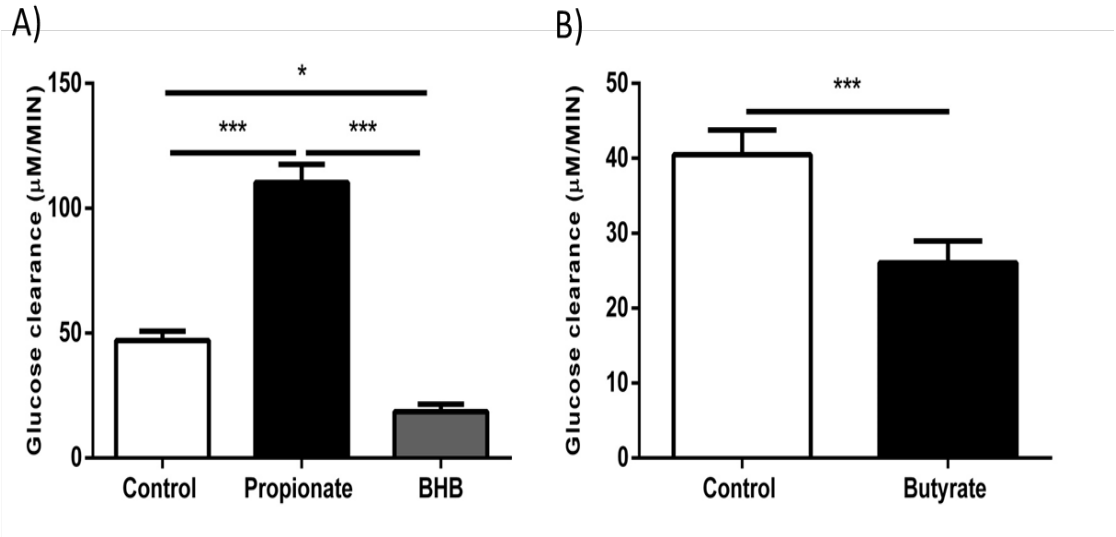

Figure 31: Glucose clearance in astrocytes treated with 2Mm propionate, butyrate and β-Hydroxy butyrate. (A) Glucose clearance was significantly higher in propionate treated cells compared to control and BHB treated cells(both, $p< 0.001$) .BHB treated cells had lower glucose clearance rate than control cells ($p < 0.05$). (B) Glucose clearance was lower in butyrate treated cells compared to control cells ($p < 0.05$). Data are expressed as the mean ± SD. Statistical analysis was performed using one-way analysis of variance (ANOVA) with a post-hoc Tukey's multiple comparison test (GraphPad). All results were considered statistically significant at $p<0.05$, ***$p < 0.001$;*$p < 0.05$.

7.3.6. Lactate production in astrocytes treated with 2Mm propionate and butyrate: Lactate is the end product of glycolysis in astrocytes(Magistretti and Allaman, 2018). As we observed that under propionate condition there was an increased glucose consumption (either by glycolysis or oxidative metabolism) and increased glucose depletion rate (as response of blockage of mitochondrial function), we wanted to assess whether those effects may represent an increased glycolytic rate. We analysed the concentration of lactate in the culture medium of the cells treated under different conditions. We observed that cells treated with 2mM propionate had no difference in lactate concentration compared to control cells (Fig. 32A), whereas in 2mM butyrate treated cell's culture medium there was significant decrease in lactate concentration compared to control cells ($p < 0.05$) (Fig. 32B).

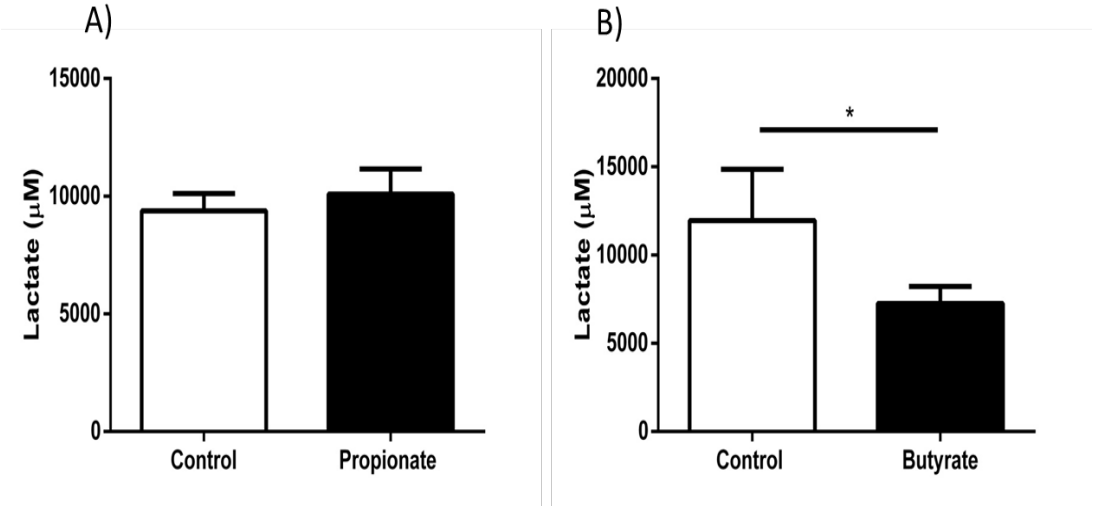

Figure 32: Lactate concentration in culture medium of astrocytes treated with 2Mm propionate and butyrate: (A) No significant difference were observed in lactate concentration between Propionate treated cells and control cells. (B) Lactate concentration was significantly lower in butyrate treated cells compared to control cells ($p < 0.05$). Data are expressed as the mean ± SD. Statistical analysis was performed using one-way analysis of variance (ANOVA) with a post-hoc Tukey's multiple comparison test (GraphPad). All results were considered statistically significant at $p<0.05$, *$p < 0.05$.

CONCLUSION PART II

In this in-vitro study, we investigated the impact of propionate and butyrate on astrocyte metabolism. We utilized a well validated method to assess glucose metabolic fate in a mix neuron /astrocyte cell culture (Valdebenito et al., 2015). Under this conditions, we were able to resemble a physiological condition where neurons modulates astrocytes metabolism. As said before, astrocytes produces lactate, a metabolic product used by neurons as preferred metabolic source (Magistretti and Allaman, 2018).

We incubated neuron/asctrocyte cell culture with propionate, butyrate or BHB (2mM) during 3 days. We observed that when mitochondrial function was blocked by Azide, propionate pre-treated astrocytes presented an increased glucose depletion rate. This means, pre-incubation with propionate enhance the metabolic rate in astrocytes (dependent on mitochondria function), but when mitochondria was blocked, a compensatory mechanism was needed in order to overdue this lack of metabolic machinery, resulting in an increased glycolysis. This scenario was different under butyrate and BHB pre-treatment, as under those conditions, the glycolytic rate was decreased along with a decreased lactate production, similar to previous reports (Valdebenito et al., 2015). BHB and butyrate pre-treatment affects astrocytes

metabolism on a similar manner, as they are used as metabolic substrates for lactate production in astrocytes. Contrastingly, propionate metabolism seems to rely more on mitochondria function (Nguyen 2007), with no changes in lactate production. This may have important physiological implications as those SCFAs differ only by 1 -2 carbons (C2, C3, C4), but they may cause opposite effects on astrocyte metabolism.

8. GENERAL DICUSSION

In this study, we evaluated the neuroprotective effect of the ingestion of BF on a transgenic mice model of AD, and thereafter, we assess the impact of different SCFAs on astrocyte metabolism in an *in-vitro* cell culture.

In the first part, we demonstrated that the ingestion of BF diminished the main pathological markers of AD, amyloid aggregates and hyperphosphorylation of tau in TG female mice. BF also diminished neuroinflammation, synaptic and metabolic alterations, and improved working memory in TG-BF compared to TG-AIN mice, effects associated with the reduction in pro-inflammatory gut bacteria and their products. We used female 3xTg-AD mice as recent evidence indicates that women are at greater risk for developing the disease (Nebel et al., 2018), and females TG mice have more severe pathology compared to males (Wang et al., 2003; Clinton et al., 2007; Schäfer et al., 2007). Therefore, we aimed to evaluate BF´s effects on the more vulnerable gender. We concluded seven months of dietary treatment when female TG were 9 months-old, an age where they show neurogenic and neuroplastic deficits resulting in cognitive decline (Billings et al., 2005; Clinton et al., 2007; Mastrangelo and Bowers, 2008; Blanchard et al., 2010). However, at 9 months of age, the pathological hallmarks and cognitive impairment were moderately present in our 3xTg-AD strain (Morin et al., 2016a). Therefore, we assessed other markers which appear since early stages of the disease.

Mitochondrial dysfunction and enhanced oxidative stress are factors leading to AD pathology (Reddy and Beal, 2008; Wang et al., 2015). Increased production of reactive oxygen species (ROS) is associated with age- and disease-dependent loss of mitochondrial function and reduced antioxidant defence system (Tönnies and Trushina, 2017). Lipid peroxidation refers to the process in which lipids are attacked by ROS (Wang et al., 2015). The BF used in this study showed a stronger antioxidant activity versus AIN93 as assessed by the ORAC method (Table 1). Furthermore, in TG mouse cortex we detected higher MDA level, a lipid peroxidation product, but BF ingestion reduced MDA levels to WT values (Appendix. Figure 1). Thus, BF´s beneficial effects may be partially mediated by its potent anti-oxidant effect.

In 3xTg-AD mice present a strong astrogliosis (Kamphuis et al., 2012) and at 7-months of age they present an impaired astrocytic support system to fulfill the

neuronal metabolic demands (Sancheti et al., 2014). Glu is the predominant excitatory neurotransmitter in adult mammalian brain, and in excess it can cause neuronal hyperexcitability (Barker-Haliski and White, 2015). When astrocytes are chronically activated they have impairment in Glu uptake, as the glutamate-glutamine (Glu-Gln) shuttle becomes compromised (Giaume et al., 2007). This impaired Glu-Gln shuttle results in increased Glu levels in the synaptic cleft (El-ansary et al., 2017), related to hyperactivity of neighbouring neurons (Busche et al., 2008; Zilberter et al., 2013). Different TG mice strains (Palop and Mucke, 2010; Perez-Cruz et al., 2011a), including 3xTg-AD (Liu et al., 2018), are characterized by pro-convulsive seizures and neuronal circuit hyperexcitability since early stages of the disease. Increased neuronal firing (Busche et al., 2008; Arsenault et al., 2011), and faster release of Glu into the synaptic cleft (Sancheti et al., 2014) is associated with increase in Arc and PSD95 post-synaptic proteins in young TG mice (Palop and Mucke, 2010; Perez-Cruz et al., 2011a). In our present study, we also observed increased number of active astrocytes, an event accompanied by enhanced Arc and PSD95 levels in cortex of TG-AIN compared to WT-AIN mice. These data may indicate a state of neuronal over-excitation in TG mice, probably caused by impaired astrocytic function. Importantly, ingestion of BF was able to abate those synaptic alterations in hippocampus and cortex.

AD is also characterized by an early hypometabolic brain phenotype, resulting in an impaired brain bioenergetics (Yao et al., 2011; Caldwell et al., 2014). SIRT1 is consider a regulator of mitochondria biogenesis (Rodgers et al., 2008) by regulating PGC-1α, that represents an upstream inducer of genes of mitochondrial metabolism (Menzies and Hood, 2012). We measured SIRT1 immunoreactivity in different regions of the hippocampus, and observed *stratum*-specific alteration in TG mice. There was a an derease in SIRT1 immunoreactivity in *st. Pyramidale* (Appendix. Figure 2), whereas there was a an increased SIRT1 immunoreactivity in *st. radiatum* but not in *st. oriens*. In the former one there were a greater number of active astrocytes in TG-AIN compared to WT-AIN mice. We assessed the content of SIRT1 in those astrocytes, and found that in TG-AIN mice active astrocytes present increased SIRT1 levels compared to WT-AIN. SIRT1 has been mostly associated with beneficial effects, as improved cognition and neuronal plasticity (Gan and Mucke, 2008); however, less is known about its role in astrocytes. Previous reports indicate that promoting mitochondrial biogenesis – rather than glycolysis - in

astrocytes helps to protect them from Aβ 1-42 toxic effects (Aguirre-rueda et al., 2015). Moreover, upregulation of SIRT1 attenuates oxidative stress in astrocytes via upregulation of superoxide dismutase 2 and catalase (Cheng et al., 2014), whereas LPS and interferon-γ induced activation of astrocytes results in increased mitochondrial biogenesis (Wang et al., 2014). In our current study we detected significant increases of LPS in plasma of TG-AIN mice, while BF inclusion reduced LPS levels. This body of data may suggest that enhanced SIRT1 reflects a preferential oxidative metabolism in astrocytes in order to protect them from harmful agents (i.e. Aβ, LPS), while BF was able to abate those alterations.

We also measured GSK3β protein levels. GSK3β regulates mitochondrial energy metabolism in neurons and in glia. Activation of GSK3β also promotes tau hyperphosphorylation, neurofibrillary tangles, and amyloid plaques (Serenó et al., 2009; DaRocha-Souto et al., 2012). Whereas, GSK3β inhibition (pGSK3β form) attenuates the production of pro-inflammatory cytokines (IL-1β and TNF-α) and augments the production of anti-inflammatory cytokines (IL-10) *in vitro* (Maixner and Weng, 2014). Here, we observed that p-GSK3β levels were dramatically increased in TG-BF mice after ingestion of BF. This enhanced p-GSK3β could be associated with reduced tau hyperphosphorylation in hippocampus and cortex, reduced neuroinflammation and oxidative damage (MDA) in TG-BF mice.

As mentioned in the introduction, several clinical studies have highlighted the impact of a healthy diet against the onset of dementia (Masaki et al., 2000; Morris et al., 2002, 2003; Zandi et al., 2004; Solfrizzi et al., 2006; Hughes et al., 2010). However, it is not clear how the ingestion of certain foods can damper the onset of brain pathologies.

It is important to highlight the presence of pro-inflammatory bacteria and neurotoxins derived from bacterial membranes as LPS, in AD brains (Harris and Harris, 2015; Zhan et al., 2016; Cattaneo et al., 2017; Itzhaki, 2017). In addition, recent studies illustrated the role of GM in amyloid aggregation, as GM depletion by a germ-free condition (Harach et al., 2017), or by antibiotic treatment (Minter et al., 2016, 2017) reduced the amyloid burden and microglia activation in TG mice.

In order to have a clearer picture of GM alterations in AD, we have compile all studies where GM composition analysis was done in TG mice and AD patients (Tables 7 and 8). GM analysis shows a strong variation between studies, depending

on the animal model and age of individuals. Age is an important factor that impact GM composition in AD (Harach et al., 2017), and it may help to explain the contradictory data between animal and human studies. At phylum level most of the TG models coincide with increase abundance of the phylum Firmicutes and a decrease in phylum Bacteriodetes (Table.7). Whereas at family and lower taxonomical levels there is no consistency in GM data. We observed important variations depending on the TG model used and the chronological stages of the pathology. Those two factors (age and mouse strain) may influences GM composition. GM might also be influenced by type of diet, **gender** and difference in environment and handling (Mueller et al., 2006; Hufeldt et al., 2010; Sanchez-Tapia et al., 2017). All these factors may explain discrepancies in AD´s GM published data. Currently, there are no reports of GM using female TG mice. Therefore, we were not able to match our current data with previous reports, as none have used female 3xTgAD mice of 9 months of age. However, similarly to human data, we observed an increased abundance of pro-inflammatory bacteria in TG mice compared to WT controls. TG-AIN mice presented an increased abundance of *L. ruminus, S. anginosus, H. parainfluenza, A. parahaemolyticus, and P. copri* but a decrease in anti-inflammatory related bacteria, such as *A. muciniphila, B. uniformis, F. prausnitzii* in TG-AIN compared to WT-AIN mice.

L. ruminis has stimulatory effects on the secretion of tumor necrosis factor (TNFα) (Taweechotipatr et al., 2009), while *S. anginosus* cause brain abscesses, meningitis, cerebral venous system thrombophlebitis, intracranial arteritis, and inflammation (Kragha, 2016). *Actinobacillus* species are Gram-negative bacteria responsible for several disease conditions of animals (Rycroft and Garside, 2000) and *H. parainfluenzae* is considered as a gut pathogen associated with irritable bowel syndrome (IBS) (Saulnier et al., 2011) and abundantly present in autistic children (Qiao et al., 2018). Furthermore, *H. parainfluenzae* has been reported to cause meningitis (Cardines et al., 2009). *P. copri* is a well-known propionate producing bacteria (Salonen et al., 2014; Chen et al., 2017). Propionate is considered a potent neurotoxic agent that generates neuroinflammation (De Almeida et al., 2006; Thomas et al., 2010; Shultz et al., 2015). It is known that genetic diseases that affect the function of the enzyme propionyl-CoA carboxylase (Propionic Acidemia), are characterized by high levels of propionate and high incidence of dementia (Grünert et al., 2013).

Table 7: Alterations in microbiota at phylum level in AD patients and AD mice

Model	Bacterial phylum INCREASED	Bacterial phylum DECREASED	Reference
AD patients	Bacteroidetes	Firmicutes Bifidobacterium	Vogt et al., 2017
AD patients	Actinobacteria	Bacteroidetes	Zhuang et al., 2018
3xTg-AD mice 24 months		Tenericutes Cyanobacteria	Bonfili et al., 2017
3XTG-ADmice 8 month	Firmicutes		Sanguinetti et al., 2018
5xFAD mice 9 weeks	Firmicutes	Bacteroidetes	Brandscheid et al., 2016
APP/PS1 mice 8 months	Firmicutes	Bacteroidetes Proteobacteria	Park et al., 2017
APP/PS1 mice (1 month)	Firmicutes	Bacteroidetes	Harach et al., 2017
APP/PS1 mice (8 month)	Bacteroidetes Tenericutes	Firmicutes Verrucomicrobia Proteobacteria Actinobacteria	

Table 8: Alterations in microbiota in AD patients and AD mice at level lower than phylum

Model	Bacterial Species INCREASED	Bacterial Species DECREASED	Reference
AD patients	*Bacteroidaceae* *Rikenellaceae* *Gemellaceae* *Bilophila*	*Ruminococcaceae* *Turicibacteraceae* *Peptostreptococcaceae* *Clostridiaceae* *Mogibacteriaceae* *Bifidobacteriaceae*	Vogt et al., 2017
AD patients	*Ruminococcaceae* *Enterococcaceae* *Lactobacillaceae*	*Lanchnospiraceae,* *Bacteroidaceae,* *Veillonellaceae*	Zhuang et al., 2018
3XTG-AD mice (24 months)		*Tenericutes* *Cyanobacteria* *Anaeroplasmatales* *Anaerostipes*	Bonfili et al., 2017
3XTG-ADmice (8 month)	*Enterococcaceae* *Turicibacteraceae*	*S24.7* *Bifidobacteriaceae*	Sanguinetti et al., 2018
5xFAD mice (9 weeks)	*Clostridium leptum*		Brandscheid et al., 2016
APP/PS1 mice (8 months)	*Aerococcaceae* *Leuconostocaceae* *Lactobacillacea* *Pseudomonadaceae* *Caulobacteraceae* *Cytophagaceae* *Sphingobacteriaceae* *Corynebacteriaceae*	*Sphingomonadaceae ,* *Comamonadaceae* *Rhodocyclaceae* *Flavobacteriaceae*	Park et al., 2017
APP/PS1 mice (8 month)	*Rikenellacea)* *S24-7*	*Allobaculum* *Akkermansia*	Harach et al., 2017

Moreover, intraventricular infusions of propionate increased reactive astrogliosis and activate microglia (Macfabe et al., 2006), while the incubation of propionate in cultured astrocytes leads to morphological changes and phosphorylation of GFAP (De Almeida et al., 2006). We observed higher propionate concentration in the brain tissue of TG-AIN compared to that of WT-AIN mice. This was consistent with the increase in the level of FFAR3/GPR41 in brain tissue, a receptor with a high affinity for propionate (Inoue et al., 2012; Yonezawa et al., 2013). Due to the dramatic increase in the relative abundance of *P. copri* in fecal samples and the propionate levels in brain of TG-AIN mice, we decided to determine if propionate was associated with the course of AD pathology. We measured SCFAs levels in fecal samples from 3, 6 and 9 months-old TG and WT mice. Overall, the total SCFA concentration decreased with aging in both, WT and TG mice; however, this reduction was less pronounced in TG mice. At 6 months of age, propionate levels were higher in TG compared to WT mice. It has been reported that several bacterial fermentation products, such as acetate and propionate were higher in plasma and saliva of AD patients (Figueira et al., 2016; Yilmaz et al., 2017), supporting our current results.

The GM analysis also indicated that TG-AIN presented a reduced relative abundance of beneficial bacteria, such as *A. muciniphila, B. uniformis,* and *F. prausnitzii.* The role of *Akkermansia* on the gut barrier has been reported, as its presence is associated with increased mucus layer thickness alleviating metabolic endotoxemia (systemic inflammation caused by bacterial associated components, such as LPS) (Everard et al., 2013). Therefore, reductions in *A. muciniphila* in TG-AIN mice may lead to increased gut barrier leakage and free passage of LPS, whereas *A. muciniphila* relative abundance increased after BF ingestion, that could help to restore membrane permeability and reducing LPS passage to blood circulation. *F. prausnitzii*´s anti-inflammatory actions has been associated with the expression of a potent Microbial Anti-inflammatory Molecule(MAM) (Quévrain et al., 2016; Breyner et al., 2017). Therefore, all this data may indicate that TG-AIN mice lives under a predominant pro-inflammatory microbiome, supporting recent hypothesis of an infectious aetiology for AD (Bhattacharjee and Lukiw, 2013; Little et al., 2014; Maheshwari and Eslick, 2015; Itzhaki et al., 2017). Remarkably, BF supplementation reduces the relative abundance of pro-inflammatory bacteria while increases the anti-inflammatory ones.

We can propose that pro-inflammatory bacteria released substances causes on the one hand, LPS-induced immune activation of glia cells. On the other hand, uptake of propionate by astrocytes as energy source induces SIRT1 increase; both events, can be associated with an impaired Glu-Gln shuttle, resulting in synaptic dysfunction and memory impairments in TG mice. All those alterations were restored in TG mice after ingestion of BF during 7 months.

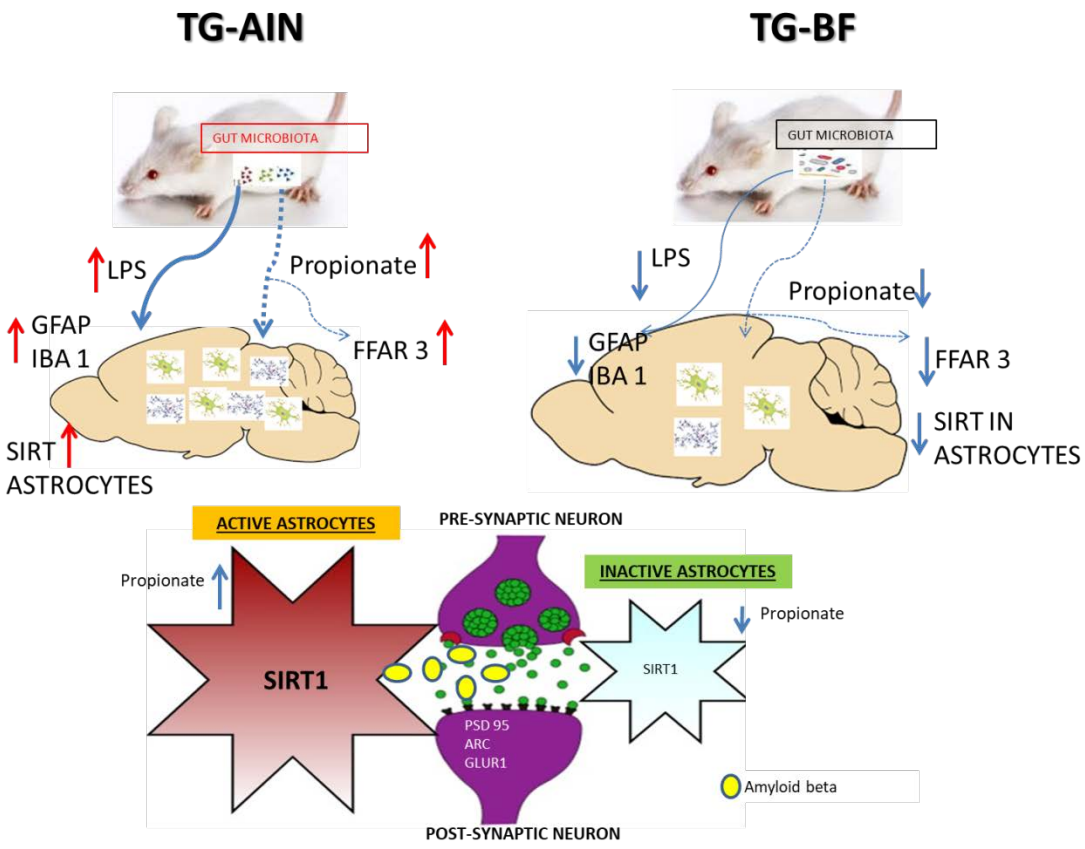

Figure 33: Proposed mechanism by which Bioactive food abates AD pathology: BF modifies microbiota and decrease LPS and propionate. This decreases inflammation in the brain resulting in2 inactive astrocytes. Inactive astrocytes are metabolically less demanding, therefore there is decrease in Sirt1, astrocytes are functionally active, therefore there is decrease in synaptic protein. Overall this decrease amyloid beta accumulation.

As we found increase in propionate concentration in the brain and increase propionate concentration in feces at 6 months of in TG mice compared to WT mice, we wanted to understand better the metabolic role of this SCFAs on astrocyte metabolism by use of cell culture.

A large portion of the glucose entering the glycolytic pathway in astrocytes is released as lactate in the extracellular space (Genc et al., 2011). Astrocyte-derived lactate is oxidized to pyruvate in neurons, a substrate for the pyruvate dehydrogenase complex that furnishes acetyl-CoA to the TCA (Magistretti, 2011), supplying neurons with substrates of energy. Under normal circumstances the brain utilizes exclusively glucose, but if alternative energy source is available (i.e. ketone bodies or SCFAs), they are efficiently utilized and a reduction of brain tissue glucose consumption is observed (Valdebenito et al., 2015). Barros and collaborators have observed in a mix neuron/astrocyte cell culture that incubation with BHB causes a reduction in glucose utilization by astrocytes. Astrocytes prefer to metabolize this ketone body releasing lactate, further use as energy substrate by neurons (Valdebenito et al., 2015). It is known that propionate is metabolized in astrocytes by oxidative phosphorylation (Nguyen et al., 2007) increasing mitochondrial function (Perry et al., 2016), but it is not known if butyrate and propionate affects astrocyte metabolism in a different manner. Thus, we determine the metabolic fate of propionate and butyrate in a mix astrocyte/neuronal culture. We observed that under propionate incubation, blockage of mitochondrial leads to an enhanced glucose clearance and glucose depletion in astrocytes. Alterations in glucose clearance could be due to changes in glucose transport or glucose consumption. Hence, we evaluated the glucose consumption rate and we observed an increased by propionate incubation. Glucose is metabolized in astrocytes by glycolysis producing lactate, however, in propionate treated astrocytes we did not observe changes in lactate production compared to control. This data indicate that glucose in propionate treated astrocytes is completely metabolized with no further production of lactate (no glycolysis). Significant increase in glucose depletion rate in propionate treated cells indicate that astrocytes were more dependent on mitochondrial metabolism (oxidative phosphorylation) and when mitochondria was blocked, there was an increased need to fulfil the increased metabolic demand caused by propionate incubation. Propionate is an agent that generates neuroinflammation (De Almeida et al., 2006; Thomas et al., 2010; Shultz et al., 2015). It has been previously observed that intraventricular infusions of propionate increased reactive astrogliosis and activated microglia (Macfabe et al., 2006), while incubation of propionate in cultured astrocyte leads to morphological changes and phosphorylation of GFAP (De Almeida et al., 2006).

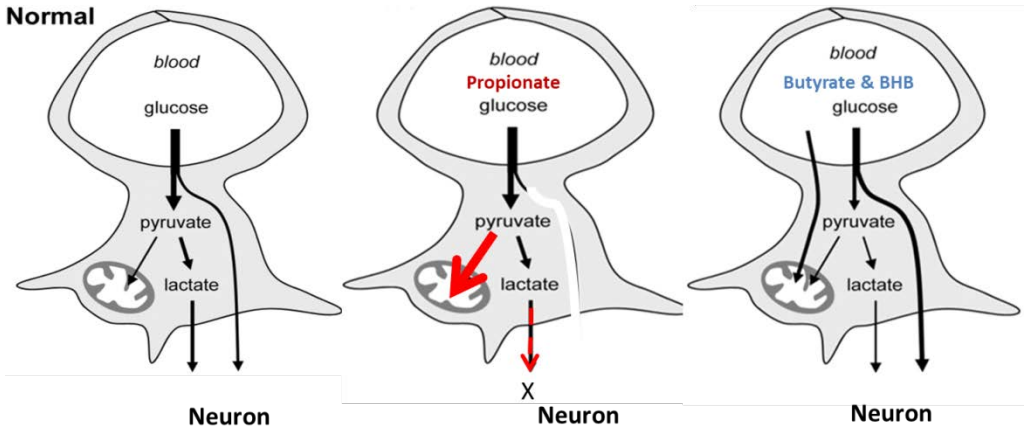

Figure 34: Proposed mechanism for differential effects of propionate and butyrate on astrocyte-neuron interaction. Propionate increases glucose metabolism in the astrocytes and it is metabolized completely by mitochondria in astrocytes. Whereas butyrate decrease glucose metabolism this decreases lactate formation, more glucose is supplied to neuron as astrocytes use butyrate for their energy needs.(Taken and modified from Valdebenito et al., 2015)

Previous reports indicate that enhanced mitochondrial respiration (oxidative phosphorylation) in astrocytes limits the substrate supply from astrocytes to neurons (Jiang and Cadenas, 2014). Moreover, astrocytes coincubated with LPS and Interferon-γ showed increase in mitochondrial biogenesis (Wang 2014). In addition, astrocytes isolated from 5xFAD mice exhibited changes in the glycolytic pathway and TCA, compared to wild type cells (Gijsel-bonnello, et al., 2017). These body of data may indicate that propionate activates astrocytes causing an enhanced mitochondrial metabolism with no release of lactate. This will neglect neuronal metabolic demands, implicating an impaired Glu-Gln shuttle.

On the other hand, we observed that butyrate pre-treatment decreased glucose clearance when glucose was depleted from culture medium. When evaluating the glucose consumption rate, we observed a strong inhibitory effect of butyrate on the consumption of glucose by astrocytes and on the capacity of astrocytic glycolysis to respond to physiological and pathological stimuli. In butyrate treated astrocytes, there was blunted response of astrocytic glycolysis to chemical anoxia, despite ATP depletion of similar extent to that observed in control cells. There was decrease in production of lactate in butyrate treated astrocytes compared to control astrocytes, parallel to decreased in rate of glucose consumption. This data is similar to previous

reports using BHB (Valdebenito et al., 2015). Butyrate has been shown anti-inflammatory and neuroprotective properties (Ricobaraza et al., 2012; Govindarajan et al., 2011). In AD, decreased butyrate in feces and brain samples have been reported in TG mice compared to WT (Zhang et al., 2017a). Administration of probiotic increases the concentration of butyrate in 3XTG-AD mice an effect associated with decrease in amyloid aggregation and neuroinflammation (Bonfili et al., 2017). In our present study we could not detect changes in butyrate in mice brains due to the low concentration present in our samples (Part I).

All this previous data supports our observation that propionate impact astrocyte metabolism causing an increased metabolic need. This effect can be correlated to the increased SIRT1 in astrocytes from TG-AIN mice, whose brains were richer in propionate concentration than WT mice. Therefore, propionate can be consider a potent neurotoxic substance related to AD pathology.

Overall the data indicates that propionate and butyrate have differential effect on metabolism of astrocytes, butyrate has similar effects as BHB, whereas propionate presented an opposite effect.

9. GENERAL CONCLUSION

- Ingestion of BF was able to diminish the pathological markers of AD, reduced neuroinflammation, synaptic hyperactivity and improved working memory in TG mice. Importantly, BF´s effects were accompanied by restoration of GM and their released products (LPS and propionate).
- Propionate and butyrate differentially alters astrocyte-neuron lactate shuttle by altering glycolysis in astrocytes.
- Based on the present data we propose that a dietary intervention in early stage of pathology is an effective strategy to abate amyloid pathology, metabolic and synaptic alteration resulting in better cognitive outcome.

10. PERSPECTIVES

- Inject propionate intraperitoneally in 3xTg-AD mice and evaluate if the pathology is exacerbated.
- Treat astrocytic culture with butyrate and propionate and determine mitochondrial dynamics under an Agilent Seahorse XF Cell and evaluate cytokines release from medium.
- Analyse the effect of butyrate and propionate in mixed astrocytes and neuronal culture from 3xTg-AD mice.

11. REFRENCES

Aguirre-rueda D, Guerra-ojeda S, Aldasoro M, Iradi A, Obrador E, Ortega A, Mauricio D, Vila JM, Valles SL (2015) Astrocytes Protect Neurons from A β 1-42 Peptide- Induced Neurotoxicity Increasing TFAM and PGC-1 and Decreasing PPAR- γ and SIRT-1. Int J Med Sci 12:48–56.

Allan K, Perez KA, Barnham KJ, Camakaris J, Burke R (2014) A commonly used Drosophila model of Alzheimer's disease generates an aberrant species of amyloid-β with an additional N-terminal glutamine residue. FEBS Lett 588:3739–3743 Available at: http://dx.doi.org/10.1016/j.febslet.2014.08.022.

Allès B, Samieri C, Féart C, Jutand MA, Laurin D, Barberger-Gateau P (2012) Dietary patterns: A novel approach to examine the link between nutrition and cognitive function in older individuals. Nutr Res Rev 25:207–222.

Alzheimer'sAssociation (2017) Alzheimer's Association. 2017 Alzheimer's Disease Facts and Figures. Alzheimers Dement.

Anastasiou CA, Yannakoulia M, Kosmidis MH, Dardiotis E, Hadjigeorgiou GM, Sakka P, Arampatzi X, Bougea A, Labropoulos I, Scarmeas N (2017) Mediterranean diet and cognitive health : Initial results from the Hellenic Longitudinal Investigation of Ageing and Diet. PLoS One 12:e0182048.

Androuin A, Potier B, Nägerl UV, Cattaert D, Danglot L, Thierry M, Youssef I, Triller A, Duyckaerts C, El Hachimi KH, Dutar P, Delatour B, Marty S (2018) Evidence for altered dendritic spine compartmentalization in Alzheimer's disease and functional effects in a mouse model. Acta Neuropathol 135:839–854 Available at: https://doi.org/10.1007/s00401-018-1847-6.

Arsenault D, Julien C, Tremblay C (2011) DHA Improves Cognition and Prevents Dysfunction of Entorhinal Cortex Neurons in 3xTg-AD Mice. PLoS One 6:e17397.

Ascencio C, Torres N, Isoard-Acosta F, Gomez-Perez FJ, Hernandez-Pando R, Tovar AR (2004) Soy Protein Affects Serum Insulin and Hepatic SREBP-1 mRNA and Reduces Fatty Liver in Rats. Am Soc Nutr Sci.

Asti A, Gioglio L (2014) Can a Bacterial Endotoxin be a Key Factor in the Kinetics of Amyloid Fibril Formation ? J Alzheimer's Dis 39:169–179.

Avila-nava A, Noriega LG, Tovar AR, Granados O, Perez-Cruz C, Pedraza-Chaverri J,

Torres N (2016) Food combination based on a pre-hispanic Mexican diet decreases metabolic and cognitive abnormalities and gut microbiota dysbiosis caused by a sucrose-enriched high-fat diet in rats. Mol Nutr Food Res 61:1–13.

Baothman OA, Zamzami MA, Taher I, Abubaker J, Abu-farha M (2016) The role of Gut Microbiota in the development of obesity and Diabetes. Lipids Health Dis:1–8 Available at: http://dx.doi.org/10.1186/s12944-016-0278-4.

Barage SH, Sonawane KD (2015) Neuropeptides Amyloid cascade hypothesis : Pathogenesis and therapeutic strategies in Alzheimer ' s disease. Neuropeptides 52:1–18 Available at: http://dx.doi.org/10.1016/j.npep.2015.06.008.

Barker-Haliski M, White HS (2015) Glutamatergic mechanimms associated with seizures and epilepsy. Cold Spring Harb Perspect Med 5:a022863.

Bhattacharjee S, Lukiw WJ (2013) Alzheimer's disease and the microbiome. Front Cell Neurosci 7:153.

Billings LM, Oddo S, Green KN, McGaugh JL, LaFerla FM (2005) Intraneuronal Aβ causes the onset of early Alzheimer's disease-related cognitive deficits in transgenic mice. Neuron 45:675–688.

Blanchard J, Wanka L, Tung YC, Cárdenas-Aguayo MDC, Laferla FM, Iqbal K, Grundke-Iqbal I (2010) Pharmacologic reversal of neurogenic and neuroplastic abnormalities and cognitive impairments without affecting Aβ and tau pathologies in 3xTg-AD mice. Acta Neuropathol 120:605–621.

Bloemen JG, Olde SWM, Venema K, Buurman WA, Jalan R, Dejong CHC (2010) Short chain fatty acids exchange : Is the cirrhotic , dysfunctional liver still able to clear them ? Clin Nutr 29:365–369 Available at: http://dx.doi.org/10.1016/j.clnu.2009.10.002.

Bonda DJ, Lee H, Camins A, Pallàs M, Casadesus G, Smith MA, Zhu X (2011) The Critical Role of the Sirtuin Pathway in Aging and Alzheimer Disease: Mechanistic and Therapeutic Considerations. Lancet Neurol 10:275–279.

Bonfili L, Cecarini V, Berardi S, Scarpona S, Suchodolski JS, Nasuti C, Fiorini D, Boarelli MC, Rossi G, Eleuteri AM (2017) Microbiota modulation counteracts Alzheimer's disease progression influencing neuronal proteolysis and gut hormones plasma levels. Sci Rep 7:1–21.

Bramham CR, Alme MN, Bittins M, Kuipers SD, Nair RR, Pai B, Panja D, Schubert M, Soule

J, Tiron A, Wibrand K (2010) The Arc of synaptic memory. Exp Brain Res 200:125–140.

Breyner NM, Michon C, de Sousa CS, Vilas Boas PB, Chain F, Azevedo VA, Langella P, Chatel JM (2017) Microbial anti-inflammatory molecule (MAM) from Faecalibacterium prausnitzii shows a protective effect on DNBS and DSS-induced colitis model in mice through inhibition of NF-κB pathway. Front Microbiol 8:1–8.

Bu X, Yao X, Jiao S, Zeng F, Liu Y, Xiang Y, Liang C, Wang Q (2014) A study on the association between infectious burden and Alzheimer ' s disease. Eur J Neurol:1–7.

Busche MA, Eichhoff G, Adelsberger H, Abramowski D, Wiederhold K, Haass C, Staufenbiel M, Konnerth A, Garaschuk O (2008) Clusters of Hyperactive Neurons Near Amyloid Plaques in a Mouse Model of Alzheimer's Disease. Science (80-) 19:1686–1689.

Buttery JE, CHAMBERLAIN BR, MILNER CR, PANNALL PR (1985) Colohmetric Measurement of Plasma Lactate. Br Sci REPORTS 84:363–365.

Caldwell CC, Yao J, Brinton RD (2014) Targeting the Prodromal Stage of Alzheimers Disease: Bioenergetic and Mitochondrial Opportunities. Neurotherapeutics 12:66–80.

Calvo-ochoa E, Arias C (2015) Cellular and metabolic alterations in the hippocampus caused by insulin signalling dysfunction and its association with cognitive impairment during aging and Alzheimer ' s disease : studies in animal models. Diabetes Metab Res Rev:1–13.

Cañete T, Blázquez G, Tobena A, Giménez-Llort A, Fernández-Teruel (2015) Cognitive and emotional alterations in young Alzheimer ' s disease (3xTgAD) mice : Effects of neonatal handling stimulation and sexual dimorphism. Behav Brain Res 281:156–171.

Cani PD, Amar J, Iglesias MA, Poggi M, Knauf C, Bastelica D, Neyrinck AM, Fava F, Tuohy KM, Chabo C, Sulpice T, Chamontin B, Gibson GR, Casteilla L, Delzenne NM, Alessi MC, Burcelin, Remy (2007) Metabolic Endotoxemia Initiates Obesity and Insulin Resistance. Diabetes 56:1761–1772.

Cantó C, Auwerx J (2009) PGC-1α, SIRT1 and AMPK, an energy sensing network that controls energy expenditure. Curr Opin Lipidol 20:98–105.

Carabotti M, Scirocco A, Antonietta M, Severi C (2015) The gut-brain axis : interactions between enteric microbiota , central and enteric nervous systems. Ann Gastroenterol:203–209.

Cardines R, Giufrè M, Atti MLCD, Accogli M, Mastrantonio P, Cerquetti M (2009)

Haemophilus parainfluenzae meningitis in an adult associated with acute otitis media. New Microbiol 32:213–215.

Carding S, Verbeke K, Vipond DT, Corfe BM, Owen LJ (2015) Dysbiosis of the gut microbiota in disease. 1:1–9.

Carlo M Di (2012) Simple model systems: a challenge for Alzheimer's disease. Immun Ageing 9:3 Available at: http://immunityageing.biomedcentral.com/articles/10.1186/1742-4933-9-3.

Carvalho C, Cardoso S, Correia SC, Santos RX, Santos MS, Baldeiras I, Oliveira CR, Moreira PI (2012) Metabolic Alterations Induced by Sucrose Intake and Alzheimer ' s Disease Promote Similar Brain Mitochondrial Abnormalities. Diabetes 61.

Cattaneo A et al. (2017) Association of brain amyloidosis with pro-inflammatory gut bacterial taxa and peripheral inflammation markers in cognitively impaired elderly. Neurobiol Aging 49:60–68.

Chandra V, Pandav R, Dodge HH, Johnston JM, Belle SH, DeKosky, S.T. et al. (2001) Incidence of Alzheimer's disease in a rural community in India: the Indo-US study. Neurology 57:985–998.

Chapman CD, Schi HB, Grillo CA, Benedict C (2018) Intranasal insulin in Alzheimer ' s disease : Food for thought. Neuropharmacology 136:196–201.

Chen T, Long W, Zhang C, Liu S, Zhao L, Hamaker BR (2017) Fiber-utilizing capacity varies in Prevotella- versus Bacteroides-dominated gut microbiota. Sci Rep 7.

Chen Y, Zhao Y, Dai C, Liang Z, Run X, Iqbal K, Liu F, Gong C (2014) Intranasal insulin restores insulin signaling , increases synaptic proteins , and reduces A β level and microglia activation in the brains of 3xTg-AD mice. Exp Neurol 261:610–619 Available at: http://dx.doi.org/10.1016/j.expneurol.2014.06.004.

Cheng A, Wan R, Yang J-L, Kamimura N, Son TG, Ouyang X, Luo Y, Okun E, Mattson MP (2012) Involvement of PGC-1α in the Formation and Maintenance of Neuronal Dendritic Spines. Nat Commun 31250.

Cheng Y, Takeuchi H, Sonobe Y, Jin S, Wang Y, Horiuchi H, Parajuli B, Kawanokuchi J, Mizuno T, Suzumura A (2014) Sirtuin 1 attenuates oxidative stress via upregulation of superoxide dismutase 2 and catalase in astrocytes. J Neuroimmunol 269:38–43 Available at: http://dx.doi.org/10.1016/j.jneuroim.2014.02.001.

Cho S, Chen XJA, Sayed F, Ward XME, Gao F, Nguyen TA, Krabbe G, Sohn PD, Lo I, Minami S, Devidze N, Zhou Y, Coppola G, Gan L (2015) SIRT1 Deficiency in Microglia Contributes to Cognitive Decline in Aging and Neurodegeneration via Epigenetic Regulation of IL-1β. Neurobiol Dis 35:807–818.

Clark IA, Vissel B (2015) Amyloid β: one of three danger-associated molecules that are secondary inducers of the proinflammatory cytokines that mediate Alzheimer's disease. Br J Pharmacol 172:3714–3727.

Clinton LK, Billings LM, Green KN, Caccamo A, Ngo J, Mcgaugh JL, Laferla FM (2007) Age-dependent sexual dimorphisms in cognition and stress response in the 3xTg-AD mice. Neurobiol Dis 28:76–82.

Creegan R, Hunt W, Mcmanus A, Rainey-smith SR (2015) Diet , nutrients and metabolism : cogs in the wheel driving Alzheimer ' s disease pathology ? British Journal of Nutrition. Br J Nutr 2050.

DaRocha-Souto B, Coma M, Pérez-Nievas BG, Scotton TC, Siao M, Sánchez-Ferrer P, Hashimoto T, Fan Z, Hudry E, Barroeta I, Serenó L, Rodríguez M, Sánchez MB, Hyman BT, Gómez-Isla T (2012) Activation of glycogen synthase kinase-3 beta mediates β-amyloid induced neuritic damage in Alzheimer's disease. Neurobiol Dis 45:425–437.

Davis KE, Burnett K, Gigg J (2017) Water and T-maze protocols are equally e ffi cient methods to assess spatial memory in 3xTg Alzheimer ' s disease mice. Behav Brain Res 331:54–66.

Davis KE, Eacott MJ, Easton A, Gigg J (2013) Episodic-like memory is sensitive to both Alzheimer ' s-like pathological accumulation and normal ageing processes in mice. Behav Brain Res 254:73–82 Available at: http://dx.doi.org/10.1016/j.bbr.2013.03.009.

Davis KE, Fox S, Gigg J (2014) Increased hippocampal excitability in the 3xTgAD mouse model for Alzheimer's disease in vivo. PLoS One 9:e91203.

De Almeida LMV, Funchal C, Gottfried C, Wajner M, Pessoa-Pureur R (2006) Propionic acid induces cytoskeletal alterations in cultured astrocytes from rat cerebral cortex. Metab Brain Dis 21:51–62.

Deacon RMJ, Rawlins JNP (2006) T-maze alternation in the rodent. Nat Protoc 1:7–12.

Dietrich MO, Andrews ZB, Horvath TL (2008) Exercise-Induced Synaptogenesis in the Hippocampus Is Dependent on UCP2-Regulated Mitochondrial Adaptation. J Neurosci

28:10766–10771.

Dineley KT, Jahrling JB, Denner L (2014) Insulin Resistance in Alzheimer's Disease. Neurobiol Dis 42:475–481.

Ding F, Yao J, Rettberg JR, Chen S, Brinton RD (2013) Early decline in glucose transport and metabolism precedes shift to ketogenic system in female aging and Alzheimer's mouse brain: Implication for bioenergetic intervention. PLoS One 8:e79977.

Do K, Laing BT, Landry T, Bunner W, Mersaud N, Matsubara T, Li P, Yuan Y, Lu Q (2018) The effects of exercise on hypothalamic neurodegeneration of Alzheimer ' s disease mouse model. :1–17.

Dong Y-TD, Cao K, Tan, Long-Chun Tanb C, Wang X-L, Qi X-L, Xiao Y, Guan, Zhi-Zhong Guana, b c (2018) Stimulation of SIRT1 Attenuates the Level of Oxidative Stress in the Brains of APP/PS1 Double Transgenic Mice and in Primary Neurons Exposed to Oligomers of the Amyloid-β Peptide. J Alzheimer's Dis:1–19.

Dorostkar MM, Zou C, Blazquez-Llorca L, Herms J (2015) Analyzing dendritic spine pathology in Alzheimer's disease: problems and opportunities. Acta Neuropathol 130:1–19.

Du H, Guo L, Yan S, Sosunov AA, Mckhann GM, Shidu S (2010) Early de fi cits in synaptic mitochondria in an Alzheimer ' s disease mouse model. PNAS 107.

Duncan SH, Louis P, Thomson JM, Flint HJ (2009) The role of pH in determining the species composition of the human colonic microbiota. Environ Microbiol 11:2112–2122.

Ebert D, Haller RG, Walton ME (2003) Energy contribution of octanoate to intact rat brain metabolism measured by13C nuclear magnetic resonance spectroscopy. J Neurosci:5928–5935.

Eder P, Reinprecht I, Schreiner E, Skofitsch G, Windisch M (2002) Increased density of glutamate receptor subunit 1 due to Cerebrolysin treatment : An immunohistochemical study on aged rats. Histochem J:1998–1999.

Edmond J, Robbins RA, Bergstrom JD, Cole RA, Vellis J De (1987) Capacity for Substrate Utilization in Oxidative Metabolism by Neurons , Astrocytes , and Oligodendrocytes From Developing Brain in Primary Culture. 561:551–561.

El-ansary A, Al-salem HS, Asma A, Al-dbass A (2017) Glutamate excitotoxicity induced by orally administered propionic acid, a short chain fatty acid can be ameliorated by bee

pollen. Lipids Health Dis 16:96.

El-ansary AK, Bacha A Ben, Kotb M (2012) Etiology of autistic features : the persisting neurotoxic effects of propionic acid. J Neuroinflammation 9:1 Available at: ??9/1742-2094-9-74.

Elder G a, Gama Sosa M a, De Gasperi R (2010) Transgenic Mouse Models of Alzheimer's Disease. Mt Sinai J Med 77:69–81.

Everard A, Belzer C, Geurts L, Ouwerkerk JP, Druart C, Bindels LB, Guiot Y (2013) Cross-talk between *Akkermansia muciniphila* and intestinal epithelium controls diet-induced obesity. Proc Nati Acad Sci USA 110:9066–9071.

Figueira J, Jonsson P, Nordin Adolfsson A, Adolfsson R, Nyberg L, Öhman A (2016) NMR analysis of the human saliva metabolome distinguishes dementia patients from matched controls. Mol BioSyst 12:2562–2571 Available at: http://xlink.rsc.org/?DOI=C6MB00233A.

Flamier A, Hajjar J El, Adjaye J, Fernandes KJ, Abdouh M, Bernier G (2018) Modeling Late-Onset Sporadic Alzheimer ' s Disease through BMI1 Deficiency. CellReports 23:2653–2666 Available at: https://doi.org/10.1016/j.celrep.2018.04.097.

Frye R, Rose S, Chacko J, Wynne R, Bennuri SC, Slattery JC, Tippett M, Delhey L, Melnyk S, Kahler SG (2016) Modulation of mitochondrial function by the microbiome metabolite propionic acid in autism and control cell lines. Transl Psychiatry 6:e927-10 Available at: http://dx.doi.org/10.1038/tp.2016.189.

Fulco M, Sartorelli V (2008) Comparing and Contrasting the Roles of AMPK and SIRT1 in Metabolic Tissues Marcella. Cell Cycle 7:3669–3679.

Gan L, Mucke L (2008) Paths of Convergence: Sirtuins in Aging and Neurodegeneration. Neuron 58:10–14.

Gardener SL, Rainey-smith SR, Barnes MB, Sohrabi HR, Weinborn M, Lim YY, Harrington K, Taddei K, Gu Y (2014) Dietary patterns and cognitive decline in an Australian study of ageing. Mol Psychiatry (2014),:1–7.

Genc S, Kurnaz IA, Ozilgen M (2011) Astrocyte - neuron lactate shuttle may boost more ATP supply to the neuron under hypoxic conditions - in silico study supported by in vitro expression data. BMC Syst Biol 5.

Gerlai R (1998) A new continuous alternation task in T-maze detects hippocampal

dysfuncion in mice. A strain comparison and lesion study. Behav Brain Res 95:91–101.

Giaume C, Kirchhoff F, Matute C, Reichenbach A, Verkhratsky A (2007) Glia: The fulcrum of brain diseases. Cell Death Differ 14:1324–1335.

Gibbs M, Shleper M, Mustafa T, Burnstock G, Bowser DN (2011) ATP derived from astrocytes modulates memory in the chick. Neuron Glia Biol 7:177–186.

Giliberto L, Zhao H, Chandakkar P, Wu Q, Simon JE, Janle EM, Lobo J, Ferruzzi MG, Davies P, Marambaud P (2010) AMP-activated Protein Kinase Signaling Activation by Resveratrol Modulates Amyloid-ℕ Peptide Metabolism * □ S Valé rie Vingtdeux. J Biol Chem.

Giménez-Llort L, García Y, Buccieri K, Revilla S, Suñol C, Cristofol R, Sanfeliu C (2010) Gender-Specific Neuroimmunoendocrine Response to Treadmill Exercise in 3xTg-AD Mice. Int J Alzheimers Dis 2010:128354 Available at: http://www.hindawi.com/journals/ijad/2010/128354/.

Govindarajan N, Agis-Balboa RC, Walter J, Sananbenesi F, Fischer A (2011) Sodium butyrate improves memory function in an alzheimer's disease mouse model when administered at an advanced stage of disease progression. J Alzheimer's Dis 26:187–197.

Grabher BJ (2018) Alzheimer's Disease and the Effects it has on the Patient and their Family. J Nucl Med Technol:1–27.

Grünert SC et al. (2013) Propionic acidemia: Clinical course and outcome in 55 pediatric and adolescent patients. Orphanet J Rare Dis 8:1–9.

Gu Y, Brickman AM, Stern Y, Habeck CG, Razlighi QR, Luchsinger JA, Manly JJ, Schupf N, Mayeux R, Scarmeas N (2015) Mediterranean diet and brain structure in a multiethnic elderly cohort. Neurology 85:1744–1751.

Guevara-cruz M, Tovar AR, Aguilar-salinas CA, Medina-vera I, Gil-zenteno L, Herna I, Lo P, Ordaz-nava G, Canizales-quinteros S, Pineda LEG, Torres N (2012) A Dietary Pattern Including Nopal , Chia Seed , Soy Protein , and Oat Reduces Serum Triglycerides and Glucose Intolerance in Patients with Metabolic Syndrome 1 – 4. J Nutr.

Guzmán-Ramos K, Moreno-castilla P, Castro-cruz M, Laferla FM, Mcgaugh JL, Martı H, Bermu F (2012) Restoration of dopamine release deficits during object recognition memory acquisition attenuates cognitive impairment in a triple transgenic mice model of

Alzheimer ' s disease. Learn Mem:453–460.

Haim L Ben, Sauvage MC, Ceyzériat K, Curtin JF (2015) Elusive roles for reactive astrocytes in neurodegenerative diseases Edited by : Citation : Front Cell Neurosci 9:1–27.

Harach T, Marungruang N, Duthilleul N, Cheatham V, Mc Coy KD, Frisoni G, Neher JJ, Fåk F, Jucker M, Lasser T, Bolmont T (2017) Reduction of Abeta amyloid pathology in APPPS1 transgenic mice in the absence of gut microbiota. Sci Rep 7:41802.

Harris SA, Harris EA (2015) Herpes Simplex Virus Type 1 and Other Pathogens are Key Causative Factors in Sporadic Alzheimer's Disease. J Alzheimer's Dis 48:319–353.

Hashimoto M, Hossain S (2011) Neuroprotective and Ameliorative Actions of Polyunsaturated Fatty Acids Against Neuronal Diseases : Beneficial Effect of Docosahexaenoic Acid on Cognitive Decline in Alzheimer ' s Disease. J Pharmacol Sci 162:150–162.

Heneka MT et al. (2015) Neuroinflammation in Alzheimer's disease. Lancet Neurol 14:388–405.

Herline K, Prelli F, Mehta P, MacMurray C, Goñi F, Wisniewski T (2018) Immunotherapy to improve cognition and reduce pathological species in an Alzheimer's disease mouse model. Alzheimers Res Ther 10:54 Available at: http://www.ncbi.nlm.nih.gov/pubmed/29914551%0Ahttp://www.pubmedcentral.nih.gov/articlerender.fcgi?artid=PMC6006698.

Hill JM, Lukiw WJ (2015) Microbial-generated amyloids and Alzheimer ' s disease. Front Aging Neurosci 7:9.

Hooper C, Killick R, Lovestone S (2008) The GSK3 hypothesis of Alzheimer's disease. J Neurochem 104:1433–1439.

Hoyer S (2004) Causes and consequences of disturbances of cerebral glucose metabolism in sporadic Alzheimer disease: therapeutic implications. Adv Exp Med Biol 541:135–152.

Hoyles L, Snelling T, Umlai U, Nicholson JK, Carding SR, Glen RC, Mcarthur S (2018) Microbiome – host systems interactions : protective effects of propionate upon the blood – brain barrier. Microbiome:1–13.

Hufeldt MR, Nielsen DS, Vogensen FK, Midtvedt T, Hansen AK (2010) Variation in the Gut

Microbiota of Laboratory Mice Is Related to Both Genetic and Environmental Factors. Comp Med 60:336–342.

Hughes TF, Andel R, Small BJ, . Borenstein, Amy R Mortimer JA, Wolk A, Johansson B, Fratiglioni L, Pedersen, Nancy L Gatz M (2010) Midlife Fruit and Vegetable Consumption and Risk of Dementia in Later Life in Swedish Twins. Am J Geriatr Psychiatry 18:413–420.

Inoue D, Kimura I, Wakabayashi M, Tsumoto H, Ozawa K, Hara T, Takei Y, Hirasawa A, Ishihama Y, Tsujimoto G (2012) Short-chain fatty acid receptor GPR41-mediated activation of sympathetic neurons involves synapsin 2b phosphorylation. FEBS Lett 586:1547–1554 Available at: http://dx.doi.org/10.1016/j.febslet.2012.04.021.

Ishii H, Shirai T, Makino C, Nishikata T (2014) Mitochondrial inhibitor sodium azide inhibits the reorganization of mitochondria-rich cytoplasm and the establishment of the anteroposterior axis in ascidian embryo. Dev Growth Differ 56:175–188.

Itzhaki RF et al. (2017) Microbes and Alzheimer's disease. Handb Infect Alzheimer's Dis 51:3–8.

Itzhaki RF (2017) Herpes simplex virus type 1 and Alzheimer's disease: possible mechanisms and signposts. FASEB J 31:3216–3226.

Jacka FN, Neil AO, Opie R, Itsiopoulos C, Cotton S, Mohebbi M, Castle D, Dash S, Mihalopoulos C, Chatterton M Lou, Brazionis L, Dean OM, Hodge AM, Berk M (2017) A randomised controlled trial of dietary improvement for adults with major depression (the ' SMILES ' trial). BMC Med 15:1–13.

Jiang Q, Jin S, Jiang Y, Liao M, Feng R (2017) Alzheimer's Disease Variants with the Genome-Wide Significance are Significantly Enriched in Immune Pathways and Active in Immune Cells. Mol Neurobiol 54:594–600 Available at: http://dx.doi.org/10.1007/s12035-015-9670-8.

Jolivalt CG, Lee CA, Beiswenger KK, Smith JL, Orlov M, Torrance MA (2016) Defective insulin signaling pathway and increased GSK-3 activity in the brain of diabetic mice: parallels with Alzheimer's disease and correction by insulin. J Neurosci res 86:3265–3274.

Julien C, Tremblay C, Émond V, Lebbadi M, Jr NS, Bennett DA, Calon F (2009) SIRT1 Decrease Parallels the Accumulation of tau in Alzheimer Disease. J Neuropathol Exp Neurol 68:1–26.

Kamphuis W, Mamber C, Moeton M, Kooijman L, Sluijs JA, Jansen AHP, Verveer M, de Groot LR, Smith VD, Rangarajan S, Rodríguez JJ, Orre M, Hol EM (2012) GFAP isoforms in adult mouse brain with a focus on neurogenic astrocytes and reactive astrogliosis in mouse models of Alzheimer disease. PLoS One 7:e42823.

Katsouri L, Lim YM, Blondrath K, Eleftheriadou I, Lombardero L, Birch AM (2016) PPAR γ -coactivator-1 α gene transfer reduces neuronal loss and amyloid- β generation by reducing β -secretase in an Alzheimer ' s disease model. 113.

Katsouri L, Parr C, Bogdanovic N, Willem M, Sastre M (2014) PPAR γ -coactivator-1 α gene transfer reduces neuronal loss and amyloid- β generation by reducing β -secretase in an Alzheimer ' s disease model. J Alzheimer's Dis 25:151–162.

Kitazawa M, Medeiros R, M. LaFerla F (2012) Transgenic Mouse Models of Alzheimer Disease: Developing a Better Model as a Tool for Therapeutic Interventions. Curr Pharm Des 18:1131–1147 Available at: http://www.eurekaselect.com/openurl/content.php?genre=article&issn=1381-6128&volume=18&issue=8&spage=1131.

Kragha KO (2016) Multiple Brain Abscesses due to Streptococcus anginosus: Prediction of Mortality by an Imaging Severity Index Score. Case Rep Radiol 2016:7040352 Available at: http://www.ncbi.nlm.nih.gov/pubmed/27034878%0Ahttp://www.pubmedcentral.nih.gov/articlerender.fcgi?artid=PMC4791499.

Laferla FM, Green KN (2012) Animal Models of Alzheimer Disease. cold spring Harb Perspect Med 2:a006320.

Lauderback CM, Hackett JM, Huang FF, Keller JN, Szweda LI, Markesbery WR, Butter DA (2001) The glial glutamate transporter , GLT-1 , is oxidatively modified by 4-hydroxy-2-nonenal in the Alzheimer ' s disease brain : the role of Abeta 1-42. J Neurochem 78:413–416.

Lee JW, Lee YK, Yuk DY, Choi DY, Ban SB, Oh KW, Hong JT (2008) Neuro-inflammation induced by lipopolysaccharide causes cognitive impairment through enhancement of beta-amyloid generation. J Neuroinflammation 5:37.

Li Q, Han Y, Dy ABC, Hagerman RJ (2017) The Gut Microbiota and Autism Spectrum Disorders. Front Cell Neurosci 11.

Li Z, Okamoto K, Hayashi Y, Sheng M (2004) The Importance of Dendritic Mitochondria in

the Morphogenesis and Plasticity of Spines and Synapses. Cell 119:873–887.

Lin J, Puigserver P, Donovan J, Tarr P, Spiegelman BM (2002) Peroxisome Proliferator-activated Receptor Coactivator 1 (PGC-1), A Novel PGC-1-related Transcription Coactivator Associated with Host Cell Factor. J Biol Chem 277:1645–1649.

Lindenburg L, Merkx M (2014) Engineering genetically encoded FRET sensors. Sensors 14:11691–11713.

Little CS, Joyce TA, Hammond CJ, Matta H, Cahn D, Appelt DM, Balin BJ (2014) Detection of bacterial antigens and Alzheimer's disease-like pathology in the central nervous system of BALB/c mice following intranasal infection with a laboratory isolate of Chlamydia pneumoniae. Front Aging Neurosci 6:1–9.

Liu D, Lu H, Stein E, Zhou Z, Yang Y, Mattson MP (2018) Brain regional synchronous activity predicts tauopathy in 3×TgAD mice. Neurobiol Aging 70:160–169.

Liu Y, Liu F, Grundke-iqbal I, Iqbal K, Gong C (2011) Deficient brain insulin signalling pathway in Alzheimer ' s disease. J Pathol:54–62.

Livingston G et al. (2017) Dementia prevention, intervention, and care. Lancet 390:2673–734.

Ma T, Chen Y, Vingtdeux V, Zhao H, Viollet B, Marambaud P, Klann E, York N, Cochin I, Inserm U (2014) Inhibition of AMP-Activated Protein Kinase Signaling Alleviates Impairments in Hippocampal Synaptic Plasticity Induced by Amyloid beta. J Neurosci 34:12230–12238.

Macfabe DF, Cain DP, Rodriguez-capote K, Franklin AE, Hoffman JE, Boon F, Taylor AR, Kavaliers M, Ossenkopp K (2006) Neurobiological effects of intraventricular propionic acid in rats : Possible role of short chain fatty acids on the pathogenesis and characteristics of autism spectrum disorders. Behav Brain Res 176:149–169.

Macklin L, Griffith CM, Cai Y, Rose GM, Yan X, Patrylo PR (2016) Department of Anatomy and Neurobiology , Central South University Xiangya School of Center for Integrated Research in Cognitive and Neural Sciences , Southern Illinois University. Exp Gerontol Available at: http://dx.doi.org/10.1016/j.exger.2016.12.019.

Magistretti PJ, Allaman I (2015) A Cellular Perspective on Brain Energy Metabolism and Functional Imaging. Neuron 86:883–901 Available at: http://dx.doi.org/10.1016/j.neuron.2015.03.035.

Magistretti PJ, Allaman I (2018) Lactate in the brain : from metabolic end-product to signalling molecule. Nat Publ Gr 19:235–249 Available at: http://dx.doi.org/10.1038/nrn.2018.19.

Maheshwari P, Eslick GD (2015) Bacterial infection and Alzheimer's disease: A meta-analysis. J Alzheimer's Dis 43:957–966.

Maixner DW, Weng H-R (2014) The Role of Glycogen Synthase Kinase 3 Beta in Neuroinflammation and Pain. J Pharm Pharmacol 1:001.

Maldonado RF, Isabel S, Valvano MA (2016) Lipopolysaccharide modification in Gram-negative. FEMS Microbiol Rev 40:480–493.

Masaki KH, Losonczy KG, Izmirlian G, Foley DJ, Ross GW, Petrovitch H, Havlik R, White LR (2000) Association of vitamin E and C supplement use with cognitive function and dementia in elderly men. Neurology 54:1265–1272.

Mastrangelo MA, Bowers WJ (2008) Detailed immunohistochemical characterization of temporal and spatial progression of Alzheimer's disease-related pathologies in male triple-transgenic mice. BMC Neurosci 9:1–31.

Menzies KJ, Hood DA (2012) The role of SirT1 in muscle mitochondrial turnover. Mitochondrion 12:5–13 Available at: http://dx.doi.org/10.1016/j.mito.2011.03.001.

Miklossy J (2011) Emerging roles of pathogens in Alzheimer disease. Expert Rev Mol Med 13:1–34.

Minter MR, Hinterleitner R, Meisel M, Zhang C, Leone V, Zhang X, Oyler-Castrillo P, Zhang X, Musch MW, Shen X, Jabri B, Chang EB, Tanzi RE, Sisodia SS (2017) Antibiotic-induced perturbations in microbial diversity during post-natal development alters amyloid pathology in an aged APPSWE/PS1ΔE9 murine model of Alzheimer's disease. Sci Rep 7:1–18.

Minter MR, Zhang C, Leone V, Ringus DL, Zhang X, Oyler-Castrillo P, Musch MW, Liao F, Ward JF, Holtzman DM, Chang EB, Tanzi RE, Sisodia SS (2016) Antibiotic-induced perturbations in gut microbial diversity influences neuro-inflammation and amyloidosis in a murine model of Alzheimer's disease. Sci Rep 6:30028.

Moloney AM, Griffin RJ, Timmons S, Connor RO, Ravid R, Neill CO (2010) Defects in IGF-1 receptor , insulin receptor and IRS-1 / 2 in Alzheimer ' s disease indicate possible resistance to IGF-1 and insulin signalling. Neurobiol Aging 31:224–243.

Morin J-P, Ceron-Solano G, Velazquez-Campos G, Pacheco-Lopez G, Bermudez-Rattoni F, Diaz-Cintra S (2016a) Spatial Memory Impairment is Associated with Intraneural Amyloid-beta Immunoreactivity and Dysfunctional Arc Expression in the Hippocampal-CA3 Region of a Transgenic Mouse Model of Alzheimer's Disease. J Alzheimers Dis 51:69–79.

Morin JP, Cerón-Solano G, Velázquez-Campos G, Pacheco-López G, Bermúdez-Rattoni F, Díaz-Cintra S (2016b) Spatial Memory Impairment is Associated with Intraneural Amyloid-β Immunoreactivity and Dysfunctional Arc Expression in the Hippocampal-CA3 Region of a Transgenic Mouse Model of Alzheimer's Disease. J Alzheimer's Dis 51:69–79.

Morris MC, C. C, Wang Y, M.Sacks F, David A Bennett NTA (2016) MIND Diet Associated with Reduced Incidence of Alzheimer's Disease. Alzheimers Dement 11:1007–1014.

Morris MC, Evans DA, Bienias JL, Tangney CC, Bennett DA, Wilson RS, Aggarwal N, Schneider J (2003) Consumption of Fish and n-3 Fatty Acids and Risk of Incident Alzheimer Disease. Arch Neurol 60:940–946.

Morris MC, Evans DA, Bienias JL, Tangney CC, Wilson RS (2002) Vitamin E and Cognitive Decline in Older Persons. Arch Neurol 59:1125–1132.

Mruk DD, Cheng CY (2011) Enhanced chemiluminescence (ECL) for routine immunoblotting. Spermatogenesis 1:121–122 Available at: http://www.tandfonline.com/doi/abs/10.4161/spmg.1.2.16606.

Mucke L, Masliah E, Yu G, Mallory M, Rockenstein EM, Tatsuno G, Hu K, Kholodenko D, Johnson-wood K, Mcconlogue L (2000) High-Level Neuronal Expression of A $^{N}_{L}$ 1 – 42 in Wild-Type Human Amyloid Protein Precursor Transgenic Mice : Synaptotoxicity without Plaque Formation. J Neurosci 20:4050–4058.

Mueller S et al. (2006) Differences in Fecal Microbiota in Different European Study Populations in Relation to Age , Gender , and Country : a Cross-Sectional Study Differences in Fecal Microbiota in Different European Study Populations in Relation to Age , Gender , and Country : Appl Environ Microbiol:1027–1033.

Muhič M, Vardjan N, Chowdhury HH, Zorec R, Kreft M (2015) Insulin and insulin-like growth factor 1 (IGF-1) modulate cytoplasmic glucose and glycogen levels but not glucose transport across the membrane in astrocytes. J Biol Chem 290:11167–11176.

Nakahata Y, Kaluzova M, Grimaldi B, Sahar S, Chen D, Guarente LP, Sassone-corsi P (2012) The NAD+ -Dependent Deacetylase SIRT1 Modulates CLOCK- Mediated Chromatin Remodeling and Circadian Control. Cell 134:329–340.

Natarajaseenivasan K, Cotto B, Shanmughapriya S, Lombardi AA, Datta PK, Madesh M, Elrod JW, Khalili K, Langford D (2018) Astrocytic metabolic switch is a novel etiology for Cocaine and HIV-1 Tat-mediated neurotoxicity. Cell Death Dis:415.

Nebel RA, Aggarwal NT, Barnes LL, Gallagher A, Goldstein JM, Kantarci K, Mallampalli MP, Mormino EC, Scott L, Yu WH, Maki PM, Mielke MM (2018) Understanding the Impact of Sex and Gender in Alzheimer's Disease: A Call to Action. Alzheimer's Dement 14:1171–1183.

Neth BJ, Craft S (2017) Insulin Resistance and Alzheimer ' s Disease : Bioenergetic Linkages. Front Aging Neurosci 9:1–20.

Nguyen NHT, Morland C, Gonzalez SV, Rise F, Storm-Mathisen J, Gundersen V, Hassel B (2007) Propionate increases neuronal histone acetylation, but is metabolized oxidatively by glia. Relevance for propionic acidemia. J Neurochem 101:806–814.

Nichols M, Zhang J, Polster BM, Elustondo PA, Thirumaran A, Pavlov E V., Robertson GS (2015) Synergistic neuroprotection by epicatechin and quercetin: Activation of convergent mitochondrial signaling pathways. Neuroscience 308:75–94 Available at: http://dx.doi.org/10.1016/j.neuroscience.2015.09.012.

Noebels JL (2011) A Perfect Storm: Converging Paths of Epilepsy and Alzheimer's Dementia Intersect in the Hippocampal Formation. epil 52:39–46.

Nyffeler M, Zhang W, Feldon J, Knuesel I (2007) Differential expression of PSD proteins in age-related spatial learning impairments. Neurobiol Aging 28:143–155.

Oddo S, Caccamo A, Kitazawa M, Tseng BP, Laferla FM (2003a) Amyloid deposition precedes tangle formation in a triple transgenic model of Alzheimer ' s disease. Neurobiol Aging 24:1063–1070.

Oddo S, Caccamo A, Shepherd JD, Murphy MP, Golde TE, Kayed R, Metherate R, Mattson MP, Akbari Y, Laferla FM (2003b) Triple-Transgenic Model of Alzheimer ' s Disease with Plaques and Tangles : Intracellular A ^{N_L} and Synaptic Dysfunction. Neuron 39:409–421.

Ontiveros-Torresa AM, Luna-herrera C, Perry G, Luna-arias JP (2016) Fibrillar Amyloid-?

Accumulation Triggers an Inflammatory Mechanism Leading to Hyperphosphorylation of the Carboxyl-Terminal End of Tau Polypeptide in the Hippocampal Formation of the 3×Tg-AD Transgenic Mouse. J Alzheimer's Dis.

Palop J, Mucke L (2010) Amyloid-beta Induced NeuronalDisease : From Synapses toward Neural Networks. Nat Neurosci 13:812–818.

Pelletier A, Barul C, Catherine F, Samieri C (2015) Mediterranean diet and preserved brain structural connectivity in older subjects. Alzheimer's Dement:1–9.

Perez-Cruz C, Nolte MW, Gaalen, Marcel M van Rustay NR, Annelies T, Tanghe A, Kirchhoff F, Ulrich E (2011a) Reduced Spine Density in Specific Regions of CA1 Pyramidal Neurons in Two Transgenic Mouse Models of Alzheimer's Disease. J Neurosci 31::3926–3934.

Perez-Cruz C, Nolte MW, van Gaalen MM, Rustay NR, Termont A, Tanghe A, Kirchhoff F, Ebert U (2011b) Reduced spine density in specific regions of CA1 pyramidal neurons in two transgenic mouse models of Alzheimer's disease. J Neurosci 31:3926–3934.

Piquet J, Toussay X, Hepp R, Lerchundi R, Douce J Le, Faivre É, Guiot E, Bonvento G, Cauli B (2018) Supragranular Pyramidal Cells Exhibit Early Metabolic Alterations in the 3xTg-AD Mouse Model of Alzheimer ' s Disease. 12:1–16.

Povova J, Ambroz P, Bar M, Pavukova V, Sery O, Tomaskova H, Janout V (2012) Epidemiological of and risk factors for Alzheimer ' s disease : A review. 156:108–114.

Qiao Y, Wu M, Feng Y, Zhou Z, Chen L, Chen F (2018) Alterations of oral microbiota distinguish children with autism spectrum disorders from healthy controls. Sci Rep 8:1–12.

Qin W, Haroutunian V, Katsel P, Cardozo CP, Ho L, Buxbaum JD, Pasinetti GM (2009) PGC-1α Expression Decreases in the Alzheimer Disease Brain as a Function of Dementia Weiping. Arch Neurol 66:352–361.

Quévrain E et al. (2016) Identification of an anti-inflammatory protein from Faecalibacterium prausnitzii, a commensal bacterium deficient in Crohn's disease. Gut 65:415–425.

Rayasam GV, Tulasi VK, Sodhi R, Davis JA, Ray A (2009) Glycogen synthase kinase 3 : more than a namesake. :885–898.

Reddy PH, Beal MF (2008) Amyloid beta, mitochondrial dysfunction and synaptic damage: implications for cognitive decline in aging and Alzheimer's disease. Trends Mol Med

14:45–53.

Reeves PG (1997) Components of the AIN-93 Diets as Improvements in the AIN-76A Diet. J Nutr 127:838–841.

Ricobaraza A, Cuadrado-Tejedor M, Marco S, Pérez-Otaño I, García-Osta A (2012) Phenylbutyrate rescues dendritic spine loss associated with memory deficits in a mouse model of Alzheimer disease. Hippocampus 22:1040–1050.

Riemer J, Kins S (2012) Axonal Transport and Mitochondrial Dysfunction in Alzheimer ' s Disease. Neurodegener Dis 12:111–124.

Ríos-Covián D, Ruas-Madiedo P, Margolles A, Gueimonde M, De los Reyes-Gavilán CG, Salazar N (2016) Intestinal short chain fatty acids and their link with diet and human health. Front Microbiol 7:1–9.

Ríos-covián D, Ruas-madiedo P, Margolles A, Gueimonde M, Reyes-gavilán CGDL, Salazar N (2016) Intestinal Short Chain Fatty Acids and their Link with Diet and Human Health. 7:1–9.

Robinson A, Mett J, Grosgen S, Zimmer VC, Haupenthal VJ, Stahlmann CP, Hundsd B, Hartmann T, Slobodskoy Y, Ulrike CM, Stein R, Grimm MOW (2014) Upregulation of PGC-1a expression by Alzheimer's disease-associated pathway: presenilin 1/amyloid precursor protein (APP)/intracellular domain of APP. Aging Cell:263–272.

Rodgers J, Lerin C, Gerhart-Hines Z, Puigserver P (2008) Metabolic Adaptations through the PGC-1α and SIRT1 Pathways. FEBS Lett 582:46–53.

Rodriguez-Callejas JD, Fuchs E, Perez-Cruz C (2016) Evidence of tau hyperphosphorylation and dystrophic microglia in the common marmoset. Front Aging Neurosci 8.

Rodriguez-ortiz CJ, Baglietto-vargas D, Martinez-coria H (2014) Upregulation of miR-181 Decreases c-Fos and SIRT-1 in the Hippocampus of 3xTg-AD Mice. J Alzheimer's Dis 42:1229–1238.

Rycroft AN, Garside LH (2000) Actinobacillus species and their role in animal disease. Vet J 159:18–36.

Salminen A, Kaarniranta K (2012) AMP-activated protein kinase (AMPK) controls the aging process via an integrated signaling network. Ageing Res Rev:230–241.

Salonen A, Lahti L, Salojärvi J, Holtrop G, Korpela K, Duncan SH, Date P, Farquharson F,

Johnstone AM, Lobley GE, Louis P, Flint HJ, de Vos WM (2014) Impact of diet and individual variation on intestinal microbiota composition and fermentation products in obese men. ISME J 8:2218–2230 Available at: http://www.nature.com/doifinder/10.1038/ismej.2014.63.

Sancheti H, Patil I, Kanamori K, Díaz Brinton R, Zhang W, Lin AL, Cadenas E (2014) Hypermetabolic state in the 7-month-old triple transgenic mouse model of Alzheimer's disease and the effect of lipoic acid: A 13 C-NMR study. J Cereb Blood Flow Metab 34:1749–1760.

Sanchez-Tapia M, Aguilar-López M, Perez-Cruz C, Pichardo-Ontiveros E, Wang M, Donovan S, Tovar A, Torres N (2017) Nopal (Opuntia ficus indica) protects from metabolic endotoxemia, improving carbohydrate and lipid metabolism and cognitive function by modifying gut microbiota in a rat model of high fat and sucrose feeding. Sci Rep 7:4716.

Sánchez-Tapia M, Aguilar-López M, Pérez-Cruz C, Pichardo-Ontiveros E, Wang M, Donovan SM, Tovar AR, Torres N (2017) Nopal (Opuntia ficus indica) protects from metabolic endotoxemia by modifying gut microbiota in obese rats fed high fat/sucrose diet. Sci Rep 7:1–16.

Sanguinetti E, Collado MC, Marrachelli VG, Monleon D, Selma-royo M, Pardo-tendero MM, Burchielli S, Iozzo P (2018) Microbiome-metabolome signatures in mice genetically prone to develop dementia , fed a normal or fatty diet. Sci Rep:1–13 Available at: http://dx.doi.org/10.1038/s41598-018-23261-1.

Saulnier D, Riehle K, Mistretta T, Diaz M, Mandal D, Raza S, Weidler E, Qin X, Coarfa C, Milosavljevic A, Petrosino J, Highlander S, Gibbs R, Lynch S, Shulman R, Versalovic J (2011) Gastrointestinal Microbiome Signatures of. Gastroenterology 141:1782–1791.

Savioz A, Leuba G, Vallet PG (2014) A framework to understand the variations of PSD-95 expression in brain aging and in Alzheimer ' s disease. Ageing Res Rev 18:86–94 Available at: http://dx.doi.org/10.1016/j.arr.2014.09.004.

Scarmeas N, Stern Y, Tang M, Luchsinger JA (2006) Mediterranean Diet and Risk for Alzheimer's Disease Nikolaos. Ann Neurol 59:912–921.

Schäfer S, Wirths O, Multhaup G, Bayer TA (2007) Gender dependent APP processing in a transgenic mouse model of Alzheimer's disease. J Neural Transm 114:387–394.

Schulz JG, Antonio, AnnetteGartner LVH, Vilain S, Bastianen J, Veldhoven PP Van, Dotti

CG (2015) Glial b-Oxidation regulates Drosophila Energy Metabolism. Sci Rep:1–9.

Serenó L, Coma M, Rodríguez M, Sánchez-Ferrer P, Sánchez MB, Gich I, Agulló JM, Pérez M, Avila J, Guardia-Laguarta C, Clarimón J, Lleó A, Gómez-Isla T (2009) A novel GSK-3β inhibitor reduces Alzheimer's pathology and rescues neuronal loss in vivo. Neurobiol Dis 35:359–367.

Serrano-pozo A, Frosch MP, Masliah E, Hyman BT (2011) Neuropathological Alterations in Alzheimer Disease. Cold Spring Harb Perspect Med 1:a006189.

Shultz SR, Aziz NAB, Yang L, Sun M, MacFabe DF, O'Brien TJ (2015) Intracerebroventricular injection of propionic acid, an enteric metabolite implicated in autism, induces social abnormalities that do not differ between seizure-prone (FAST) and seizure-resistant (SLOW) rats. Behav Brain Res 278:542–548 Available at: http://dx.doi.org/10.1016/j.bbr.2014.10.050.

Sidorova-darmos E, Wither RG, Shulyakova N, Fisher C, Ratnam M, Aarts M, Lilge L, Philippe P (2014) Differential expression of sirtuin family members in the developing , adult , and aged rat brain. Front Aging Neurosci 6:1–20.

Singh B, Ajay K. Parsaik, Mielke MM, Erwinc PJ, Knopman DS, Petersen RC, Roberts RO, ChB (2014) Association of Mediterranean diet with Mild Cognitive Impairment and Alzheimer's disease: A Systematic Review and Meta-Analysis Balwinder. J Alzheimers Dis 39:271–282.

Solfrizzi V, Colacicco AM, D'Introno A, Capurso C, Torres F, Rizzo C, Capurso A, Panza F (2006) Dietary intake of unsaturated fatty acids and age-related cognitive decline: A 8.5-year follow-up of the Italian Longitudinal Study on Aging. Neurobiol Aging 27:1694–1704.

Solfrizzi V, Custodero C, Lozupone M, Imbimbo BP (2017) Relationships of Dietary Patterns , Foods , and Micro- and Macronutrients with Alzheimer ' s Disease and Late-Life Cognitive Disorders : A Systematic Review. J Alzheimer's Dis 59:815–849.

Steen E, Terry BM, Rivera EJ, Cannon JL, Neely TR, Tavares R, Xu XJ, Wands JR, Monte SM De (2005) Impaired insulin and insulin-like growth factor expression and signaling mechanisms in Alzheimer ' s disease – is this type 3 diabetes ? J Alzheimer's Dis 7:63–80.

Sterniczuk R, Antle MC, Laferla FM, Dyck RH (2010) Characterization of the 3xTg-AD mouse model of Alzheimer ' s disease : Part 2 . Behavioral and cognitive changes.

Brain Res 1348:149–155 Available at: http://dx.doi.org/10.1016/j.brainres.2010.06.011.

Streit WJ, Braak HQ-S, Xue Ingo B (2009) Dystrophic (senescent) rather than activated microglial cells are associated with tau pathology and likely precede neurodegeneration in Alzheimer's disease. Acta Neuropathol 118:475–485.

Streit WJ, Sammons NW, Kuhns AJ (2004) Dystrophic Microglia in the Aging. Glia 212:208–212.

Sun B, Li W, Zhu C, Fan WJ (2018) Clinical Research on Alzheimer ' s Disease : Progress and Perspectives. Neurosci Bull Available at: https://doi.org/10.1007/s12264-018-0249-z.

Swerdlow RH, Khan SM (2004) A " mitochondrial cascade hypothesis " for sporadic Alzheimer ' s disease. Med Hypotheses 63:8–20.

Szablewski L (2018) Human Gut Microbiota in Health and Alzheimer's Disease. J Alzheimer's Dis 62:549–560.

Talbot K, Wang H, Kazi H, Han L, Bakshi KP, Stucky A, Fuino RL, Kawaguchi KR, Samoyedny AJ, Wilson RS, Arvanitakis Z, Schneider JA, Wolf BA, Bennett DA, Trojanowski JQ, Arnold SE (2012) Demonstrated brain insulin resistance in Alzheimer ' s disease patients is associated with IGF-1 resistance , IRS-1 dysregulation , and cognitive decline. J Clin Invest 122:1316–1338.

Taweechotipatr M, Iyer C, Spinler JK, Versalovic J, Tumwasorn S (2009) Lactobacillus saerimneri and Lactobacillus ruminis: Novel human-derived probiotic strains with immunomodulatory activities. FEMS Microbiol Lett 293:65–72.

Thomas RH, Foley KA, Mepham JR, Tichenoff LJ, Possmayer F, MacFabe DF (2010) Altered brain phospholipid and acylcarnitine profiles in propionic acid infused rodents: Further development of a potential model of autism spectrum disorders. J Neurochem 113:515–529.

Tippmann F, Hundt J, Schneider A, Endres K, Fahrenholz F (2009) Up-regulation of the ⎵ -secretase ADAM10 by retinoic acid receptors and acitretin. FASEB J:1643–1654.

Tlaskalová-hogenová H, Štˇ R, Cukrowska B, Lodinová-žádn R, Kozáková H, Rossmann P, Sokol D, Funda DP, Borovská D, Reháková Z (2004) Commensal bacteria (normal microflora), mucosal immunity and chronic inflammatory and autoimmune diseases. Immunol Lett 93:97–108.

Tönnies E, Trushina E (2017) Oxidative Stress, Synaptic Dysfunction, and Alzheimer's Disease. J Alzheimer's Dis 57:1–17.

Tovar AR, Díaz-Villaseñor A, Cruz-Salazar N, Ordáz G, Granados O, Palacios-González B, Tovar-Palacio C, López P, Torres N (2011) Dietary Type and Amount of Fat Modulate Lipid Metabolism Gene Expression in Liver and in Adipose Tissue in High-fat Diet-fed Rats. ARCMED.

Tovar AR, Torre-Villalvazo I, Ochoa M, Elías AL, Ortíz V, Ag CA, Uilar-Salinas, Torres N (2005) Soy protein reduces hepatic lipotoxicity in hyperinsulinemic obese Zucker fa/fa rats. J Lipid Res.

Ursell LK, Metcalf JL, Laura Wegener Parfrey, Knight R (2013) Defining the Human Microbiome. Nutr rev 70:1–12.

Valdebenito R, Ruminot I, Garrido-Gerter P, Fernández-Moncada I, Forero-Quintero L, Alegría K, Becker HM, Deitmer JW, Barros LF (2015) Targeting of astrocytic glucose metabolism by beta-hydroxybutyrate. J Cereb Blood Flow Metab 36:1813–1822.

Valls-Pedret C, Sala-Vila A, Serra-Mir M, Corella D, De La Torre R, Martínez-González MÁ, Martínez-Lapiscina EH, Fittó M, Pérez-Heras A, Salas-Salvadó J, Estruch R, Ros E (2015) Mediterranean diet and age-related cognitive decline: A randomized clinical trial. JAMA Intern Med 175:1094–1103.

Vandal M, White PJ, Tremblay C, St-Amour I, Chevrier G, Emond V, Lefranc¸ois D, Virgili J, Planel E, Giguere Y, Marette A, Calon F (2014) Insulin reverses the high-fat diet-induced increase in brain Aβ and improves memory in an animal model of Alzheimer disease. Diabetes 63:4291–4301.

Varamini B, Sikalidis AK, Bradford KL (2013) Resveratrol increases cerebral glycogen synthase kinase phosphorylation as well as protein levels of drebrin and transthyretin in mice : an exploratory study. 7486:1–8.

Vingtdeux V, Giliberto L, Zhao H, Chandakkar P, Wu Q, Simon JE, Janle EM, Lobo J, Ferruzzi MG, Davies P, Marambaud P (2010) AMP-activated Protein Kinase Signaling Activation by Resveratrol Modulates Amyloid-beta Peptide Metabolism. J Biol Chem 285:9100–9113.

Vinolo MAR, Rodrigues HG, Nachbar RT, Curi R (2011) Regulation of Inflammation by Short Chain Fatty Acids. Nutrients:858–876.

Walker AW, Duncan SH, Leitch ECM, Child MW, Flint HJ (2005) pH and Peptide Supply Can Radically Alter Bacterial Populations and Short-Chain Fatty Acid Ratios within Microbial Communities from the Human Colon. Appl Environ Microbiol 71:3692–3700.

Wang HM, Zhao YX, Zhang S, Liu GD, Kang WY, Tang, H.D. et al. (2010) PPAR gamma agonist curcumin reduces the amyloid-beta-stimulated inflammatory responses in primary astrocytes. J Alzheimers Dis 20:1189–1199.

Wang J, Varghese M, Ono K et al. (2014) Cocoa extracts reduce oligomerization of amyloid-beta: implications for cognitive improvement in Alzheimer's disease. J Alzheimers Dis 41:643–650.

Wang J, BiW, Cheng A et al. (2014) Targeting multiple pathogenic mechanisms with polyphenols for the treatment of Alzheimer's disease – experimental ap- proach and therapeutic implications. Front Aging Neurosci 6.

Wang J, Tanila H, Puoliväli J, Kadish I, Van Groen T (2003) Gender differences in the amount and deposition of amyloidβ in APPswe and PS1 double transgenic mice. Neurobiol Dis 14:318–327.

Wang L, Thagaard C, Joseph M, Jacobus S, Gerber P, Therese M, Michael A, Conlon A (2012) Elevated Fecal Short Chain Fatty Acid and Ammonia Concentrations in Children with Autism Spectrum Disorder. Dig Dis Sci 57:2096–10.

Wang X, Wang W, Li L, George P, Hyoung-gon L, Xiongwei Z (2015) Oxidative Stress and Mitochondrial Dysfunction in Alzheimer's Disease. Biochem Biophys acta 1842:1240–1247.

Wang Y, Chen Z, Zhang Y, Fang S, Zeng Q (2014) Mitochondrial biogenesis of astrocytes is increased under experimental septic conditions. Chin Med J 127:1837–1842.

Waniewski RA, Martin DL (1998) Preferential utilization of acetate by astrocytes is attributable to transport. J Neurosci 18:5225–5233 Available at: http://www.ncbi.nlm.nih.gov/pubmed/9651205.

Waniewski RA, Martin DL (2004) Astrocytes and Synaptosomes Transport and Metabolize Lactate and Acetate Differently *. Neurochem Res 29:209–217.

Weaver CM (2018) Bioactive Foods and Ingredients for Health 1 , 2. Adv Nutr 5:306S–311S.

Weller J, Budson A (2018) Current understanding of Alzheimer ' s disease diagnosis and treatment. F1000Research 7:1–9.

Wilson RS, Segawa E, Boyle PA, Anagnos SE, Hizel LP, Bennett DA (2012) The Natural History of Cognitive Decline in Alzheimer ' s Disease. Psychol Aging 27:1008–1017.

Wiltrout DW, Satter LD (1972) Contribution of Propionate to Glucose Synthesis in the Lactating and Nonlactating Cow 1. J Dairy Sci 55:307–317 Available at: http://dx.doi.org/10.3168/jds.S0022-0302(72)85487-0.

Wong, JM, , de Souza R, Kendall CW, Emam A JD (2006) Colonic Health : Fermentation and Short Chain Fatty Acids. J Clin Gastroenterol 40:235–243.

Wu J, Petralia RS, Kurushima H, Patel H, Jung M, Chowdhury S, Shepherd JD, Dehoff M, Li Y, Huganir RL, Price DL, Scannevin R, Troncoso JC, Wong PC, Worley PF (2011) Arc/Arg 3.1 Regulates an Endosomal Pathway Essential for Activity-Dependent B-amyloid generation. Cell 147:615–628.

Wu L, Rosa-neto P, Hsiung GR, Sadovnick AD, Masellis M, Black SE, Jia J, Gauthier S (2012) Early-Onset Familial Alzheimer 's Disease (EOFAD). Can J Neurol Sci 39:436–445.

Wu L, Sun D (2017) Adherence to Mediterranean diet and risk of developing cognitive disorders : An updated systematic review and meta-analysis of prospective cohort studies. Sci Rep 7:41317 Available at: http://dx.doi.org/10.1038/srep41317.

Wyss MT, Magistretti PJ, Buck A, Weber B (2011) Labeled Acetate as a Marker of Astrocytic Metabolism. J Cereb Blood Flow Metab 31:1668–1674 Available at: http://journals.sagepub.com/doi/10.1038/jcbfm.2011.84.

Yang J-T, Wang Z-J, Cai H-Y, Yuan L, Hu M-M, Wu M-N, Qi J-S (2018) Sex Differences in Neuropathology and Cognitive Behavior in APP/PS1/tau Triple-Transgenic Mouse Model of Alzheimer's Disease. Neurosci Bull Available at: http://link.springer.com/10.1007/s12264-018-0268-9.

Yang T, Santisteban MM, Rodriguez V, Li E, Ahmari N, Sahay B, Pepine CJ, Raizada MK (2016) GUT MICROBIOTA DYSBIOSIS IS LINKED TO HYPERTENSION. Hypertension 65:1331–1340.

Yao J, Irwin RW, Zhao L, Nilsen J, Hamilton RT, Brinton RD (2009) Mitochondrial bioenergetic deficit precedes Alzheimer ' s pathology in female mouse model of Alzheimer ' s disease. PNAS 106:14670–14675.

Yao J, Rettberg JR, Klosinski LP, Cadenas E, Brinton RD (2011) Shift in brain metabolism in

late onset Alzheimer's disease: Implications for biomarkers and therapeutic interventions. Mol Aspects Med 32:247–257.

Yilmaz A, Geddes T, Han B, Bahado-singh RO, Wilson GD (2017) Diagnostic Biomarkers of Alzheimer ' s Disease as Identified in Saliva using H NMR-Based Metabolomics. J Alzheimer's Dis 58:355–359.

Yonezawa T, Kurata R, Yoshida K, Murayama M a, Cui X, Hasegawa A (2013) Free fatty acids-sensing G protein-coupled receptors in drug targeting and therapeutics. Curr Med Chem 20:3855–3871 Available at: http://www.ncbi.nlm.nih.gov/pubmed/23862620.

Zandi PP, Anthony JC, Khachaturian AS, Stone S V, Gustafson D, Tschanz JT, Norton MC, Welsh-bohmer KA (2004) Reduced Risk of Alzheimer Disease in Users of Antioxidant Vitamin Supplements. Arch Neurol 61:82–88.

Zbeida M, Goldsmith R, Shimony T, Vardi H, Naggan L, Shahar DR (2014) MEDITERRANEAN DIET AND FUNCTIONAL INDICATORS AMONG OLDER ADULTS IN NON-MEDITERRANEAN AND MEDITERRANEAN COUNTRIES. J Nutr Health Aging:1–8.

Zetterberg H, Mattsson N (2014) Expert Review of Neurotherapeutics Understanding the cause of sporadic Alzheimer ' s disease Understanding the cause of sporadic Alzheimer ' s disease. Expert Rev Neurother 7175.

Zhan X, Stamova B, Lee-Way J, DeCarli C, Phinney B, Sharp FR (2016) Gram-negative bacterial molecules associate with Alzheimer disease pathology. Neurology 88:2338.

Zhang C, Browne A, Child D, Tanzi RE (2010) Curcumin decreases amyloid-beta peptide levels by attenuating the maturation of amyloid-beta precursor protein. J Biol Chem 285:28472–28480.

Zhang L, Wang Y, Xiayu X, Shi C, Chen W, Song N (2017a) Altered Gut Microbiota in a Mouse Model of Alzheimer's Disease. 60:1241–1257.

Zhang Q, Wang S, Fleuriel C, Leprince D, Rocheleau J, Piston D, Goodman R (2007) Metabolic regulation of SIRT1 transcription via a HIC1:CtBP corepressor complex. Proc Natl Acad Sci 104:829–33.

Zhang Z-H, Wu Q-Y, Zheng R, Chen C, Chen Y, Liu Q, Hoffmann PR, Ni J-Z, Song G-L (2017b) Selenomethionine mitigates cognitive decline by targeting both tau hyperphosphorylation and autophagic clearance in an Alzheimer's disease mouse

model. J Neurosci 37::2449–2462.

Zhao G, Nyman M, Jönsson JÅ (2006) Rapid determination of short-chain fatty acids in colonic contents and faeces of humans and rats by acidified water-extraction and direct-injection gas chromatography. Biomed Chromatogr 20:674–682.

Zhao Y, Cong L, Lukiw WJ (2017) Lipopolysaccharide (LPS) accumulates in neocortical neurons of Alzheimer's disease (AD) brain and impairs transcription in human neuronal-glial primary co-cultures. Front Aging Neurosci 9:1–9.

Zhao Y, Dua P, Wj L (2015a) Microbial Sources of Amyloid and Relevance to Amyloidogenesis and Alzheimer ' s Disease (AD) Alzheimer ' s Disease & Parkinsonism. J Alzheimer's Dis Park 5:117.

Zhao Y, Jaber V, Lukiw WJ (2015b) Microbial Sources of Amyloid and Relevance to Amyloidogenesis and Alzheimer's Disease (AD). J Alzheimers Dis Park 5:177.

Zhu X, Han Y, Du J, Liu R, Jin K, Yi W (2017) Microbiota-gut-brain axis and the central nervous system. Oncotarget 8:53829–53838.

Zilberter M, Ivanov A, Ziyatdinova S, Mukhtarov M, Anton M, Alpár A, Tortoriello G, Botting CH, Lívia F, Osypov AA, Asla P, Tanila H, Harkany T, Zilberter Y (2013) Dietary energy substrates reverse early neuronal hyperactivity in a mouse model of Alzheimer's disease. J Neurochem 125:157–171.

12. APPENDIX

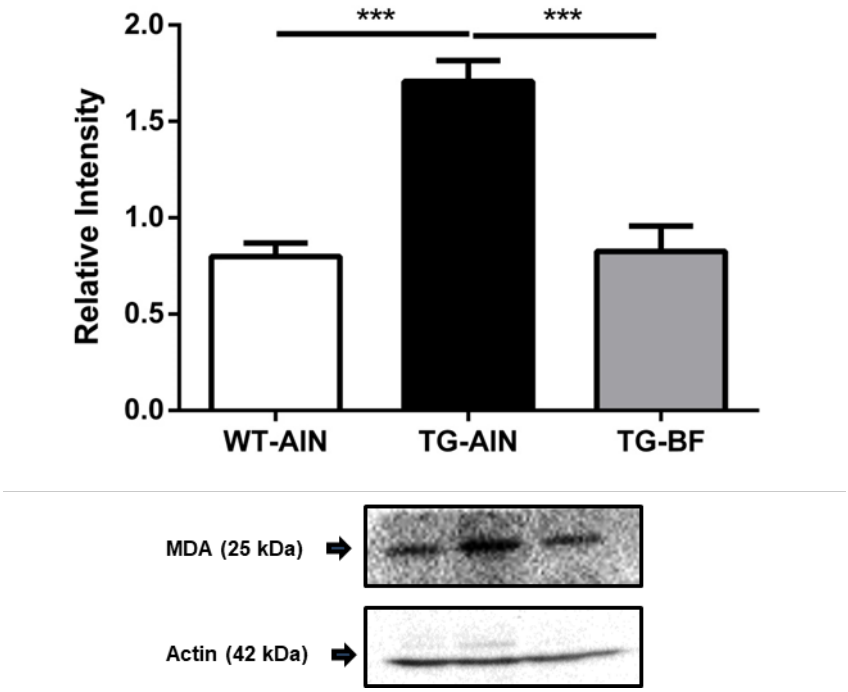

Figure 1 (Appendix 1). Protein levels of MDA in the brain cortex: MDA levels were higher in TG-AIN compared to WT-AIN ($p < 0.001$), while in TG-BF mice MDA levels were even lower than TG-AIN ($p < 0.01$). Images below graphs are representative blots for each protein done five times, in pool samples. Data represents mean ± S.D. ***p <0.001.

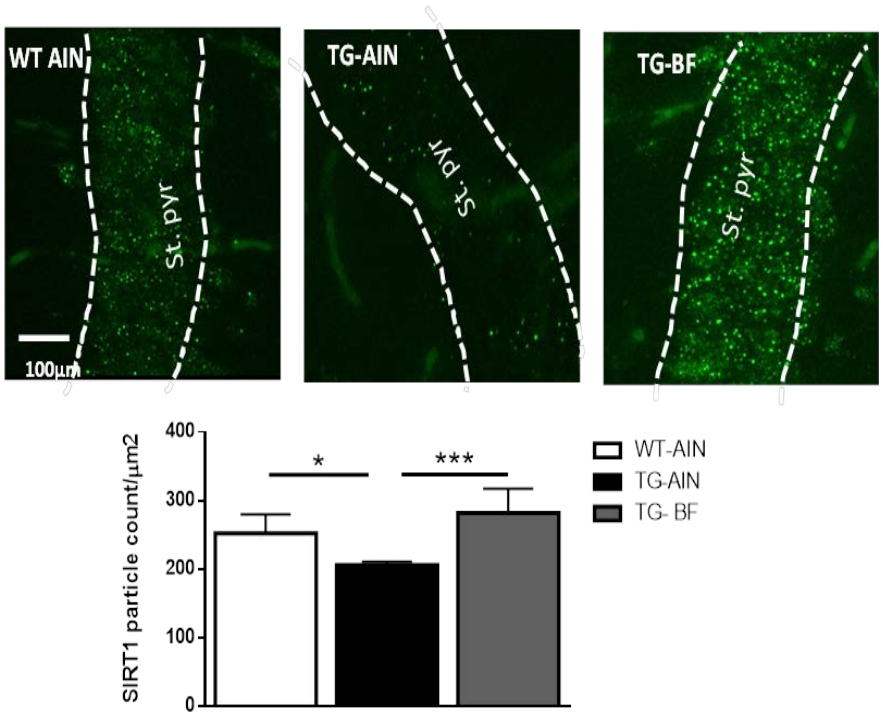

Figure 2 (Appendix 1): Effect of bioactive food on SIRT1 in st. *pyramidale* of the hippocampus. Representative images of SIRT1 labelling in st. *pyramidale.* Scale bar 100 µm. In st. *pyramidale.* TG-AIN mice had less number of SIRT1 particles compared to WT-AIN ($p < 0.01$) and TG-BF ($p<0.001$). Data are expressed as the mean ± S.D. *$p < 0.05$, **$p < 0.001$